

THE MICROSTRUCTURE OF LOESS
AND ITS RELATIONSHIP TO
ENGINEERING PROPERTIES

By

RUDOLPH V. MATALUCCI

Bachelor of Science
University of New Hampshire
Durham, New Hampshire
1960

Master of Science
Oklahoma State University
Stillwater, Oklahoma
1962

Submitted to the Faculty of the
Graduate College of the
Oklahoma State University
in partial fulfillment of
the requirements for
the Degree of
DOCTOR OF PHILOSOPHY
May, 1969

SEP 29 1969

THE MICROSTRUCTURE OF LOESS
AND ITS RELATIONSHIP TO
ENGINEERING PROPERTIES

Thesis Approved:

W. Abell-Hardy

Thesis Adviser

L. Allan Halburton

J. V. Parcker

R. L. James

John W. Shelton

D. D. Durham

Dean of the Graduate College

724980

TO MY WIFE:

for her patience, sacrifice,
understanding, and
encouragement

ACKNOWLEDGMENT

The writer wishes to acknowledge Dr. M. Abdel-Hady, Chairman of the Advisory Committee, and Drs. R. L. Janes, J. W. Shelton, J. V. Parcher, and T. A. Haliburton, Committee Members, for their interest and contribution to this research, and for their review of the manuscript.

Sincere appreciation is extended to Professor Abdel-Hady, Thesis Adviser, for his guidance, inspiration, and continued encouragement throughout the entire progress of this research.

The writer is grateful for the assistance provided by Professor Shelton, Geology Department, whose expert knowledge was of benefit in the geological considerations of this thesis.

Professor Parcher's support and advice in the many phases of this research was gratefully appreciated.

The cooperation and interest provided by Professor Haliburton was invaluable in successfully conducting laboratory tests.

The United States Air Force Institute of Technology is acknowledged for sponsorship of the writer during his pursuit of graduate studies. The U. S. Air Force Weapons Laboratory is recognized for the partial financial support of this research and for the interest shown during its progress.

The author is grateful to the Office of Engineering Research and the School of Civil Engineering for partial financial support and assistance which made the purchase of necessary equipment possible.

Shell Development Company is recognized for donating the dielectric anisotropy instrument to Oklahoma State University and for kindly allowing use of it for part of this research. Halliburton Company is acknowledged for kindly supplying the needed materials for consolidation of the samples.

The writer is grateful to Dr. E. L. Krinitzsky, of the Waterways Experiment Station, Vicksburg, Mississippi, for his excellent introduction to the loess of that region and for his interest and assistance during collection of undisturbed samples. Appreciation is also extended to Dan Marks for his assistance during the collection of the material tested.

The writer is grateful to Samuel Ng for his advice and assistance in the photographic and computer work of this thesis.

The programming assistance provided by Larry Mills, Oklahoma State University Computer Center, is acknowledged.

Appreciation is expressed to Eldon Hardy and Velda Davis for their assistance in preparing the illustrations and typing the manuscript.

TABLE OF CONTENTS

Chapter	Page
I. INTRODUCTION	1
A. General	1
B. Purpose and Scope of Study	3
C. Source of Material	4
II. LITERATURE REVIEW	6
A. Geology of Loess	6
1. Geographical Distribution	6
2. Origin of Loess	9
3. General Description	13
4. Certain Areal Properties	15
B. Physical Properties of Loess	19
C. Microstructure of Loess	21
III. COMPOSITION AND TEXTURE	23
A. Mineralogy	23
B. Partial Chemical Analysis	24
C. Grain Shape	25
D. Grain Size Distribution	25
1. General	25
2. Statistical Parameters	27
3. Procedure	32
4. Descriptive Measures	33
5. Regression Equations	40
6. Discussion	43
E. Physical Properties	45
F. Fabric Elements and Cementation	47
IV. GRAIN ORIENTATION	50
A. Introduction	50
B. Preparation of Samples	52
C. Grain Orientation Measurements	54
D. Data Analysis Methods	59
E. Discussion of Results	61
V. INFLUENCE OF GRAIN ORIENTATION ON DIRECT SHEAR STRENGTH	65

Chapter	Page
V. CHAPTER V (Continued)	
A. Introduction	65
B. Procedure	66
C. Shear Strength Results.	70
D. Analysis of Data	75
E. Failure Surfaces	79
F. Shear Plane Development	81
G. Discussion	83
VI. INFLUENCE OF MICROSTRUCTURE ON SHEAR STRENGTH: TRIAXIAL TESTS	87
A. Introduction	87
B. Procedure	88
C. Test Results	92
D. Discussion	99
VII. SUMMARY AND CONCLUSIONS	104
A. Summary	104
B. Conclusions	109
C. Recommendations for Further Research.	111
BIBLIOGRAPHY	113
APPENDIX A - RAPID PROCEDURE USED FOR MOUNTING GRAINS	120
APPENDIX B - RELATIONSHIP BETWEEN FREQUENCY-BY- NUMBER AND WEIGHT-PER CENT GRAIN- SIZE DISTRIBUTIONS	122
APPENDIX C - GRAIN-SIZE DISTRIBUTION REGRESSION DATA	126
APPENDIX D - PROCEDURE FOR IMPREGNATING SAMPLES FOR THIN SECTIONS	130
APPENDIX E - PROCEDURE FOR PREPARING SAMPLES FOR DIELECTRIC ANISOTROPY MEASUREMENTS	132
APPENDIX F - COMPUTERIZED GRAIN ORIENTATION STATISTICAL ANALYSIS	137

LIST OF TABLES

Table	Page
I. Range in Values of Engineering Properties of Loess in the United States (after Sheeler, 1968)	20
II. Definitions of Grain-Size Distribution Statistical Parameters	30
III. Summary of Grain-Size Distribution Statistical Parameters	39
IV. Some Physical Properties of Loess	46
V. Summary of Statistical Parameters for Grain Orientation	62
VI. Summary of Direct Shear Tests	76
VII. Analysis of Variance	78
VIII. Summary of Triaxial Compression Tests	101
IX. Phi Values Derived by Plotting Cumulative Curves on Probability Paper	127
X. Grain Orientation by Vector Magnitude Method	139
XI. Grain Orientation by Chayes' Minimum Variance Technique	142

LIST OF FIGURES

Figure	Page
1. Geographical Distribution of Loess Deposits Excluding North America (modified after Berg, 1947)	7
2. General Loess Deposits of the United States Excluding Alaska (after Gibbs and Holland, 1960)	7
3. Eastward Thinning of the Loess Blanket From the Mississippi River (modified after Wascher, et al., 1948)	17
4. Thin Section Photomicrograph of Vicksburg Loess; Crossed Nicols; 80x	26
5. Grain Mount Photomicrograph of Vicksburg Loess; Crossed Nicols; 80x	26
6. Graphical Representation of Statistical Parameters for Grain-Size Distribution Analysis	31
7. Cumulative Grain-Size Distribution Curves for Vicksburg Loess	34
8. Cumulative Grain-Size Distribution Curves for Pre-Vicksburg Loess	35
9. Cumulative Grain-Size Distribution Curves for Vicksburg Loess on Probability Paper	37
10. Cumulative Grain-Size Distribution Curves for Pre-Vicksburg Loess on Probability Paper	38
11. Regression Lines for Grain-Size Distribution Analysis	42
12. Snail Shells and Calcareous Root Tubules and Concretions in Vicksburg Loess; Scale in Inches	49

Figure	Page
13. Thin Section Photomicrograph of Vicksburg Loess Illustrating Discrete Calcite Grains (Shaded Arrows), and Secondary Calcite Rim of a Root Tubule (Unshaded Arrow), Crossed Nichols; 80x	49
14. Grain Orientation in the Horizontal Plane of Vicksburg Loess	55
15. Grain Orientation in the Vertical Plane of Vicksburg Loess Parallel to the Horizontal Fabric Mean	55
16. Grain Orientation in the Horizontal Plane of Pre-Vicksburg Loess	56
17. Grain Orientation in the Vertical Plane of Pre-Vicksburg Loess Parallel to the Horizontal Fabric Mean	56
18. Typical Chart Tracing From a Dielectric Anisotropy Measurement of a Vicksburg Loess Plug; Showing Fabric Mean of N 83°W	58
19. Orientation of the Shear Planes in Undisturbed Vicksburg Loess Specimens Used for Direct Shear Tests	68
20. Direct Shear Device Mounted on Vertical Strain Controlled Loading Machine	69
21. Effect of Imbrication on Direct Shear Tests of Dry Specimens	71
22. Effect of Imbrication on Direct Shear Tests of Moist Specimens	72
23. Effect of Preferred Grain Orientation on Direct Shear Tests of Dry Specimens	73
24. Effect of Preferred Grain Orientation on Direct Shear Tests of Moist Specimens	74
25. Exposed Direct Shear Surfaces (2" x 2") of Moist Vicksburg Loess. Large Arrows Indicate Direction of Movement; Small Arrows Indicate Steps Facing Oncoming Opposed Surface	80

Figure	Page
26. Exposed Direct Shear Surfaces (2" x 2") of Dry Vicksburg Loess. Large Arrows Indicate Direction of Movement; Small Arrows Indicate Steps Facing Oncoming Opposed Surface.	80
27. Thin Sections Illustrating Sequential Development of Failure Pattern (a, b, c, d) in Moist Specimens Sheared Normal to Grain Orientation; Crossed Polars	82
28. Thin Sections Illustrating Failure Pattern in Moist Specimens Sheared (a) Normal to Imbrication, and (b) Parallel to Imbrication. Crossed Polars; 1" x 2" Sections	82
29. Photomicrograph of a Failure Plane in Specimen H(EW). Arrows Indicate Direction of Shear and Outline Indicates Steps Facing a Direction Which Apparently Opposes Movement; Crossed Nicols; 10x.	84
30. Photomicrograph of a Failure Plane in Specimen V(V). Arrows Indicate Direction of Shear and Outline Indicates Steps Facing a Direction Which Apparently Opposes Movement; Crossed Nicols; 20x	84
31. Strength and Stress-Deformation Characteristics of Cemented Soils (after Means and Parcher, 1963)	89
32. Triaxial Compression Tests on Undisturbed Vicksburg Loess	93
33. Triaxial Compression Tests on Undisturbed (45°) Vicksburg Loess	94
34. Triaxial Compression Tests on Remolded Vicksburg Loess	95
35. Triaxial Compression Strength Envelopes for Vicksburg Loess	96
36. Average Stress-Strain Triaxial Test Results for Dry Vicksburg Loess	97
37. Average Stress-Strain Triaxial Test Results for Moist Vicksburg Loess	98

Figure	Page
38. Axial Strains at Failure in Triaxial Compression Tests of Vicksburg Loess	100
39. Perfectly Normal Grain-Size Distribution Curves Plotted on Probability Paper	124
40. Apparatus for Standard Impregnation of Soils	134
41. Apparatus for Consolidation of Soil Specimens	134

CHAPTER I

INTRODUCTION

A. General

Strength and stability considerations in soil mechanics problems are concerned with various studies to determine whether the shearing resistance of a soil material is sufficient to prevent failure. Such studies essentially consist of analyzing several factors which influence shear strength such as friction angle, cohesion, intergranular pressure, colloidal phenomena, structural strength, and others. The principal factor which has the largest bearing on this investigation is structural strength.

The nature of structural strength is not completely known. Numerous investigations have established the effects that size and shape of grains as well as mineralogical composition have on over-all structural strength. The arrangement, orientation, and the interlocking of soil grains, and the various characteristics of the water film surrounding some soil grains, have also contributed to a better understanding of the structural strength of cohesive and noncohesive soils. Recent developments in techniques for examining and evaluating microstructural patterns in soils have further contributed to an understanding of

structural strength and have provided more quantitative measures for expressing fabric variations in soil masses.

In a complex material such as soil, the individual components consisting of skeleton grains, soil matrix (plasma), and pores (intrapedal voids) are arranged in a continuous system commonly referred to as structural or fabric pattern. In most soils, these patterns are usually observed microscopically. The two principal aspects of structural patterns involve spatial distribution and spatial orientation of the soil elements. Spatial distribution is concerned with the position and arrangement of the individual components relative to the other surrounding soil components. This aspect is commonly described in terms of the frequency of contacts between similar or dissimilar elements within the soil pattern. Spatial orientation describes preferred dimensional alignment of individual components according to the external geometric shape of each. Consequently, dimensional orientation can only occur where the axes of individual soil elements considered are not equidimensional. Orientational patterns are generally determined by directly plotting the relative frequency of elongated elements versus the direction of orientation.

Strength theories used in soil mechanics assume that soils are generally isotropic. Even early studies, however, recognized the occurrence of depositional or stress-induced fabrics in soils. Whether these structural

anisotropies resulted in significant strength anisotropy was not completely established. Recent studies, primarily of clay soils, have indicated that the role of structural anisotropies in soils would eventually lead to new appraisals of the controlling factors in soil strength (Mitchell, 1956; Ingles and Lafeber, 1966; and others).

B. Purpose and Scope of Study

The purpose of this study was to examine the microstructure of a loess soil in an attempt to correlate any noted structural anisotropies within the soil fabric with variations in strength. Thin sections were prepared of undisturbed loess and measurements were made on photomicrographs to determine the degree of preferred orientation of silt grains. Grain orientation was also determined using a dielectric anisotropy instrument. Subsequently, the influence of grain orientation on shear strength of undisturbed loess stressed on different planes was examined. The over-all effect of grain orientation on strength variation was studied through an evaluation of direct shear and triaxial compression test results, and through an examination of the mode of failure along the shear plane.

A study of soil microstructure is not considered complete without an investigation of the composition and texture of the material in question. Since extensive mineralogical studies on this particular loess had been

performed by other investigators, this study concentrated on the chemical composition, physical properties, grain shape, and grain size distribution of the material.

A detailed analysis of grain size distribution was performed to ascertain the degree of correlation of thin section and grain mount measurements with hydrometer and dry sieve analyses. Grain shape was determined for descriptive purposes and to assure that elongation of skeleton grains exists. Chemical composition and physical properties were determined to assist in the evaluation of the strength parameters of the loess.

The composition and textural properties of two loessial soils studied are presented in Chapter III, and grain orientation of the same materials are presented in Chapter IV. Although grain orientation, composition, and texture were determined for two independent loess materials, evaluation of the effect of grain orientation on strength was made only for the younger loess soil. The effect of grain orientation on directional shear strength of so-called Vicksburg loess, presented in Chapters V and VI, is based on direct shear and triaxial compression tests.

C. Source of Material

All of the loess examined in this study was obtained from the Vicksburg, Mississippi area. Undisturbed samples of Vicksburg loess were obtained at a recently exposed vertical cut at the Battlefield Shopping Center. Samples

of older deposits recognized as Pre-Vicksburg loess were obtained at a highway cut on U. S. Highway 61 Bypass, north of Vicksburg, a locality noted by Krinitzsky and Turnbull (1967). The samples of Vicksburg and Pre-Vicksburg loess were situated at depths from the original surface of 30 feet and 70 feet, respectively. Wooden boxes were utilized for transporting the samples intact to the laboratory where they were air dried for several months.

The Vicksburg loess exemplifies the typical tan or buff-colored, unweathered loess deposits of the Mississippi area. The Pre-Vicksburg loess is a reddish brown, clayey silt, which at the sampling site was overlain by 60 feet of leached and unleached Vicksburg loess. Both materials carry an abundance of gastropod shells, tubules, and calcareous concretions. Vertical jointing and vertical road cuts are other typical features of the two materials of this region. Both materials are considered Late Pleistocene - Early Recent in age by Krinitzsky and Turnbull (1967) who have made a rather extensive geologic investigation of the two loess materials.

The word "loess" itself was derived from the German name löss. Apparently the name was initially used in scientific work to describe the silt deposits in the Rhine Valley. The term was subsequently used to describe similar deposits in other parts of Europe, Russia, and America.

CHAPTER II

LITERATURE REVIEW

A. Geology of Loess

1. Geographical Distribution

Loess was first identified in the valley of the Rhine during the early nineteenth century, but was later found to be extensively deposited in many other locations throughout the world. Literature is not consistent in its interpretation of loess deposits because of differences in definition, and as a result its areal extent and distribution are sometimes questionable. The literature also provides conflicting data on the thickness of loess deposits throughout the world because of an apparent confusion over actual thickness and elevation. In any event, Berg (1947) provided a distribution map of loess deposits of the world, shown exclusive of North America (Figure 1), and Gibbs and Holland (1960) mapped the major loess deposits of the United States exclusive of Alaska (Figure 2).

Loess that has been derived principally from glacial outwash is found in Europe along the Rhine, Rhone, and Danube valleys and very extensively in the Ukraine region of Russia. Loess of similar origin is distributed in

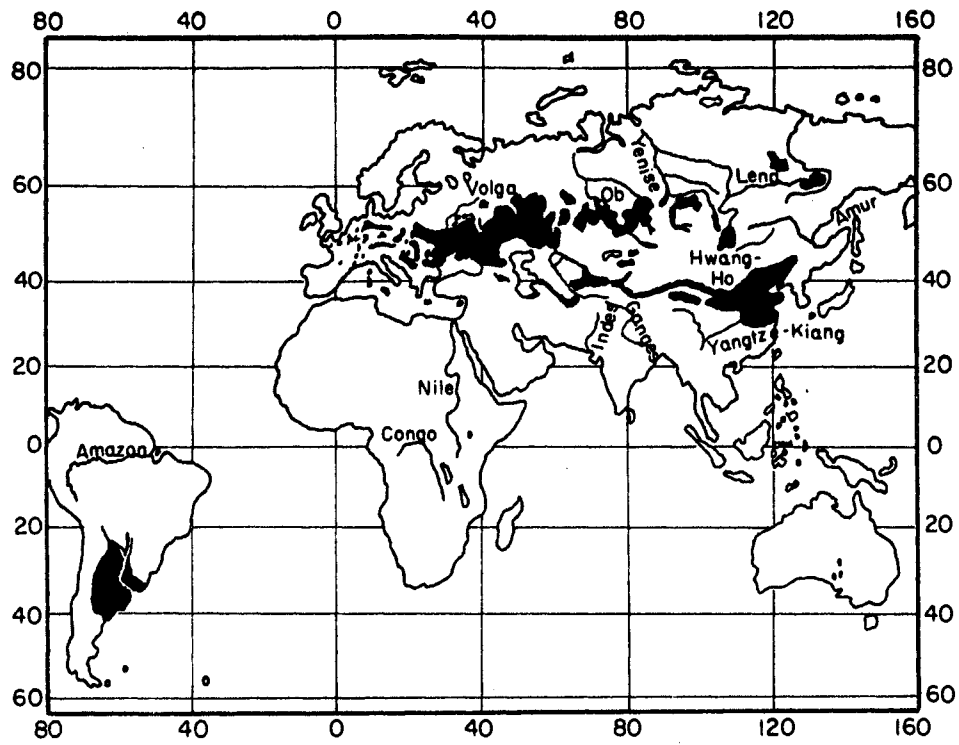


Figure 1. Geographical Distribution of Loess Deposits Excluding North America (modified after Berg, 1947)



Figure 2. General Loess Deposits of the United States Excluding Alaska (after Gibbs and Holland, 1960)

North America along the Mississippi, Missouri, Ohio, and Wabash valleys. The states exhibiting loess deposits include Nebraska, Kansas, Iowa, Wisconsin, Illinois, Idaho, Washington, Missouri, Kentucky, Tennessee, and Mississippi. Loess also exists and is still being deposited in the floodplain of the Tanana River of central Alaska (Péwé, 1951).

Loess deposits exist in northeastern China, and parts of Mongolia and Manchuria which appear to have been derived from the Gobi Desert. The deposits cover about 300,000 square miles and the actual thickness along the Yangtze Valley of China is believed to be from 180-250 feet. Loess deposits of Russia are found in the steppe region of Siberia and in Turkestan east of the Caspian Sea. Scattered deposits exist also in Australia.

The loess deposits of Argentina are the most extensive in the southern hemisphere. These deposits average 90 feet in thickness, and maximum thicknesses of 210 feet have been recorded (Teruggi, 1957).

As can be noted in Figures 1 and 2, loess is generally not present in the tropics and polar regions. According to approximate estimates, the area covered by loess is 5 million square miles which includes approximately 2.5 per cent of the earth's total land surface. Based on an average thickness of 30 feet, it would be possible to cover the entire surface of the continents with three feet of loess (Berg, 1947).

2. Origin of Loess

Until recently, the origin of loess had been a puzzling question among geologists around the world. Theories on origin which have been advanced involve some twenty geological processes. Scheidig (1934), Russell (1944), and Berg (1947) have provided a comprehensive treatment of the different theories developed by geologists and soil scientists.

As a preliminary consideration of origin, it is of importance to recall that there are essentially two problems of loess: a problem of origin of the material, and a problem of deposition. Because loess is composed of very fine and uniform material, it is generally agreed that it is a product of some extensive disaggregating erosional process which could have been aqueous, subaerial, or glacial. Furthermore, regardless of the ultimate source, it was most probably not produced at the place where it is found.

Berg (1947) reviewed numerous opinions concerning the origin of loess but mentioned five that he considered most important. These include the aquatic-glacial (from glacial "mud"), eolian (wind transported dust), alluvial (stream), alluvial-eolian (water and wind transported), and eluvial (soil, in-situ weathering and soil formation). Berg considered loess a product of weathering and soil-formation.

The Quaternary geology of the lower Mississippi Valley

has reflected the ideas particularly of two outstanding workers, H. N. Fisk and R. J. Russell, who also rejected an eolian origin of loess (Fisk, 1944, 1951; Russell, 1944). Russell (1944) suggested that the lower Mississippi Valley loess was derived from backswamp deposits of Pleistocene formations through a process of "loessification". The suggested process involves the weathering of these backswamp deposits which accumulate on slopes through mass movement and subsequently change to loess as carbonate is added by ground water.

Richthofen is generally given credit for advancing initially the eolian hypothesis for loess formation. He, writing in 1870 in Shanghai, elaborated on the origin of the Chinese loess. Although American geologists initially did not accept his hypothesis, by the end of the century many joined the beliefs of European investigators in favor of the idea. Aside from objections by some Louisiana State University geologists, loess in America, including that of the Mississippi Valley, has long been considered wind-laid and its source has been considered to be the fine sediments on the floodplains of the Pleistocene rivers (e.g., Chamberlin, 1897; Chamberlin and Salisbury, 1907; Smith, 1942; Swineford and Frye, 1944, 1951; Leighton and Willman, 1950).

Loess deposits of Kansas are considered by Swineford and Frye (1951) to be of eolian origin for the following reasons: (1) deposits exist on highest elements of local

topography, (2) texture is similar to that of modern wind-transported silt, (3) composition is uniform over large areas even where it rests on varying materials, (4) thickness and median diameter decrease away from source, (5) zones of terrestrial snails are regionally persistent, (6) lateral persistence of buried soil profiles show no evidence of erosion or creep, (7) gradational contact of overlying loess units exists on buried soils, and (8) apparent simultaneous deposition of uniform silts on sharply discordant topographic levels. Earlier mechanical analyses by the same authors illustrated the similarity between wind-blown dust and loess (Swineford and Frye, 1945). Moreover, Péwé (1951), in his observations of loess being formed by winds in the floodplain of the Tanana River in central Alaska, also noted the similarity of grain-size distributions between windblown material of the area and the loess of Kansas and Illinois.

Gibbs and Holland (1960), following the eolian origin, considered certain conditions which must exist for the development of loessial soils. These were: (1) a source of intermixed silt and clay sufficiently adequate to account for the known deposit, (2) a long period of strong wind prevailing in one direction, and (3) a place for deposition. In addition, after deposition and development of the cohesive fabric, the climate conditions were to remain arid to semi-arid to preclude collapse of the open structure. Further discussions pertaining to geological

evidence of climatic conditions during loess deposition are presented elsewhere (Shapley, 1953; Vischer, 1922; and others).

Perhaps one of the strongest single pieces of evidence in support of the eolian hypothesis is the terrestrial character of the loessial fauna. The occurrences of other than land shells are sporadic and in many places nonexistent. As such, there is no question that the vast majority of the organic remains of loess are those of animals which lived on land. On the other hand, the mere presence of land snails in fluvial, lacustrine, and marine deposits is not considered unusual, but the absence of aqueous forms from most loess deposits is significant. In other words, it is not the occurrence of terrestrial forms, but the absence of any others that so strongly favors the hypothesis that loess is deposited over a dry land surface.

As explained in the eolian theory, vegetation may have contributed to collecting and holding the soil particles together during deposition. If the loess had been deposited on a surface devoid of vegetation, it could subsequently have been eroded by wind. In Illinois, relatively thin loess deposits were found where it was believed that vegetation had been scarce during the period of deposition (Smith, 1942). The assumed presence of this vegetation has subsequently led to the belief that root hairs encouraged the precipitation of carbonate along them to form the existing tubules.

Recent investigators continue to support the eolian origin of loess in the United States (e.g., Snowden, 1966; Krinitzsky and Turnbull, 1967). Although the eolian hypothesis has long been a subject of much debate, there is now general agreement that loess was wind transported, and that the sediments were of glacio-fluvial origin. Furthermore, it is believed that other uniform silt deposits such as loess, of other than eolian origin, are not commonly formed.

3. General Description

Russell's definition of loess includes the following essential characteristics:

Loess is unstratified, homogeneous, porous, calcareous silt; it is characteristic that it is yellowish or buff, tends to split along vertical joints, maintains steep faces, and ordinarily contains concretions and snail shells. From the quantitative standpoint, at least 50% by weight must fall within the grain size fraction 0.01-0.05 mm., and it must effervesce freely with dilute hydrochloric acid.

Gibbs and Holland (1960) describe the material, in part, as follows:

Loess is a quartzose, somewhat feldspathic clastic sediment composed of a uniformly sorted mixture of silt, fine sand, and clay particles arranged in an open, cohesive fabric frequently resulting in a natural dry density of 70-90 pounds per cubic foot. Deposits may reach considerable thicknesses.

Krinitzsky and Turnbull (1967) stated the following:

Loess may be described as a well-sorted, porous, slightly indurated, eolian silt. It may or may not be calcareous. It has

excellent vertical slope stability if well drained and protected from rainwash.

The color of loess is ordinarily tan or buff; however, it may vary from ash grey to red depending on source and degree of weathering. Color is partly related to the chemical state and contents of iron oxide coatings on individual particles (clay or silt). Color depends also on the calcium carbonate content. Moisture to some degree influences the ultimate color; however, color change due to seepage is primarily associated with chemical alteration or weathering of the loess to a more clayey material.

Vertical exposures occurring principally in construction cuts or stream cuts and remaining stable for years have received much attention. Explanation of stability basically includes a combination of mechanical or adhesive cementation and formation of vertically oriented root tubules. It was suggested that vertical faces were the result of flat particles horizontally packed "like sheets of paper". However, this suggestion was rejected because particles were not found to be tabular in shape. Therefore, tubular internal structure, vertically oriented, and calcite and clay cement, formed during weathering, provides an adequate explanation of vertical stability.

The translation of calcite in loess is achieved through leaching and precipitation by soil moisture. Some of the calcite can conceivably form a "crust" on exposed faces by evaporation of moisture at the face and subsequent precipitation of calcite in the pore spaces. This crust

best explains the durability of these vertical exposures. After prolonged weathering, the crust thickens and "slabbing" at the face sometimes develops.

Loess generally drapes the upland hills in conformity to the pre-existing erosional surfaces; a feature which supports the eolian hypothesis. Underlying materials contribute nothing to the characteristics of the overlying loess except where it is believed there has been some intermixing by colluviation or gravity. Where present in the United States, the thickness of this loess mantle varies from a few inches to over one hundred feet and generally presents a smooth rolling upland topography. Where loess is adjacent to streams or gullies, the typical vertical slopes are immediately recognized. Drainage patterns on aerial photographs are feather-shaped and generally completely uniform.

4. Certain Areal Properties

In support of the eolian origin, several investigators have noted a consistent pattern of decreasing thickness and increasing plasticity of loess with distance from the source area. According to a study in Mississippi by Krumbein (1937), the thickness of loess decreases exponentially with respect to the distance from the bluffs of the Mississippi River in the area between two and nine miles from the bluffs. He speculated that particle size also decreased exponentially.

Across two long traverses in Iowa, Simonson and Hutton (1954) noted a linear-logarithmic thinning of loess with distance from the Missouri River. The Wisconsin loess of Iowa is characterized by an increasing clay content as well as decreasing thickness eastward from the Missouri River (Davidson et al., 1960).

The loess in Illinois shows a linearly decreasing particle size with respect to the logarithm of the distance from the Mississippi River bluffs (Smith, 1942). It was also found that the rate of thinning of the same loess was a linear function of the logarithm of the distance from the river.

In an investigation of the Lower Mississippi Valley loess, Wascher et al., (1948) mapped an eastward thinning of loess on the east side of the Mississippi River (Figure 3). Krinitzsky and Turnbull (1967) have also noted an eastward decrease in thickness as well as a decreasing particle size (for a distance of 40 miles) from the bluffs at Vicksburg, Mississippi.

Swineford and Frye (1951) investigating some textural properties of the Peoria loess in Kansas found that the median particle diameter decreased with distance away from source. The linear relationship established in this study was based on the logarithm of the median diameter plotted against distance in miles.

Of some interest at this point is a study based on a statistical theory of atmospheric turbulence. A linear

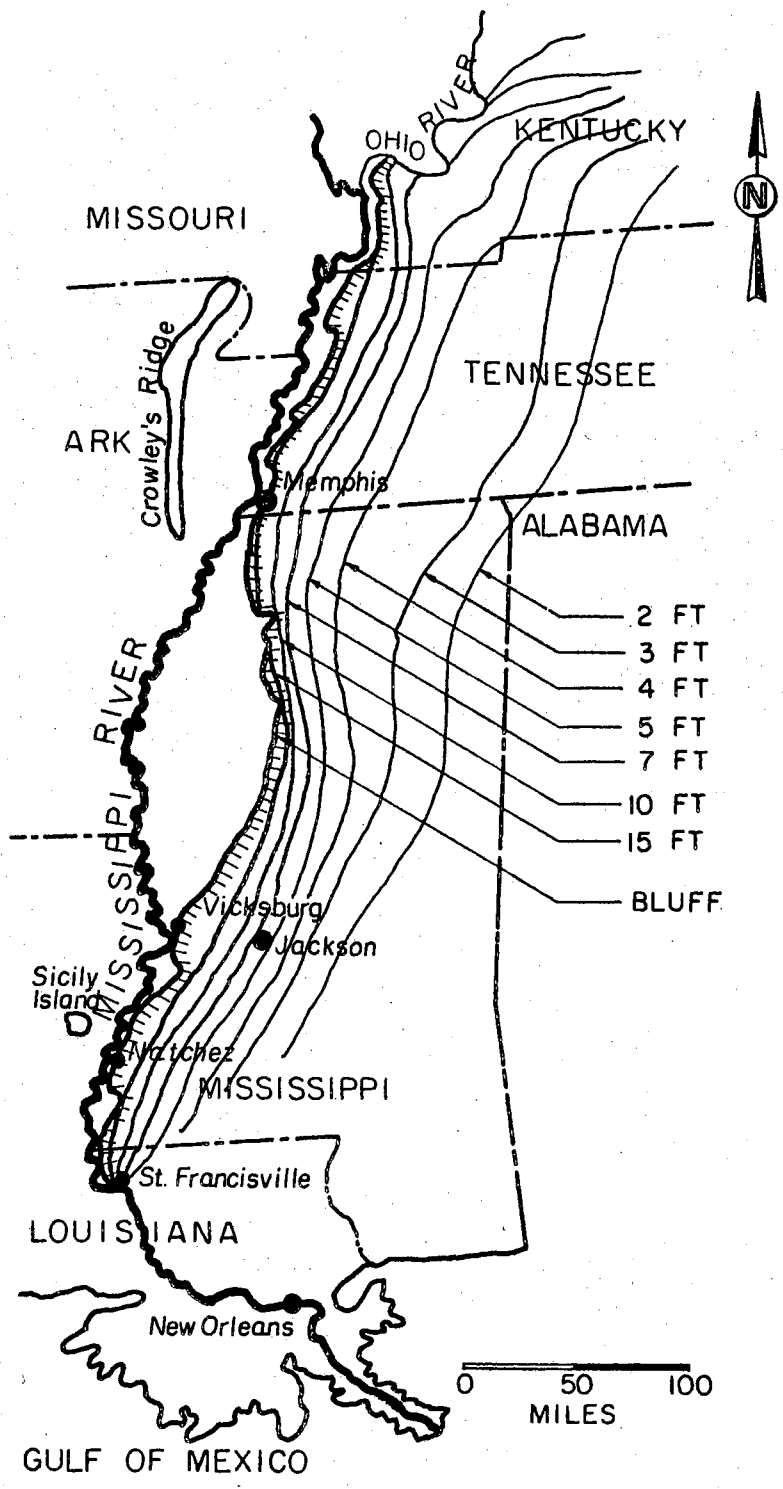


Figure 3. Eastward Thinning of the Loess Blanket From the Mississippi River (modified after Wascher et al., 1948)

relationship was derived which was used to predict the change in depth of loess blankets with distance from the source of the wind-blown material (Waggoner and Bingham, 1961). The predictions were shown to explain adequately loess thickness east of the Mississippi, Illinois, and Missouri Rivers.

Emerson (1918), following the eolian origin for loess of Louisiana and southern Mississippi, proposed that the principal paleowinds of this region were westerly and southerly. This conclusion was based on the width and thickness of the loess, as well as the "lime, potash, and phosphoric acid" contents.

The decreasing thickness of loess with distance from the bluffs in the Vicksburg area provides a means for ascertaining predominant wind direction during deposition (Figure 3). Constructing perpendicular lines at each contour from Vicksburg to Jackson results in an average paleowind azimuth of 290 degrees (N 70° W). In addition, the eastward decrease in grain size in the same area indicates that westerly winds were perhaps more frequent and effective during deposition.

An analysis of modern wind directions revealed that at Vicksburg, 43 per cent of the high winds were from the west, 29 per cent from the north, 16 per cent from the south, and 11 per cent from the east (Emerson, 1918). However, recent surface wind direction data compiled by the U. S. Weather Bureau (1967) for this same area indicate

that westerly winds are not as predominant at the present as they were earlier or apparently during the loess-depositing period.

B. Physical Properties of Loess

A number of recent studies have been made concerning the physical and engineering properties of loess in the United States (e.g., Clevenger, 1956; Gibbs and Holland, 1960; Davidson et al, 1960; Royster and Rowan, 1968; Lohnes and Handy, 1968; Sheeler, 1968). Aside from local variation, it is interesting to note that basically the behavior of loess is similar worldwide.

General characteristics of loess noted by Sheeler (1968) are summarized below and are given in some detail in Table I:

1. Loess is a soil of predominantly silt particles with small amounts of sand.
2. The physical characteristics of gradation, compaction, plasticity, and classification are uniform.
3. The structure is open and porous.
4. Bonding is primarily due to thin clay coatings.
5. In-situ densities range from 66 to 104 pounds per cubic foot.
6. Large settlements are uncommon for in-situ densities of over 90 pounds per cubic foot.
7. Natural moisture contents range from 4 to 49 per cent which are generally well below saturation.
8. Bearing capacity depends primarily on the in-situ density.

TABLE I

RANGE IN VALUES OF ENGINEERING PROPERTIES OF LOESS IN
THE UNITED STATES (AFTER SHEELER, 1968)

PROPERTY	LOCATION							
	Iowa	Nebraska	Tennessee	Mississippi	Illinois	Alaska	Washington	Colorado
SPECIFIC GRAVITY	2.68-2.72	2.57-2.69	2.65-2.70	2.66-2.73		2.67-2.79		
MECHANICAL ANALYSIS								
Sand, percent	0-27	0-41	1-12	0-8	1-4	2-21	2-21	30
Silt, percent	56-85	30-71	68-94	75-85	48-64	65-93	60-90	50
Clay, percent	12-42	11-49	4-30	0-25	35-49	3-20	8-20	20
ATTERBERG LIMITS								
LL, percent	24-53	24-52	27-39	23-43	39-58	22-32	16-30	37
PL, percent	17-29	17-28	23-26	17-29	18-22	19-26		20
PI	3-34	1-24	1-15	2-20	17-37	NP-8	<8	17
CLASSIFICATION								
Textural	SL,SCL,SC	SL,SCL,SC	SL,SCL,SC	SL,SCL	SC,C	SL,SCL		SL
AASHO	A-4 A-7-6	A-4 A-6	A-4 A-6	A-4 A-6	A-6 A-7-6	A-4		A-6
Unified	ML,CL,CH	ML,CL	ML,CL	ML,CL	CL,CH	ML,CL-ML		CL
DENSITY TEST DATA								
Standard OM, percent	15-20		14-16			13-18		
Modified OM, percent	13-18							
Standard MD, pcf	103-112		100-108			103-112		
Modified MD, pcf	113-119							
In-place MD, pcf	66-99			80-104				76-95
Field moisture, percent	4-31		12-25	19-38		11-49		8-10
SHEAR STRENGTH								
Unconfined compression test				2-8				
Unconsolidated undrained triaxial shear,								
c, psi		0-67		2-10				
ϕ		31-36°		0-28°				
Consolidated undrained triaxial shear,								
c, psi	0-8			3-8				
ϕ	28-31°			26°				
Consolidated drained direct shear,								
c, psi	0.3-1.8			0				
ϕ	24-25			32-33°				
CBR				10-13				

9. Consolidation proceeds rapidly under load when loess is saturated.
10. Shearing strength is greatly dependent on moisture content.

C. Microstructure of Loess

Literature review does not reflect extensive studies on the microstructure of loess in the United States except those limited to the petrographic properties (e.g., Swineford and Frye, 1951; Gibbs and Holland, 1960; Davidson et al., 1960; Krinitzsky and Turnbull, 1967). These examinations were primarily concerned with qualitative description of the fabric elements such as skeletal grains, clay matrix, intrapedal voids, cementation, and root tubules. The descriptions primarily consider particle size and shape, composition, porosity, and the nature and distribution of clay matrix and secondary carbonate.

Conclusions derived from the petrographic analyses of loess, however, have been used to explain certain engineering properties. The high compressibility of loess, for example, has been attributed to the open-structural peculiarities. The strength of the material has been considered a function of the clay bond and the continuous system of silt grains. Strength properties have also been considered to be dependent on texture, and on arrangement of chemical and mineral constituents. All of these fabric components have generally been used to explain engineering behavior of loess; however, few studies actually correlated

quantitative measurements of loess fabric with engineering data. None has analyzed grain orientation of loess.

Microstructure of loess has been a subject of considerable interest to many Russian engineers, as exemplified by the works of Larionov (1965). Larionov (1965) and others have studied methods of evaluating loess soils in light of new data obtained from studying loess structure under an electron microscope. Earlier studies in Russia revealed that the skeletal grains were not in contact with each other, but floated in a fine dispersed mass. Consequently, loess soil strength was believed to be primarily dependent on the composition and microstructure of the surrounding matrix. More recent examination of electron micrographs have shown that certain arrangements of these clay particles and accumulation of fine quartz and carbonates on the planes of these clay particles formed zones of weakness.

CHAPTER III

COMPOSITION AND TEXTURE

A. Mineralogy

Early mineralogical studies of lower Mississippi Valley loess were made by Doeglas (1949) and Wascher, Humbert, and Cady (1948). The most recent mineralogical analyses of loess from this region were presented by Snowden (1966) and Krinitzsky and Turnbull (1967). In these recent studies, the material referred to as calcareous is comparable to the Vicksburg loess studied herein, and the leached is comparable to the Pre-Vicksburg loess. General findings of a comprehensive mineralogical investigation of loess in this region by Snowden (1966) are summarized below:

<u>Leached</u>		<u>Calcareous</u>	
Quartz	75 per cent	Quartz	65 per cent
Clay minerals	18 per cent	Carbonates	20 per cent
Feldspars	4 per cent	Clay minerals	7 per cent
Carbonates	2 per cent	Feldspars	6 per cent
Heavy minerals	1 per cent	Heavy minerals	2 per cent

Average Accessory Heavy Minerals

Mica	63 per cent
Opagues	21 per cent
Non-Opagues	16 per cent

<u>Micas</u>	<u>Opagues</u>	<u>Non-Opagues</u>	
Biotite-chlorite	Hematite	Hornblende	59 per cent
Muscovite	Limonite	Epidote	21 per cent
	Ilmenite	Zircon	9 per cent
	Magnetite	Garnet	8 per cent
		Tourmaline	1 per cent
		Others	2 per cent

X-ray diffraction methods indicate that montmorillonite (+ vermiculite) is a moderate to strong component of the clay fraction. Small amounts of illite and slight amounts of kaolinite are also present in the loess.

B. Partial Chemical Analysis

In the Vicksburg loess, hydrochloric acid treatment revealed an average carbonate content of 30.5 per cent by weight. The organic matter, determined by hydrogen peroxide treatment, averaged 0.5 per cent by weight. Based on an average clay content of 9.0 per cent, determined by sedimentation and hydrometer analyses, the remaining mineral grains average 60.0 per cent by weight. The same analytical method for Pre-Vicksburg loess revealed 3.8 per cent carbonates, 1.9 per cent organic, 17.9 per cent clay, and 76.4 per cent other mineral grains.

C. Grain Shape

Grain shape analyses are usually based on concepts of sphericity and roundness. Sphericity is concerned with the degree of conformity of the shape of the particle to that of a sphere. Roundness is concerned with the sharpness of the corners irrespective of sphericity. A perfectly spherical grain would have a roundness and sphericity of 1.0.

Several equations have been advanced to calculate sphericity and roundness values; however, a visual estimation for this study was considered adequate. Therefore, based on a chart for visual estimation prepared by Krumbein and Sloss (1955), the sphericity of Vicksburg and Pre-Vicksburg loess ranges from 0.6 to 0.8. From the same chart, roundness averages 0.3-0.4. Based on a similar chart by Powers (1953), grain shape of both materials is considered subangular with some angular and subrounded particles. An average width to length axial ratio of grains is approximately 1:1.6 which does indicate some degree of elongation. The shape of grains is illustrated in a photomicrograph of a thin section (Figure 4) and of a grain mount (Figure 5).

D. Grain Size Distribution

1. General

Numerous methods are used in practice to determine

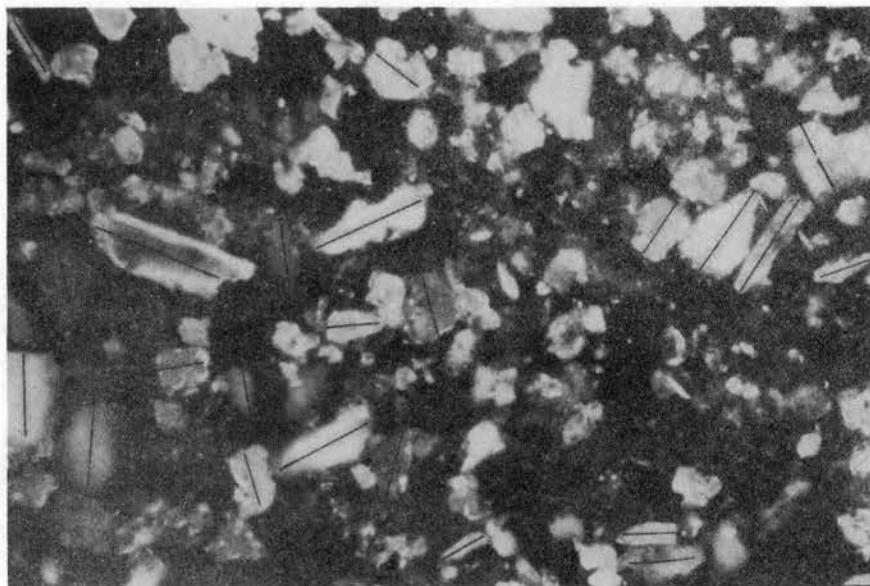


Figure 4. Thin Section Photomicrograph of Vicksburg Loess; Crossed Nicols; 80x

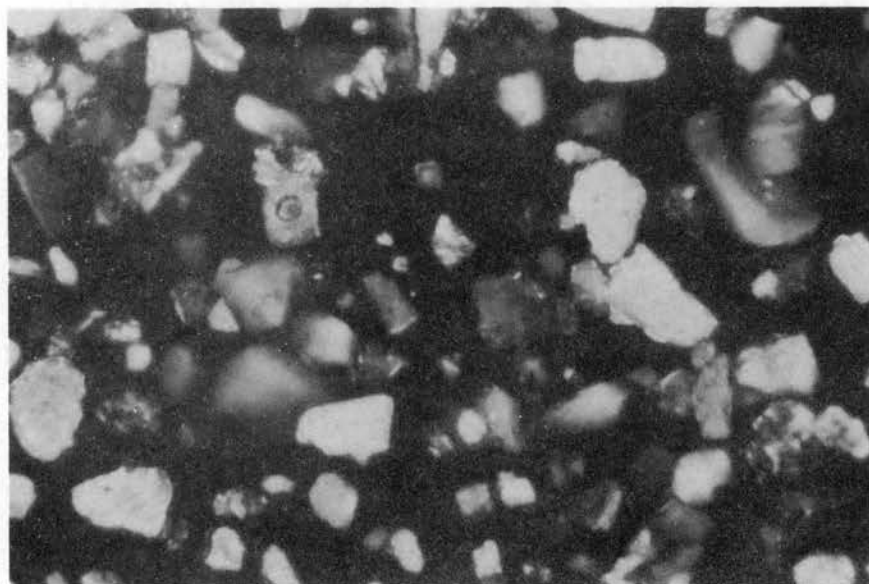


Figure 5. Grain Mount Photomicrograph of Vicksburg Loess; Crossed Nicols; 80x

grain-size distribution of soils which include sieving and direct measuring of particles. Other methods are based on Stokes' law. Likewise, numerous descriptive measures obtained from these grain-size analyses are used to indicate salient features of the soil. These measures range from those obtained by more complex statistical computation of the grain-size distribution of a sample to those obtained by graphically selecting points on a cumulative distribution curve. Aside from utilizing grain-size distribution studies for classification purposes and genetic interpretation, the statistical parameters derived from these studies may be useful in engineering problems of frost action, seepage, and of moisture movement in different phases.

Grain-size distributions for Vicksburg and Pre-Vicksburg loess were obtained from independent analyses by hydrometer, dry sieve, thin section, and grain mount methods. The descriptive parameters of the distribution were based on a graphical solution outlined in subsequent sections.

2. Statistical Parameters

Although diameter of grains can be measured in several units, a millimeter has been found a convenient unit of measure for most fine-grained soils. In many mechanical analyses, the data are further assembled in classes according to a scale in which each succeeding grade is one-half

as large as its predecessor. In addition, it has been found that grain-size distribution curves become more symmetrical when the logarithm of the diameter instead of the diameter is plotted as the independent variable. As such, these curves usually approach log-normal distributions which lend themselves to a more convenient statistical analysis.

The phi (Φ) scale (Krumbein, 1934) is the standard grade scale used in geology for size analysis. It is derived from the equation:

$$d = 2^{-\Phi}$$

where d = diameter of the particle in millimeters
and, Φ = a value along the phi scale.

Then,

$$\Phi = -\log_2 d.$$

In the phi notation, therefore, values of 0, 1, 2, 3, 4, etc., correspond to particle diameters in millimeters of 1, $1/2$, $1/4$, $1/8$, $1/16$, etc., respectively. A conversion chart for phi and diameters in millimeters is available (Inman, 1952).

In a normal frequency distribution curve, 68.27 per cent of the population occurs between plus and minus one standard deviation to either side of the mean, (or median since both are equal for normal distributions) and 95.45 per cent occurs between two standard deviations either

side of the mean. Therefore, the 16th and 84th percentiles of a normal grain size cumulative curve represents one standard deviation either side of the mean. Similarly, the 2.5 and 97.5 percentiles represent diameters two standard deviations either side of the mean. From cumulative curves of numerous analyses of sediments, the Φ_{16} and the Φ_{84} were found to provide a sufficiently accurate measure of standard deviation, and the Φ_5 and Φ_{95} a working approximation of two standard deviations.

Other descriptive parameters such as skewness and kurtosis were derived from further statistical considerations of frequency distribution curves of soils and sediments. The equations which define these parameters were derived independently by Inman (1952) and Folk and Ward (1957). These equations are provided in Table II. A graphical illustration of some of the descriptive parameters for a typical grain size distribution is presented in Figure 6.

Treatment of grain-size data depends on the information required. One method in practice for treating grain-size distributions utilizes central tendency, degree of sorting, skewness, and kurtosis for describing the distribution curves. Central tendency is an assessment of both a mean and median diameter. The degree of sorting defines the standard deviation of a distribution. The measure of skewness describes the deviation of the distribution curve from the symmetry of the normal. Skewness

TABLE II
DEFINITIONS OF GRAIN-SIZE DISTRIBUTION
STATISTICAL PARAMETERS

IDENTIFICATION	MEASURE	NOMENCLATURE	DEFINITION
INMAN (1952)	CENTRAL TENDENCY	PHI MEDIAN DIAMETER	$Md_{\phi} = \phi_{50}$
		PHI MEAN DIAMETER	$M_{\phi} = \frac{1}{2} (\phi_{16} + \phi_{84})$
	DISPERSION (SORTING)	PHI DEVIATION MEASURE	$\sigma_{\phi} = \frac{1}{2} (\phi_{84} - \phi_{16})$
	SKEWNESS	PHI SKEWNESS MEASURE	$\alpha_{\phi} = \frac{M_{\phi} - Md_{\phi}}{\sigma_{\phi}}$
		2nd PHI SKEWNESS MEASURE	$\alpha_{2\phi} = \frac{\frac{1}{2}(\phi_5 + \phi_{95}) - Md_{\phi}}{\sigma_{\phi}}$
KURTOSIS (PEAKEDNESS)	PHI KURTOSIS MEASURE	$\beta_{\phi} = \frac{\frac{1}{2}(\phi_{95} - \phi_5) - \sigma_{\phi}}{\sigma_{\phi}}$	
FOLK AND WARD (1957)	MEAN		$M_z = \frac{1}{3} (\phi_{16} + \phi_{50} + \phi_{84})$
	SORTING, STANDARD DEVIATION		$\sigma_{\phi} = \frac{1}{4} (\phi_{84} - \phi_{16}) + \frac{1}{6.6} (\phi_{95} - \phi_5)$
	SKEWNESS		$Sk_i = \frac{\phi_{16} - \phi_{84} - 2\phi_{50}}{2(\phi_{84} - \phi_{16})} + \frac{\phi_5 + \phi_{95} - 2\phi_{50}}{2(\phi_{95} - \phi_5)}$
	KURTOSIS		$Kg = \frac{(\phi_{95} - \phi_5)}{2.44 (\phi_{75} - \phi_5)}$

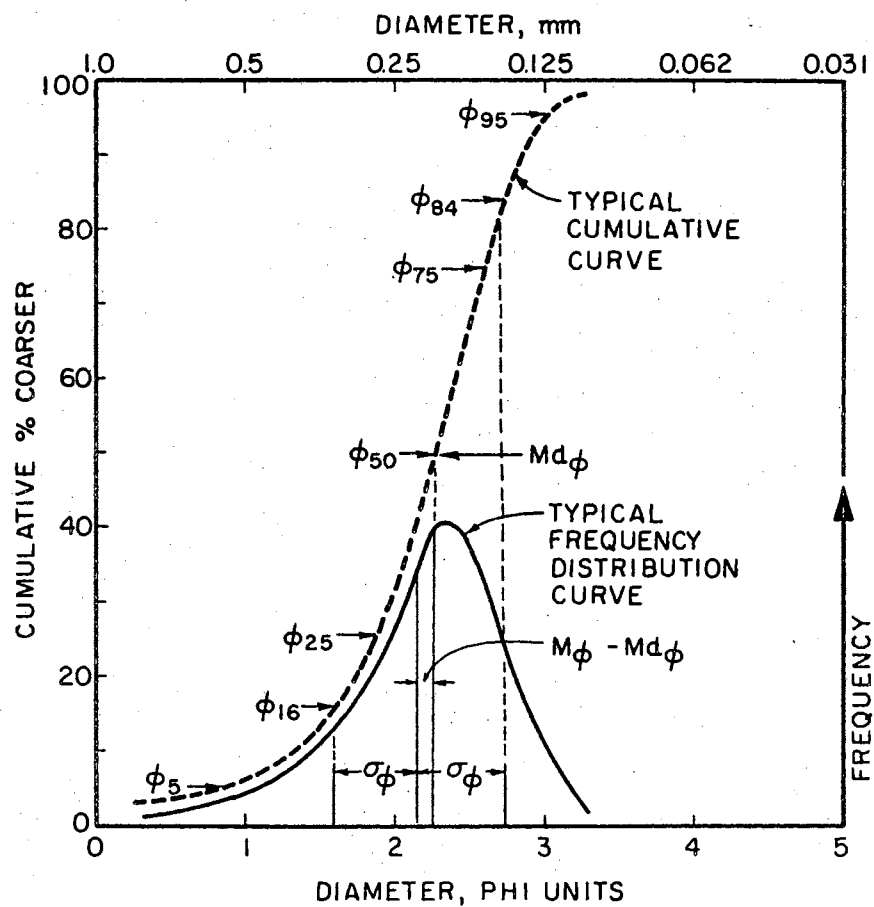


Figure 6. Graphical Representation of Statistical Parameters for Grain-Size Distribution Analysis

varies from -1.00 to +1.00, so that a value of 0.00 is a perfectly symmetrical distribution. Kurtosis is a measure of the degree of peakedness of a distribution. From Inman's (1952) equations, a kurtosis measure for a normal curve is 0.65; such that values less than 0.65 indicate more peaked than normal, and more than 0.65 less peaked. From Folk and Ward's (1957) equation, a kurtosis value of 1.00 represents a normal curve; larger values indicate excessive peakedness, smaller values indicate excessive flatness.

3. Procedure

Grain-size distributions for Vicksburg and Pre-Vicksburg loess were determined by the 151H hydrometer method in accordance with ASTM(D422-63). Distributions for both materials were also obtained by dry sieving after removing particles finer than 5μ by sedimentation and decantation. The amount of material finer than 5μ was oven dried and weighed and subsequently included in the calculation of the distribution curves.

Direct determination of grain sizes were performed by measuring long axes of particles on thin sections. The apparent long diameter of grains was measured directly from 8" x 10" enlargements of photomicrographs. A mechanical stage with a counting device described by Chayes (1949, 1956) was used to make regular traverses across the thin section. Fields of view for photographing were

selected systematically over approximately 75 per cent of the available area to minimize bias in sampling. All of the particles showing a definite outline were measured. An average of 80 grains was measured in each photomicrograph and a total of over 1500 grains was included for each material. Friedman (1957), studying several sandstones, suggested that sieve-sizes can be established from thin section data if long axes of about 500 particles are measured.

Direct measurements of short axes of particles were made from 8" x 10" photomicrograph enlargements of grain mountings for both Vicksburg and Pre-Vicksburg loess. After particles finer than 5μ were removed by sedimentation and decantation, a small representative portion of the remaining grains was spread on a gelatin base prepared on a clean glass slide. With the aid of a formalin and acetone solution, a single layer of grains was mounted prior to taking the photomicrographs. Rapid procedures for mounting mineral grains are available (Fairbairn, 1943; Nayudu, 1962), and the procedure found efficient for this study is detailed in Appendix A. The definite outline of discrete mineral grains on mountings is illustrated in Figure 5.

4. Descriptive Measures

The cumulative frequency or "ogive" curves of grain-size distribution are presented in Figures 7 and 8.

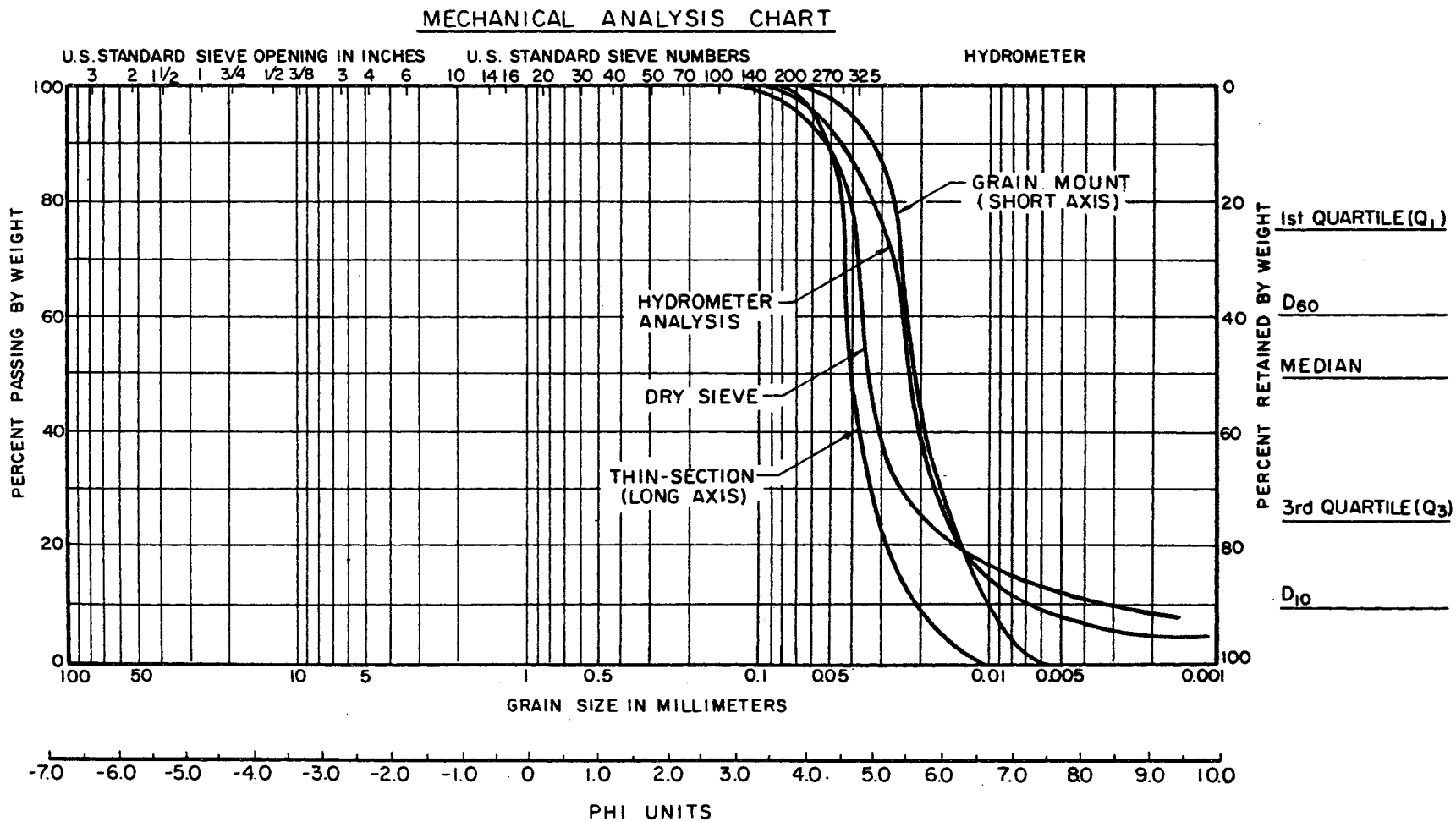


Figure 7. Cumulative Grain-Size Distribution Curves for Vicksburg Loess

MECHANICAL ANALYSIS CHART

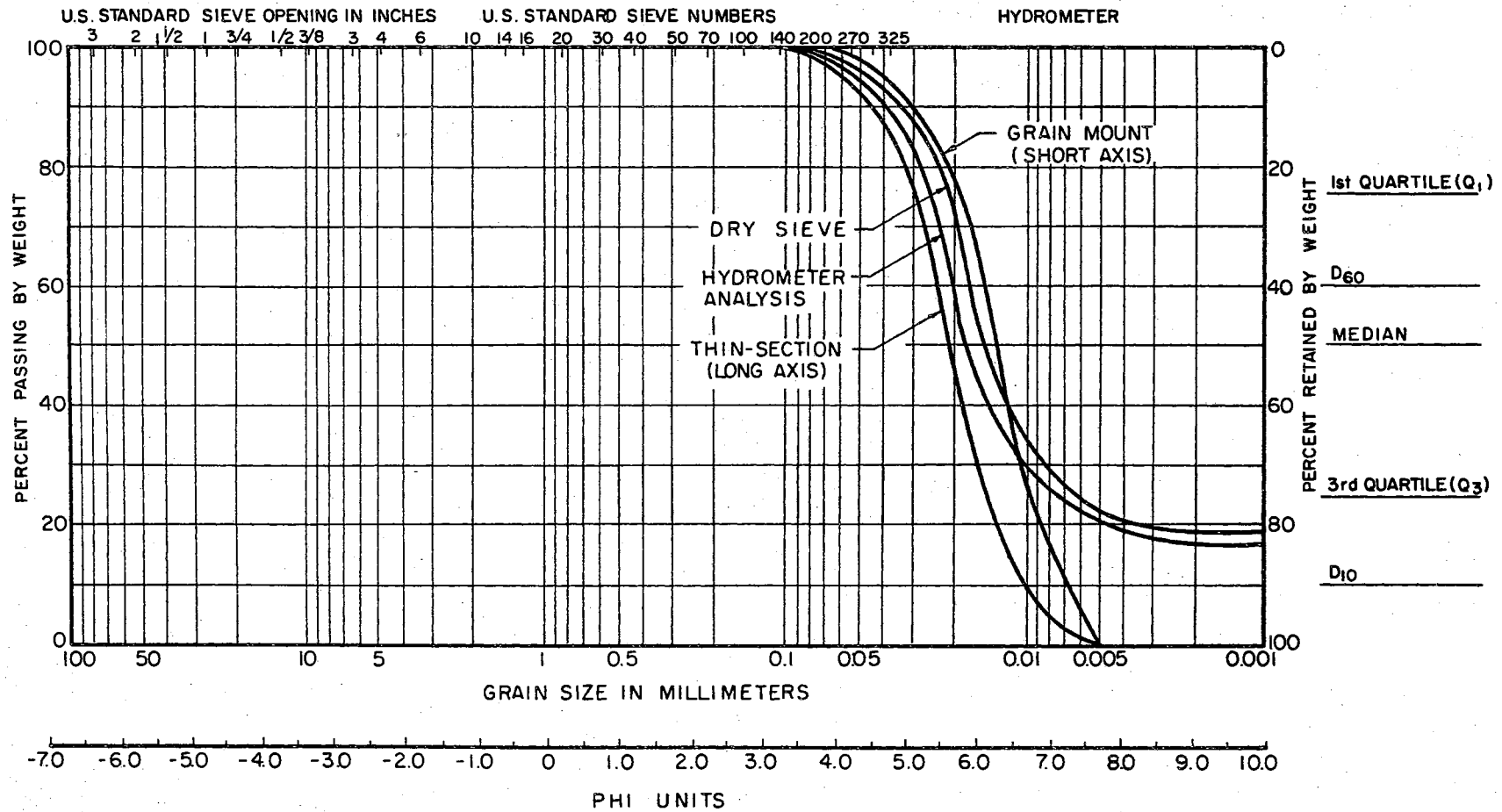


Figure 8. Cumulative Grain-Size Distribution Curves for Pre-Vicksburg Loess

Within the silt size range, the hydrometer and dry sieve analyses generally fall within the trend established by thin section and grain mount distributions. In the finer particle range, however, the differences between the two groups of curves are more pronounced. This difference is expected, however, because particles finer than 5μ could not be measured in thin section and had been removed in the grain mountings.

To facilitate curve fitting, interpolation, and visual interpretation of the data above, the cumulative "ogive" curves were plotted on arithmetic probability paper (Figures 9 and 10). Use of this paper results in a straight line plot for a normal distribution. It is apparent that for both materials, the thin section and grain mount distribution follow a straight line better than hydrometer and sieving analyses. Furthermore, in the latter case, the deviation from a straight line is more pronounced in the finer grain-size range.

In any event, from the above plots, Φ_5 , Φ_{16} , Φ_{25} , Φ_{50} , Φ_{75} , Φ_{84} , and Φ_{95} values were obtained for statistical evaluation. In some cases, because Φ_{84} and Φ_{95} values were undefined as a result of the open-ended nature of the cumulative curves, certain parameters could not be calculated. Inman's and Folk and Ward's statistical parameters, Hazen's uniformity coefficient, and Trask's sorting coefficient were calculated (Table III).

An examination of the statistical parameters (Table

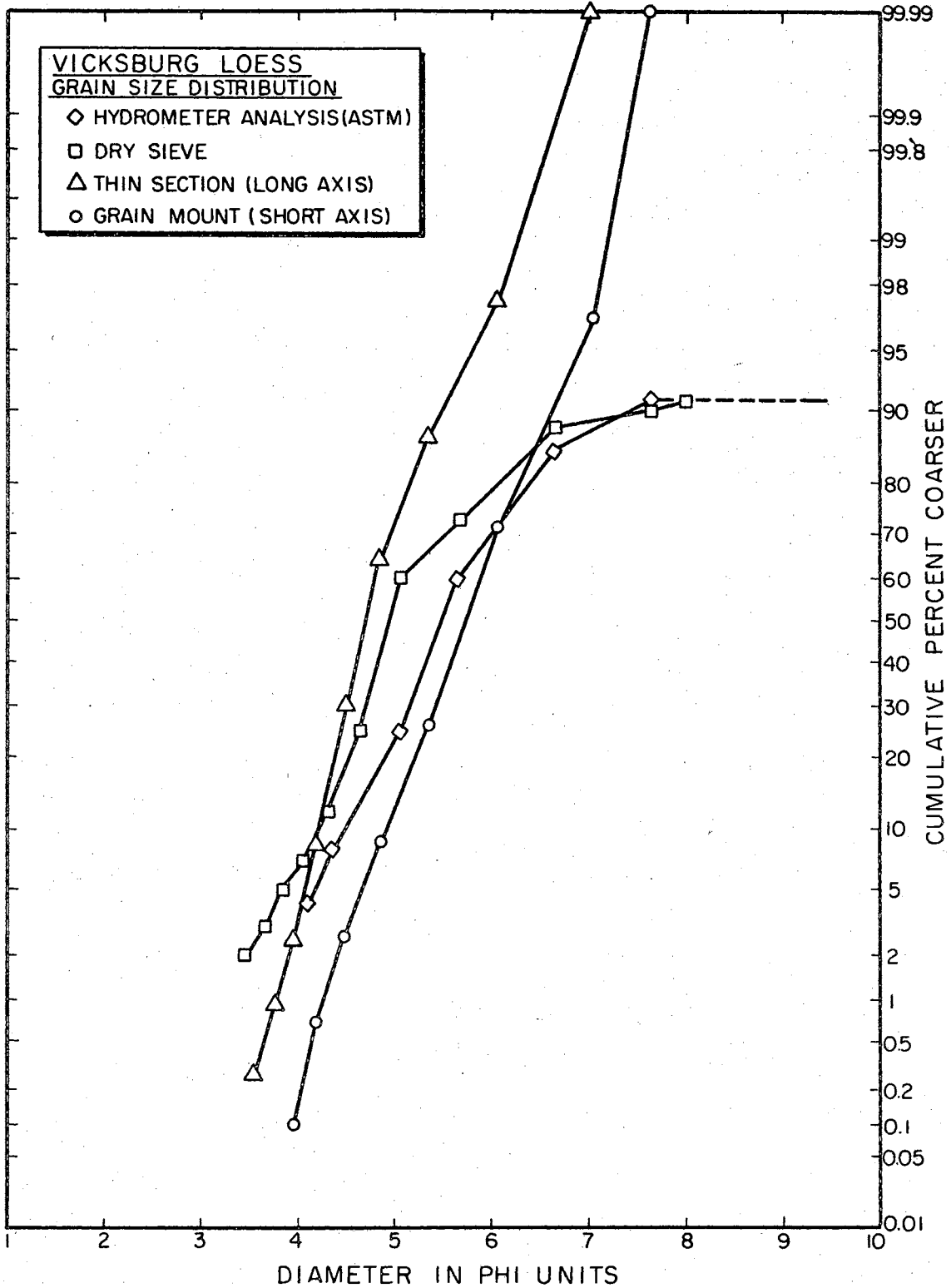


Figure 9. Cumulative Grain-Size Distribution Curves for Vicksburg Loess on Probability Paper

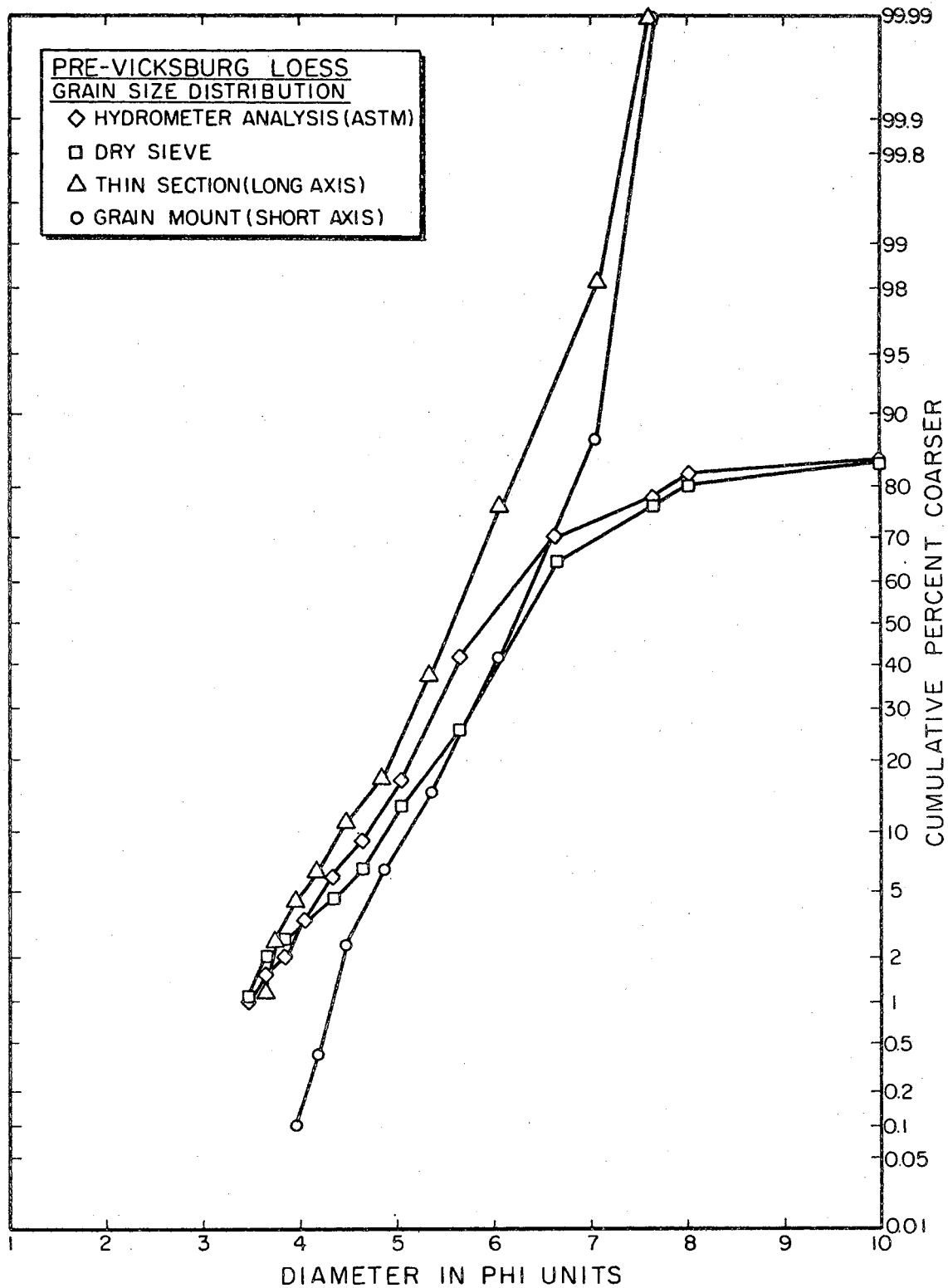


Figure 10. Cumulative Grain-Size Distribution Curves for Pre-Vicksburg Loess on Probability Paper

TABLE III
SUMMARY OF GRAIN-SIZE DISTRIBUTION
STATISTICAL PARAMETERS

$\phi = -\log_2 d$ (mm)	VICKSBURG LOESS				PRE-VICKSBURG LOESS			
	HYDROMETER ANALYSIS	DRY SIEVE	THIN SECTION	GRAIN MOUNT	HYDROMETER ANALYSIS	DRY SIEVE	THIN SECTION	GRAIN MOUNT
ϕ_5	4.20	3.85	4.05	4.65	4.25	4.40	4.05	4.75
ϕ_{16}	4.75	4.45	4.30	5.10	5.05	5.25	4.75	5.40
ϕ_{25}	5.05	4.65	4.45	5.30	5.30	5.65	5.05	5.70
ϕ_{50}	5.50	4.95	4.70	5.75	5.90	6.30	5.55	6.25
ϕ_{75}	6.20	5.80	5.05	6.20	7.25	7.50	6.05	6.75
ϕ_{84}	6.60	6.35	5.25	6.40	*	*	6.25	6.95
ϕ_{95}	*	*	5.80	6.90	*	*	6.75	7.20
TRASK Sorting Coefficient, S_0 (Trask 1932)								
$\sqrt{Q_1/Q_3}$	1.31	1.51	1.22	1.29	1.88	1.82	1.41	1.38
(Q 's in mm units)	[1.2 < S_0 < 1.4, well sorted; 1.4 < S_0 < 2.0, moderately sorted]							
INMAN'S Graphical Parameters (Based on Phi units)								
Median, $M_d\phi$	5.50	4.95	4.70	5.75	5.90	6.30	5.55	6.25
Mean, M_ϕ	5.68	5.40	4.78	5.78	*	*	5.50	6.18
Sorting, σ_ϕ	0.93	0.95	0.48	0.65	*	*	0.75	0.78
Skewness, α_ϕ	0.19	0.47	0.17	0.00	*	*	-0.07	-0.04
2nd Skewness, $\alpha_{2\phi}$	*	*	0.48	0.04	*	*	-0.20	-0.33
Kurtosis, β_ϕ	*	*	0.83	0.72	*	*	0.80	0.58
FOLK AND WARD Graphical Parameters (Based on Phi units)								
Mean, M_z	5.62	5.25	4.75	5.75	*	*	5.52	6.20
Sorting, σ_ϕ	*	*	0.51	0.67	*	*	0.79	0.73
Skewness, S_{ki}	*	*	0.21	0.01	*	*	-0.09	-0.16
Kurtosis, K_g	*	*	1.19	1.03	*	*	1.11	0.96
D_{60} (% Finer)	.025	.035	.040	.023	.020	.015	.025	.015
D_{10} (% Finer)	.006	.0035	.006	.005	*	*	.010	.0065
HAZEN'S Uniformity Coefficient								
D_{60}/D_{10}	4.16	10.0	6.67	4.60	*	*	2.50	2.32
(D 's in mm units)	[If < 2, soil considered uniform]							

*Undefined values (open-ended cumulative curves)

III) reveals that values for each descriptive measure vary slightly, depending on the method of grain-size analysis. This is also expected, however, because the direct measurements are of skeletal grains (framework); whereas, hydrometer and dry sieve include the clay fraction which forms the matrix of the loess fabric.

5. Regression Equations

In the direct measurement of particle sizes, the observed random grain diameters are not a direct reflection of hydrometer or sieve-size distributions. Sizes measured directly lead to frequency-by-number data; whereas, weight per cent is used as a scale in size analysis by sieving or using methods based on Stokes' Law. Although measured particle sizes may be exactly comparable to sieve openings, for example, large variations in specific gravity of particles tend to reduce agreement between weight and frequency distribution curves. An example is given in Appendix B. Nevertheless, a correlation between frequency and weight analyses can be established from regression equations. Because the difference between the dry sieve and hydrometer distributions is for practical purposes insignificant, an arithmetic average of the two is considered a representative distribution by weight per cent. Therefore, a correlation was developed between weight and thin section distributions, and weight and grain mount distributions based on phi units. The phi

values are obtained graphically from Figures 9 and 10, and two least squares regression lines are calculated and presented in Figure 11. Calculation and tabulation of this data are presented in Appendix C.

Based on phi units for grain sizes, the linear relationship between frequency and weight distribution is apparent. The regression equation for converting thin section distributions to sieve size, in phi units, is as follows:

$$\phi_w = -1.247 + 1.350 \phi_{T.S.}$$

where $\phi_{T.S.}$ = grain diameter of the distribution in phi units based on long axis measurement in thin section;

and ϕ_w = calculated grain diameter in phi units for a weight-per cent distribution.

Similarly, the regression equation for converting grain mount grain-size distributions to sieve size, in phi units, is as follows:

$$\phi_w = -2.390 + 1.365 \phi_{G.M.}$$

where $\phi_{G.M.}$ = grain diameter of the distribution, in phi units, based on short axis measurements in grain mounts;

and ϕ_w = calculated grain diameter in phi

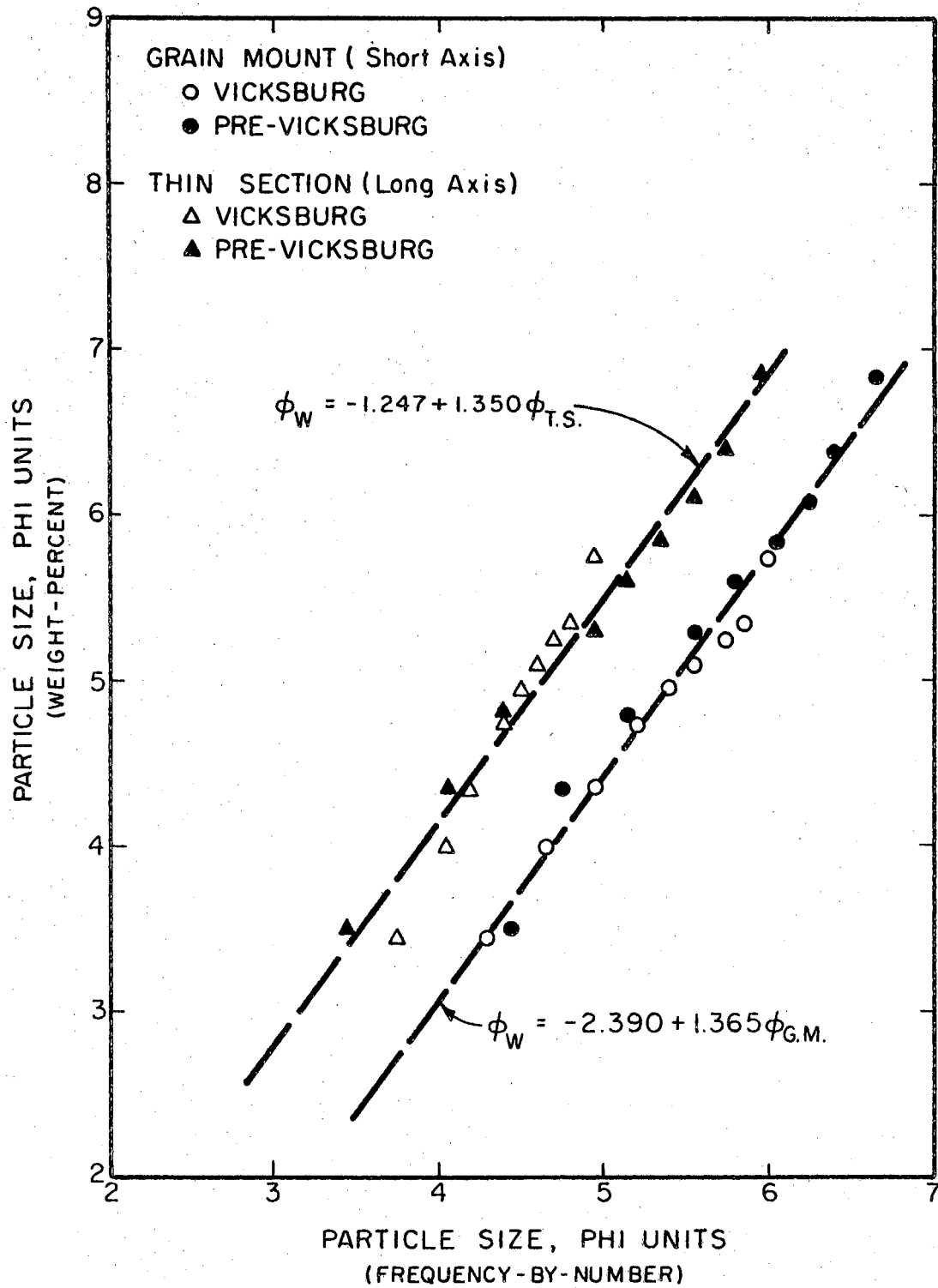


Figure 11. Regression Lines for Grain-Size Distribution Analysis

units for a weight-per cent distribution.

The regression coefficients are similar for both equations (1.350 and 1.365) and they indicate that the relationship between grain mount and thin section analyses in the loess studied can be considered a constant. Although measurement of long axes in thin section has been established statistically and empirically to provide more adequate correlation with sieve analyses, suitability of measurement of long axes in grain mounts instead of short axes requires further investigation.

6. Discussion

Geologists for many years have attempted to use grain-size parameters as environmental indicators. Although there are conflicting views on the environmental sensitivity of the textural parameters discussed above, correlations of sorting and variations in average grain size with depth have been useful in distinguishing beach and river sand.

Aside from the noted variation in the median and mean diameters (Table III), Trask's sorting coefficient, Hazen's uniformity coefficient, and the other sorting parameters generally consider both Vicksburg and Pre-Vicksburg loess moderately sorted. The Vicksburg loess reflects a slightly positive skewness toward the larger grain sizes; whereas, the Pre-Vicksburg loess values

indicate a slightly negative skewness toward finer grain sizes. This trend reflects the greater weathering and particle disaggregation which is characteristic of Pre-Vicksburg loess. The conflicting kurtosis values do not lend themselves to any conclusions. Kurtosis, according to Inman's equation, indicates less peakedness and according to Folk and Ward's equations, excessive peakedness. These results support the belief by many investigators that kurtosis is not a significant parameter of grain-size distributions.

Although a study of these parameters individually does not appear significant, valuable information which assists in the interpretation of origin and aids in the study of transportational and depositional processes can be derived by comparing the same parameters of similar materials. Furthermore, studies involving examination of degree of change in various statistical parameters as a result of mechanical manipulation, chemical treatment, or weathering could provide information of significance to soils engineers.

A further consideration in this study involves dividing the grain-size distribution of the loess into two populations. Spencer (1963) hypothesized that clastic sediments are essentially mixtures of three or less fundamental populations (gravel, sand, clay), and that the sorting in these sediments can only be recognized by the degree of truncation of the original fundamental

populations. His hypothesis would suggest a dissection of the grain-size distribution of loess into two modes (silt and clay, perhaps), and treatment of each independently. Although an analysis of this type is beyond the scope of this thesis, there is, nevertheless, belief that such considerations might be significant in origin and permeability studies of loess.

Finally, for engineering purposes, both frequency-by-number and weight per cent distributions are of significance in analysis and design problems of primarily coarser grained soils. This may be particularly significant where the grain size range is relatively large and the distribution well sorted because the variation between the two methods is greatest. In this situation, it is thought that a frequency-by-number distribution may be more reliable for establishing permeability characteristics because the actual number of grains filling void spaces is perhaps a better measuring device than the weight of the grains. A soil type which has larger amounts of heavier minerals of a uniform size should also be analyzed by direct measurement of grain sizes wherever possible.

E. Physical Properties

Some of the basic physical properties, excluding strength, of Vicksburg and Pre-Vicksburg loess are summarized in Table IV.

TABLE IV
SOME PHYSICAL PROPERTIES OF LOESS

	Vicksburg	Pre-Vicksburg
1. Specific Gravity, G_s	2.71	2.70
2. Dry Density, γ_d , (pcf) (average, volumetric measurement, water and mercury displacement)	93.5	95.5
3. Void Ratio, e , (based on average dry density)	0.81	0.77
4. Porosity, n , (based on void ratio), (per cent)	44.7	43.5
5. Standard Proctor Density (miniature test) (pcf)	101.2	102.5
6. Optimum Moisture Content (per cent)	16.0	17.5
7. Plasticity		
a. Liquid Limit (LL)	26.5	32.5
b. Plastic Limit (PL)	24.5	20.6
c. Plasticity Index (PI)	2.0	11.9
8. Lineal Shrinkage Texas Bar Method, (per cent)	1.32	5.25
9. Vertical Permeability, k , (undisturbed, using fall- ing head of kerosene) (cm/sec.)	8×10^{-4}	1.5×10^{-4}

F. Fabric Elements and Cementation

The Vicksburg loess is an eolian sediment composed of uniformly sorted silt grains of quartz, feldspars, carbonate, and minor amounts of other minerals all arranged in an open fabric and cemented primarily by a clay matrix. Carbonate minerals also participate, to some extent, in cementing the silt particles. However, their effect in developing cohesion is considered only supplementary to the clay bond. Although other eolian deposits of cohesionless silts, fine sands, and clay mixtures are capable of forming loess, it is not considered loess until the characteristic cohesion of the clay bond is developed. It is also recognized that some of the clay in loess is secondary and that cementation by the clay bond can also develop with weathering.

The photomicrograph of a thin section of Vicksburg loess (Figure 4) clearly displays the spatial distribution of skeletal grains which appear to "float" in a clay matrix. Under high magnification and crossed nicols, the effect of oriented clay particles is also noticed around the skeletal grains. Their appearance is in the form of "jackets" or "husks" and has been observed by other investigators. Apparent also in Figure 4 are the intrapedal voids which occur within the clay matrix and which are responsible for the high porosity of the material. This obvious open structure and unique cementation, therefore, distinguishes loess from other silt deposits.

There has been some discussion pertaining to the origin of the calcite in loess of the lower Mississippi Valley. It is generally agreed that root tubes, incrustations, and concretions are secondary calcite (Figure 12). Leighton and Willman (1950) postulated that the other occurrences of carbonate in loess are primary because of: (1) the presence of discrete grains, (2) their uniform distribution, (3) decreasing amounts of carbonate with distance from the bluffs, and (4) the presence of dolomite grains. Krinitzsky and Turnbull (1967), however, emphasize the predominance of the secondary state of the calcite in Vicksburg loess although both primary and secondary are present (Figure 13). Primary carbonate is in the form of single discrete grains of calcite and secondary carbonate occurs as recrystallized cement in pores or voids and as a coating rim around supposed root tubules.



Figure 12. Snail Shells and Calcareous Root Tubules and Concretions in Vicksburg Loess; Scale in Inches

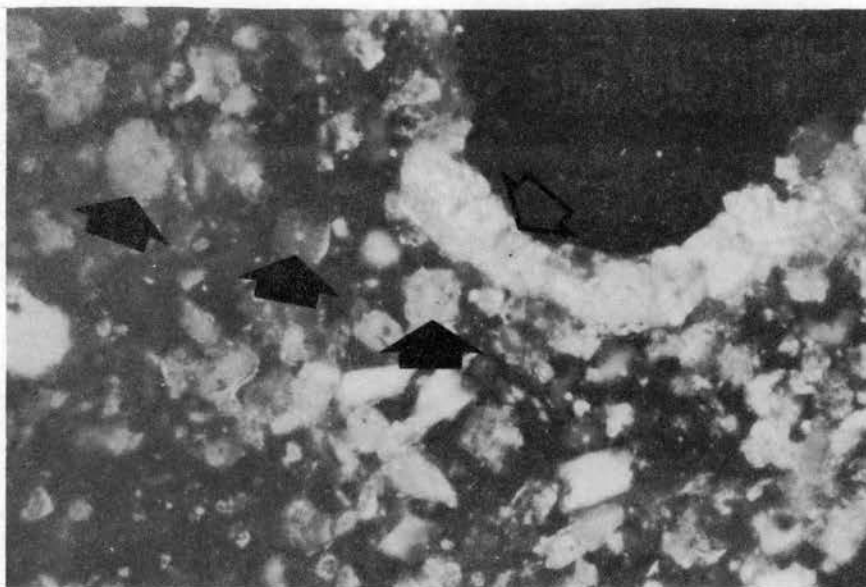


Figure 13. Thin Section Photomicrograph of Vicksburg Loess Illustrating Discrete Calcite Grains (shaded arrows) and Secondary Calcite Rim of a Root Tubule (unshaded arrow), Crossed Nichols; 80x

CHAPTER IV

GRAIN ORIENTATION

A. Introduction

Numerous fabric studies have been based on direct measurement of the apparent long axes of detrital grains seen in thin sections. Griffiths and Rosenfeld (1953), Curray (1956a), and Rusnak (1957) have made their measurements along traverses under the microscope or measured grain orientation from a reference line on a screen of a projected thin section. Dapples and Rominger (1945), Potter and Mast (1963), and Lafeber (1966) have measured grain orientation from a reference line marked on photomicrographs. Selection of grains for measurement in thin sections has been made along linear traverses, by point count techniques (Chayes, 1949, 1956), or in randomly selected fields of view. Some care and attention is required in determining the apparent long axes of mineral grains. Dapples and Rominger (1945) recognized three ways of measuring long axes of quartz grains: (1) the apparent longest dimension, (2) the least projection elongation, and (3) the center of area elongation. Potter and Pettijohn (1963, p. 42), however, regard these differences of measurement in practice as of minor importance because

little effect was found on the mean azimuth where over 100 grains were measured.

Many methods of studying fabric orientation indirectly have been advanced or suggested. Martinez (1958) developed an optical method utilizing a photometer. Arbogast and others (1960) devised a technique which utilizes the dielectric anisotropy in sediments to infer fabric direction. Nanz (1960) suggests the use of sonic, thermal, and dielectric anisotropy of materials to determine the alignment direction of quartz grains. Zimmerle and Bonham (1962) found that an electronic spot scanner which counts the number of grain-matrix contacts on a photographic film can establish the direction of preferred orientation of long axes. Mast and Potter (1963) noted that the maximum imbibition of water of a sandstone tends to be parallel to the average grain fabric. Orr (1964) developed a method for determining directional anisotropy of materials by detecting inductive conductivity anomalies within it. Rodriguez and Pirson (1968) recently used oriented and focused resistivities or conductivities recorded by a dipmeter well logging device to derive the dominant directions of sand grains.

The two methods used for this study are the visual grain measurements, and the dielectric anisotropy (DA) measurements. The visual analysis involves measuring grain orientation from a reference line on photomicrographs of thin sections. To minimize bias, fields of view

on the thin sections were selected on the basis of a systematic traversing of approximately 75 per cent of the total available area. Color photographs were used as it was found that a "sensitive tint" or "first order red" quartz plate under crossed nichols provided an excellent outline of mineral grains. In addition, some of those grains on photomicrographs were "highlighted" where ordinarily they would have been at the position of near extinction. An alternate method of photographic reproduction is described by Lafeber and Kurbanovic (1965) who use overlays of negatives and transparencies of the same image.

B. Preparation of Samples

Loess monoliths, approximately 18 inches cube of both Vicksburg and Pre-Vicksburg loess were cut from vertical exposures after marking with an appropriate azimuth. Specimens from these monolithic blocks were then oven dried in preparation for standard impregnation. One horizontal thin section was prepared from each of the three undisturbed blocks. After the preferred grain orientation was established, three vertical thin sections were prepared from the respective specimens in a direction parallel to the preferred grain orientation. These sections were analyzed for imbrication. The procedure for impregnating samples for thin sections is described in Appendix D.

From the same samples, specimens were obtained for

partial impregnation necessary for determining grain orientation by Shell Development Company's dielectric anisotropy (DA) instrument. Partial impregnation was performed in the laboratory in accordance with Shell's Eposand treatment which was slightly modified by Halliburton Company, a licensee for Shell's Eposand treatment. The treated loess samples were consolidated with only a slight reduction in porosity. These samples were then marked and plugs three-fourths inch in diameter and seven-eighths inch in height were cored with a standard diamond core bit. The plugs were then impregnated under vacuum with Dow Corning 550 fluid in preparation for DA measurements. Appendix E describes this procedure in further detail.

Several possible sources of error exist in the collection and preparation of samples for visual and dielectric grain orientation analyses. These are typical errors inherent in any assemblage of specimens for analyses of this type. Expected errors common to both visual and dielectric measurements are: (1) deviations of north arrow and other horizontal marks inscribed on blocks from true values, (2) variations caused by transferring markings from sample to specimen and from specimen to thin section or consolidated plugs. Some of the errors which exist in visual measurement of grains are: (1) misalignment of thin section markings with microscope, (2) misalignment of reference lines on photographic reproductions,

(3) improper selection of grain elongation and inaccuracy in measurement of orientation. Some errors which exist in dielectric measurements are: (1) improper selection of maximum capacitance peaks on chart recorder tracing, (2) inaccurate measurement of angle of rotation from reference mark to peak capacitance on the chart tracing. Cumulative error is estimated to be less than 10 degrees.

C. Grain Orientation Measurements

Visual grain orientation data were obtained by measuring the apparent longest axes of mineral grains. The apparent longest axes on the color prints were determined by visual selection of those grains showing definite elongation. Potter and Mast (1963) used a rule for choosing grains with an apparent longest axis which is based on a minimal axial ratio of 1:1.3. In this study, a larger axial ratio was used to visually select elongated grains. Figure 4 shows elongated grains selected for measurement on a typical photomicrograph. An adjustable transparent protractor and a drafting instrument were used to class each grain into eighteen 10-degree intervals.

The grain orientation frequencies were plotted on polar coordinate paper at the mid-point of each 10-degree interval, using a 30-degree "sliding" average. The diagrams of the actual grain count are shown in Figures 14-17 for both horizontal and vertical thin section observations. The total number of grains measured for each

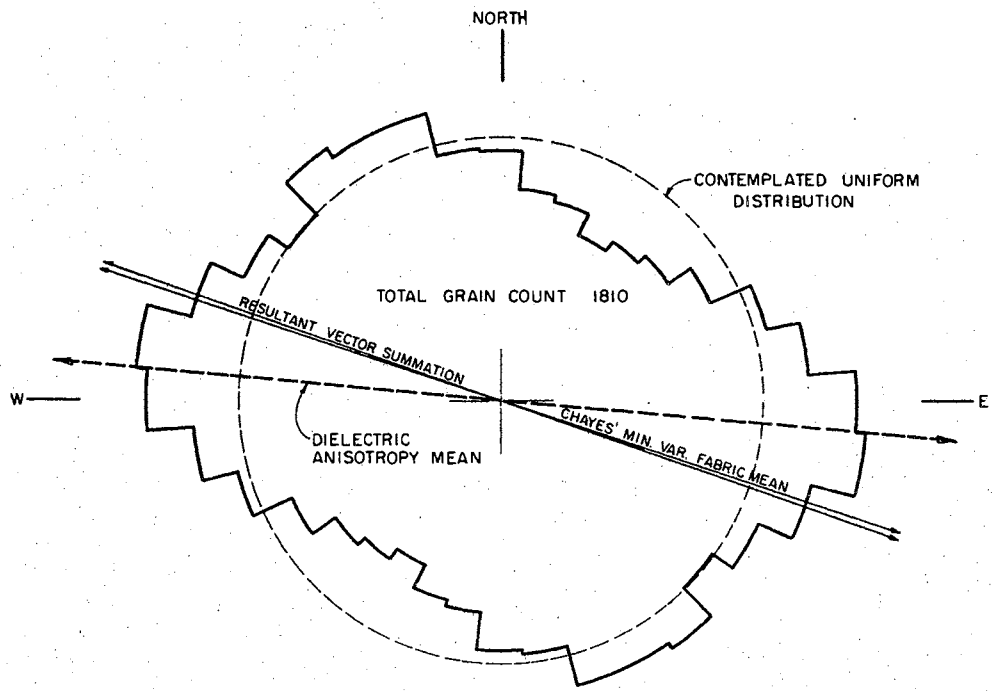


Figure 14. Grain Orientation in the Horizontal Plane of Vicksburg Loess

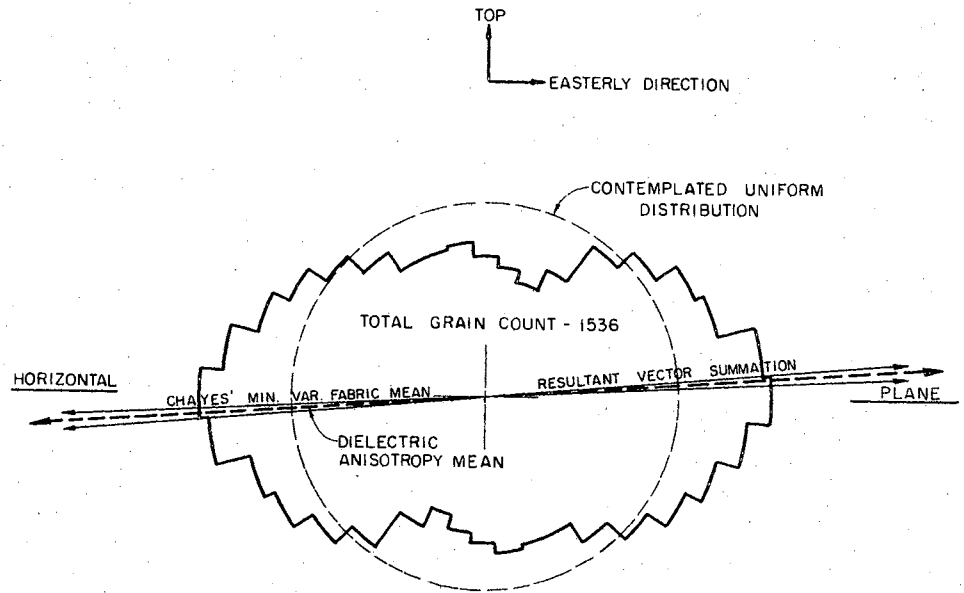


Figure 15. Grain Orientation in the Vertical Plane of Vicksburg Loess Parallel to the Horizontal Fabric Mean

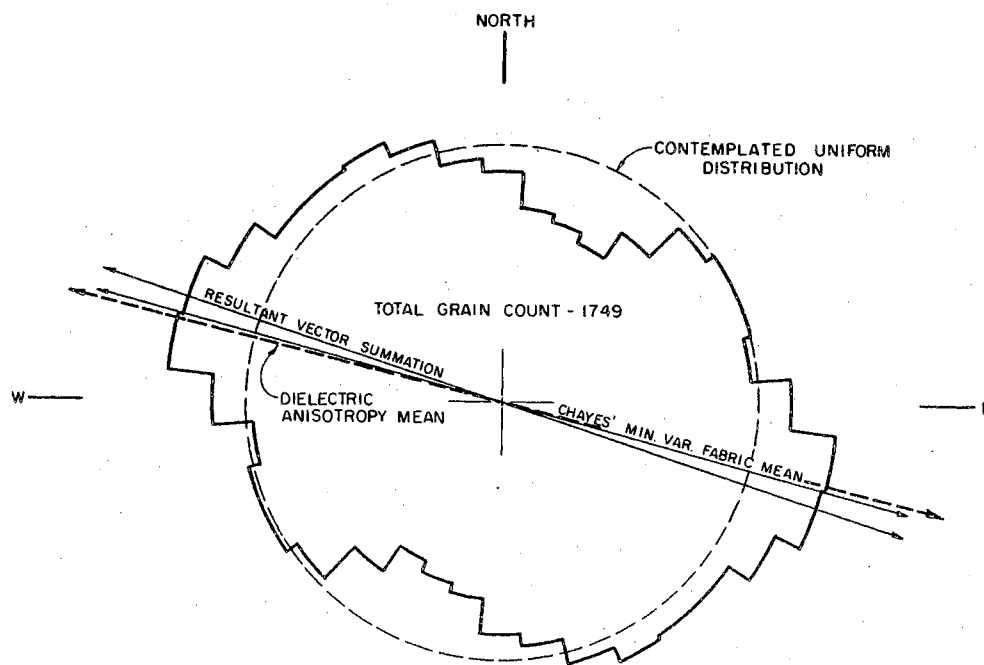


Figure 16. Grain Orientation in the Horizontal Plane of Pre-Vicksburg Loess

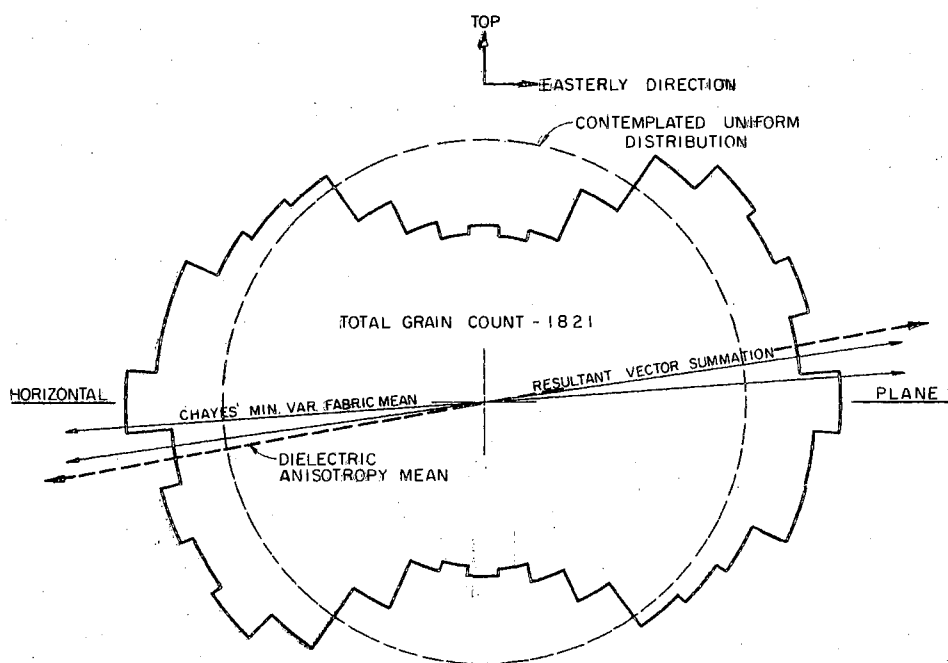


Figure 17. Grain Orientation in the Vertical Plane of Pre-Vicksburg Loess Parallel to the Horizontal Fabric Mean

plane and material is indicated, and the "contemplated" uniform distribution for each is plotted. The total grain count for Vicksburg loess includes primarily quartz grains with less than 10 per cent calcite grains. In both horizontal and vertical thin sections studied, it was found that primary calcite generally followed the same preferred orientation of the other detrital grains. No primary calcite was noticed in the Pre-Vicksburg loess.

DA measurements were made using the Shell Development Company's apparatus according to the procedure outlined by Arbogast et al. (1960) and Nanz (1960). The impregnated sample plugs were inserted as a rotatable part of the dielectric medium of a capacitance cell. During each revolution of the sample plug in the cell, two complete cycles of maximum capacitance are recorded as a sinusoidal trace on a chart recorder (Figure 18). A north-trending reference mark on each plug is aligned to correspond to the reference mark indicated on the upper trace. The maximum capacitance is considered the preferred grain orientation, the direction of which can be determined by measuring the angle of rotation from the reference mark to the first maximum value (Figure 18). Based on an average porosity of 48 per cent, and a particle size mean diameter of 0.021 mm., it is estimated that the device measures fabric maxima of approximately 30 million grains per plug.

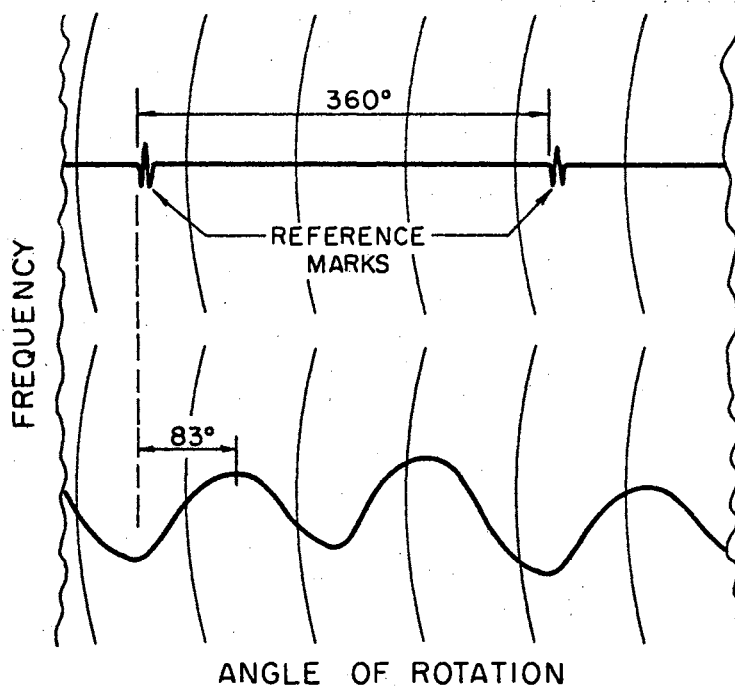


Figure 18. Typical Chart Tracing From a Dielectric Anisotropy Measurement of a Vicksburg Loess Plug; Showing Fabric Mean of N 83° W

D. Data Analysis Methods

Grain orientation data have become a more common tool in the study of sedimentologic processes and of directional properties of deposits. In particular, the long axes of particles in undeformed sediments have been used to establish directions of ancient and recent depositing currents. Statistical treatment of grain orientation data is also becoming increasingly important for interpreting the significance of patterns in sediment, soil, and rock fabrics.

Early analyses of orientational data applied radius-vector summation techniques to obtain resultant directions (Reiche, 1938; Krumbein, 1939). Later studies applied the linear normal distribution techniques to establish significance of preferred orientational directions (Chayes, 1949; Griffiths and Rosenfeld, 1953). Recognizing the effects imposed by the choice of origin for angular data treated by linear normal distribution techniques, Chayes (1954) proposed a minimum variance procedure which has been found adequate for several types of analyses (Griffiths, 1967, p. 144-163). Further excellent discussions on the development of statistical treatment for orientational data are presented elsewhere (Pincus, 1953; Curray, 1956b; Steinmetz, 1962; Jones, 1968).

The above references pertain to the most recent statistical analysis techniques which test orientational data against a circular normal distribution. Since these techniques are not sufficiently developed, no attempt has been

made to apply them to this study. Instead, the resultant vector summation method and Chayes' minimum variance technique were used for the data analysis. These methods, including IBM programs, are presented in Appendix F.

Applying the resultant vector summation method (Pincus, 1953; Curray, 1956b) to each set of grain orientation data, the azimuth of the resultant vector, θ , and the magnitude of the resultant vector in terms of per cent, L , were calculated using IBM 7040 computer (see Appendix F). Based on the number of observations (grain counts), n , and the vector magnitude, L , the Rayleigh test of significance was determined as outlined by Curray (1956b). In addition, based on the chi-square principle, the significance of the data was examined as proposed by Tukey in an unpublished communication in 1954, noted in Harrison (1957) and Rusnak (1957).

The same data were manipulated using Chayes' minimum variance technique as programmed for the IBM 1620 computer (Griffiths, 1967, p. 152). This program, converted to the IBM 7040, was used to calculate the mean, variance, standard deviation, and F-test. A review of the computer output is presented in Appendix F. Since the results of both methods discussed above for practical purposes are essentially identical, no attempt was made to evaluate them independently.

The fabric mean for azimuth and imbrication was determined from DA measurements for both Vicksburg and

Pre-Vicksburg loess using Chayes' minimum variance technique. The mean and standard deviation were calculated, and a level of significance was evaluated.

E. Discussion of Results

A visual examination of the rose diagrams readily discloses a definite degree of preferred orientation (Figures 14-17). Although regionally both materials may be considered the same, the difference in depths (30 feet versus 60-70 feet), difference in texture and composition, and the 3-mile separation between the two sites are sufficient reasons for treating the grain orientation of the two samples independently. In spite of this consideration, the similarity of horizontal grain orientation and imbrication between Vicksburg and Pre-Vicksburg loess is striking. The apparent bimodal distribution in both horizontal plots is another feature recognized. Explanation of the bimodal distribution requires further study. However, it is believed that an appropriate explanation for it involves some local variation in depositional wind direction caused by topography, turbulence, or other climatic factors.

The statistical treatment of visually determined grain orientation is tabulated in Table V. The resultant vector summation and Chayes' minimum variance techniques provide an azimuthal grain maxima range of 285-289 degrees (N 75° W-N 71° W) and imbrication of 3-8 degrees for both materials studied. The Rayleigh Test, Tukey Test, and

TABLE V
SUMMARY OF STATISTICAL PARAMETERS FOR GRAIN ORIENTATION

<u>VISUAL EXAMINATION OF THIN SECTIONS:</u>	VICKSBURG LOESS		PRE-VICKSBURG LOESS	
	NORTH AZIMUTH	IMBRICATION	NORTH AZIMUTH	IMBRICATION
Number of Thin-Sections	3	3	3	3
Total Grains Measured	1810	1536	1749	1821
Rose Diagram	Fig. 14	Fig. 15	Fig. 16	Fig. 17
Resultant Vector Summation				
a. Vector Direction, ($\bar{\theta}$)	289°	5°	288°	8°
b. Vector Magnitude, (L)	12.5%	17.9%	11.3%	16.9%
c. Rayleigh Test				
1. Significance	$<10^{-5}$	$<10^{-10}$	$<10^{-5}$	$<10^{-15}$
d. Tukey's Test				
1. Chi-square	56.8	88.4	44.8	104.9
2. Significance	$<.005$	$<.005$	$<.005$	$<.005$
Chayes' Minimum Variance				
a. Fabric Mean	288°	3°	285°	4°
b. Standard Deviation	48°	46°	48°	46°
c. Variance Ratio, F	1.17	1.26	1.17	1.27
d. Significance	$<.01$	$<.001$	$<.01$	$<.001$
<u>DIELECTRIC ANISOTROPY:</u>				
Number of Tests	16	15	8	4
Mean	275°	4°	284°	10°
Standard Deviation	20°	15°	27°	15°
Significance	$<.005$	$<.005$	$<.025$	$<.01$
Estimated Number of Grains Analyzed	5×10^8	4×10^8	3×10^8	2×10^8

Variance Ratio Test all reflect high significance against uniform distribution in both azimuth and imbrication. Imbrication analyses, however, indicate significance at much higher levels. Over 500 grains were measured from each of three thin sections, and the fabric means were compared independently for each plane and each material. There was no significant variation between respective thin sections. Consequently, only the treatment of total grain counts is presented.

The statistical treatment of DA measurements is also tabulated in Table V. The mean of all tests range from 275-284 degrees (N 85° W-N 76° W) for azimuthal grain maxima and 4-10 degrees for imbrication for both materials studied. The standard deviations fall well within the range considered excellent. The Pre-Vicksburg loess plugs were more difficult to impregnate because of the larger amount of clay material, and as a result, dielectric measurements for this material are not considered as reliable. Nevertheless, the fabric means determined by the DA instrument coincide reasonably well with visual grain orientation data (Figures 14-17).

The small difference in azimuthal preferred grain orientation between the visual and DA measurements is not completely understood (Figure 14). By comparison, this difference is less in imbrication (Figure 15). However, it seems reasonable to attribute the larger difference between visual and DA measurements for the horizontal plane

to the bimodal distribution of the visual grain count. The DA measurements result in establishing only the sum total aggregate effect of the several million grains in each plug and any actual bimodal distribution would not be identified. Nevertheless, because the larger number of grains measured by the DA instrument results in higher statistical accuracy, measurements by it can be considered more reliable for establishing preferred grain orientation.

The 285 degree average azimuth (N 75° W) of all orientational data presented coincides reasonably well with the 290 degree azimuth (N 70° W) ascertained for paleowind direction from changes in thickness (Chapter II, section 4). An average imbrication of six degrees is considered low. However, it is suspected that the low value is a result of post-depositional consolidation of the fabric grains by overburden pressures.

CHAPTER V

INFLUENCE OF GRAIN ORIENTATION ON DIRECT SHEAR STRENGTH

A. Introduction

The direct shear test performed in the traditional "shear box" has been replaced to a great extent in most soil mechanics laboratories by other shear testing devices such as triaxial and vane shear devices. Its disadvantages, such as lack of drainage control, inability of pore pressure measurement, and development of stress concentrations at the rear face of shear box, are among some of its well-known shortcomings. Nonetheless, the conventional direct shear test still has a following and its application to testing certain directional strength properties of some soils is still noteworthy.

The direct shear test has been found helpful in measuring the effect of certain anisotropies in soil microstructure. Morgenstern and Tchalenko (1967) are among the most recent investigators to use the direct shear device in microstructural studies of oriented clay. Although no significant variation was found in the directional shear strength of a consolidated kaolin slurry, the sequential failure pattern and the development of shear structures

were examined and interpreted successfully by using thin sections of direct shear specimens.

Since the examination of the microstructure of Vicksburg loess discussed in the previous chapter revealed a preferred grain orientation in both horizontal and vertical planes, the direct shear device was considered an effective tool for measuring directional strength properties. Because the direct shear test controls the plane of stress, undisturbed loess samples were trimmed to the shear box so that the shear stress would develop along selected planes. The resulting variations in shear strength were then correlated with particle orientation.

This chapter involves an examination of the effect of grain orientation and grain imbrication on shear strength of dry and moist undisturbed loess samples. The study concentrated on direct shear tests of the Vicksburg loess. The variation in strength parameters were analyzed statistically as well as graphically, and the characteristics and development of the failure plane profiles were examined and illustrated by thin sections and photomicrographs. The failure surfaces were also studied, and certain noted features were related to known displacement directions of the sheared specimens.

B. Procedure

Dry, undisturbed blocks of Vicksburg loess were cut into two-inch cube specimens with a standard diamond

blade saw. Cuts were made along predetermined markings established by preferred grain orientation and imbrication. The two-inch cubes were appropriately identified and trimmed to one-inch thickness for placing in the shear box. Additional dry specimens were marked, cut, and subsequently carefully sprayed with water until 16 per cent moisture was reached. These were wrapped to retain the moisture until tested.

Figure 19 illustrates the orientation of cut specimens and the shear directions are noted. Specimen V(EW) was sheared in a vertical plane and displaced parallel to preferred grain orientation. Specimen V(NS) was also sheared in a vertical plane, however, displaced perpendicular to preferred grain orientation. The effect of imbrication on shear strength was tested by shearing specimen H(EW) in a horizontal plane and displacing it parallel to imbrication which was practically horizontal. Specimen V(V) was sheared vertically and displaced perpendicular to imbrication or the bedding plane.

Four replicates of each specimen described were sheared in a direct shear box designed and fabricated locally for use on a strain controlled vertical loading machine (Figure 20). Constant normal loads of 8 kilograms for specimens with 16 per cent moisture, and 12 kilograms for dry specimens were applied by the pulley arrangement shown, and the shear force and displacements were recorded from appropriately positioned dial gauges. Necessary

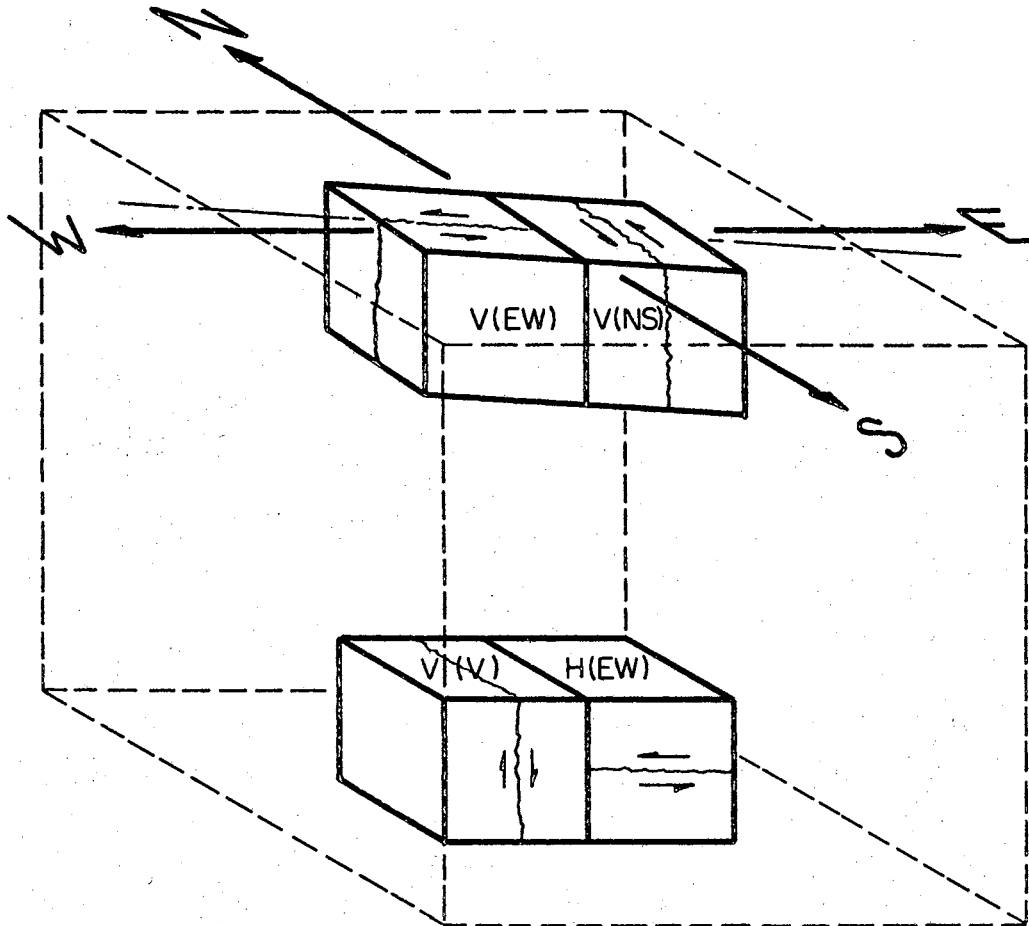


Figure 19. Orientation of the Shear Planes in Undisturbed Vicksburg Loess Specimens Used for Direct Shear Tests

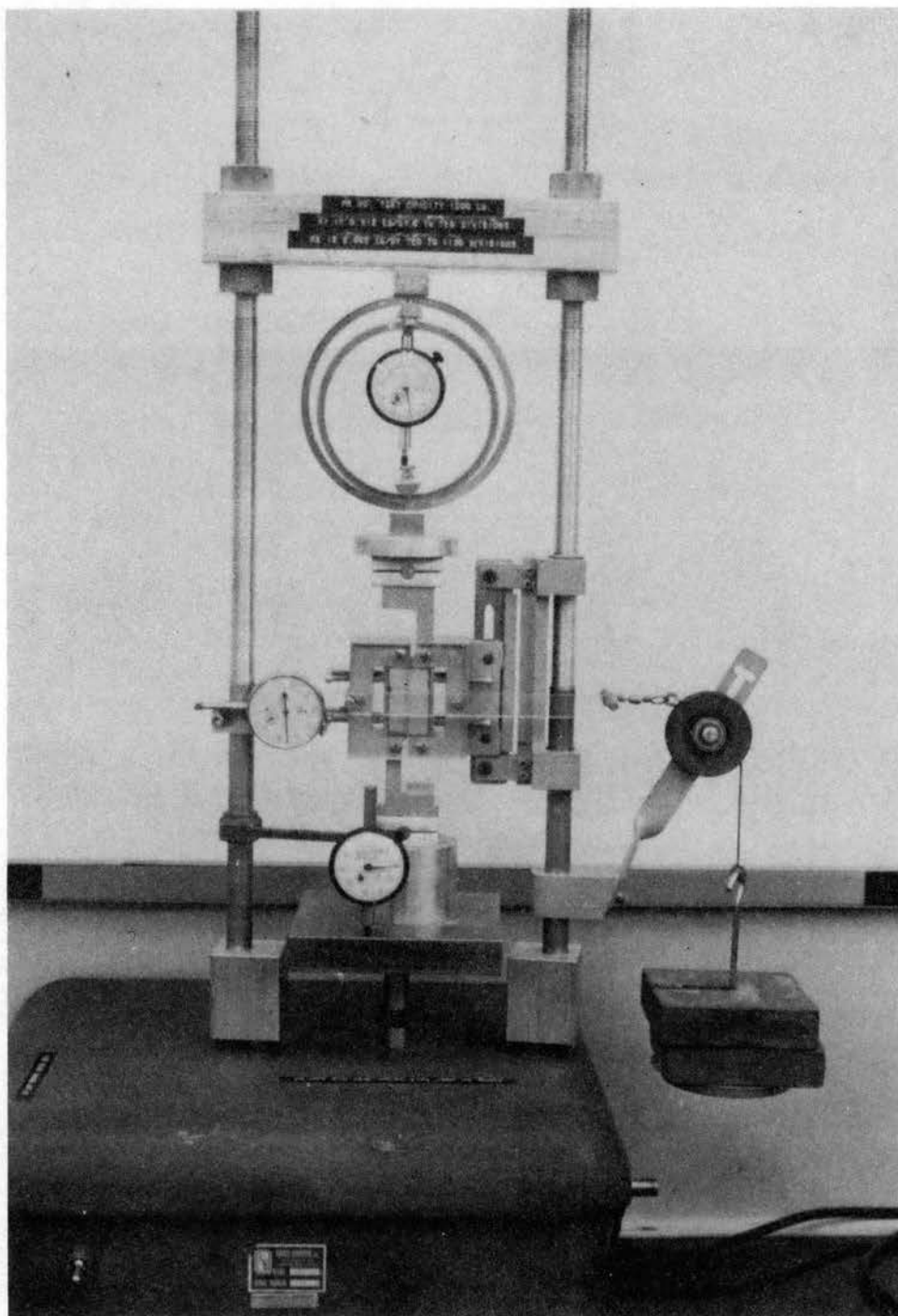


Figure 20. Direct Shear Device Mounted on Vertical Strain Controlled Loading Machine

corrections were made to account for a portion of the dead weight of the shear box and base plate. A displacement rate of 0.004 inches per minute was maintained throughout all testing. All additional procedures were in accordance with standard practice for both dry and moist specimens.

Specimens were loaded beyond failure until a constant residual stress was reached. Several failed specimens were carefully removed from the shear box intact and oven dried. These were subsequently impregnated with plastic epoxy for preparation of thin sections. After stress-strain behavior was established, two series of four separate shear tests were again conducted to examine the development of the failure plane parallel and perpendicular to imbrication. These tests were terminated at: (a) the mid-point of the quasi-elastic range, (b) the peak strength, (c) the end of unstable yielding, and (d) the end of residual strength. These were carefully removed from the shear box, oven dried, and impregnated for thin section examination.

C. Shear Strength Results

The results of the direct shear tests are graphically presented in Figures 21-24 for dry specimens and for those with 16 per cent moisture. Figures 21 and 22 illustrate variations in shear strength for specimens loaded parallel and perpendicular to imbrication, and Figures 23 and 24 illustrate shear strength variations for specimens loaded parallel and perpendicular to preferred grain orientation.

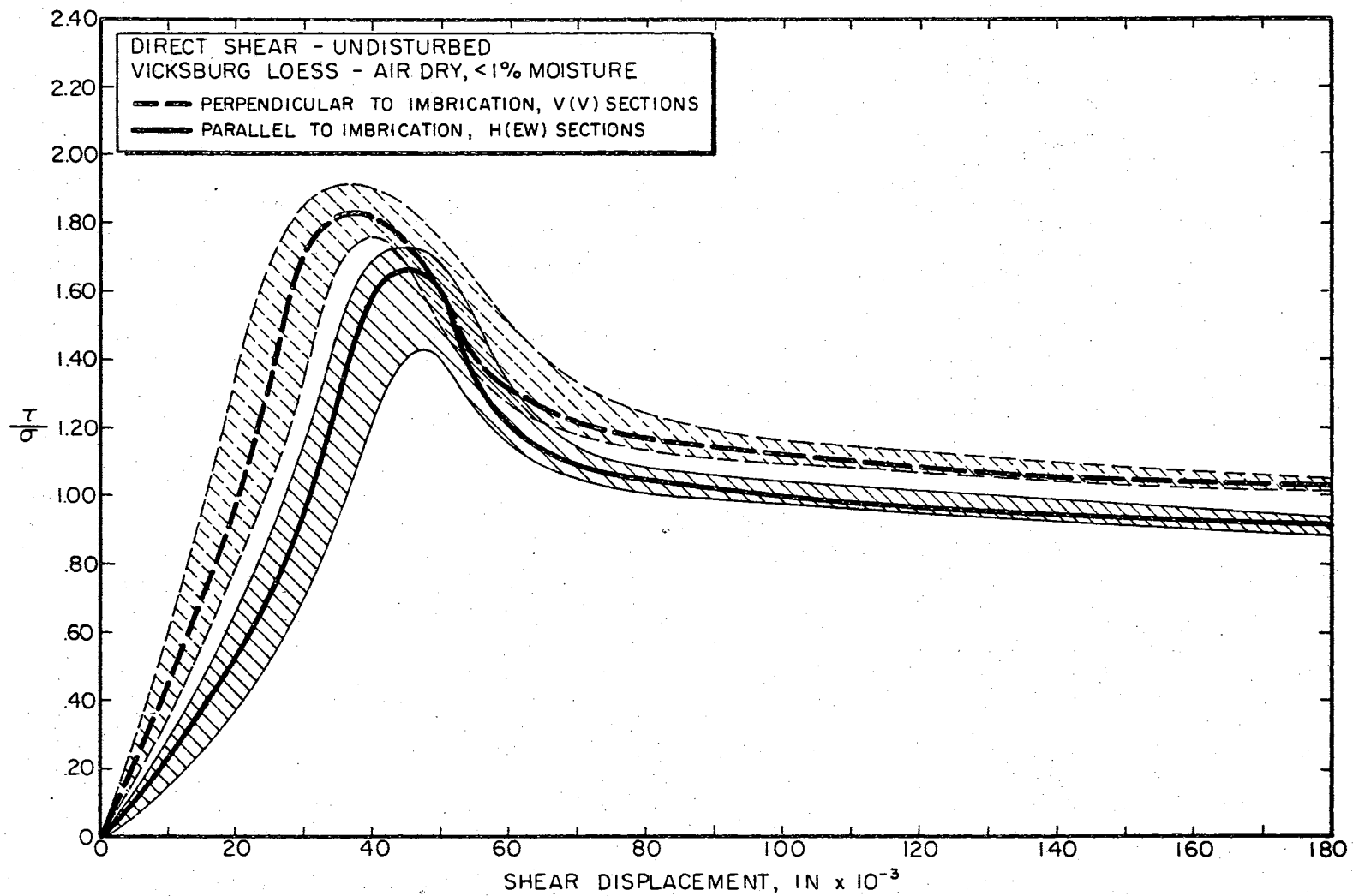


Figure 21. Effect of Imbrication on Direct Shear Tests of Dry Specimens

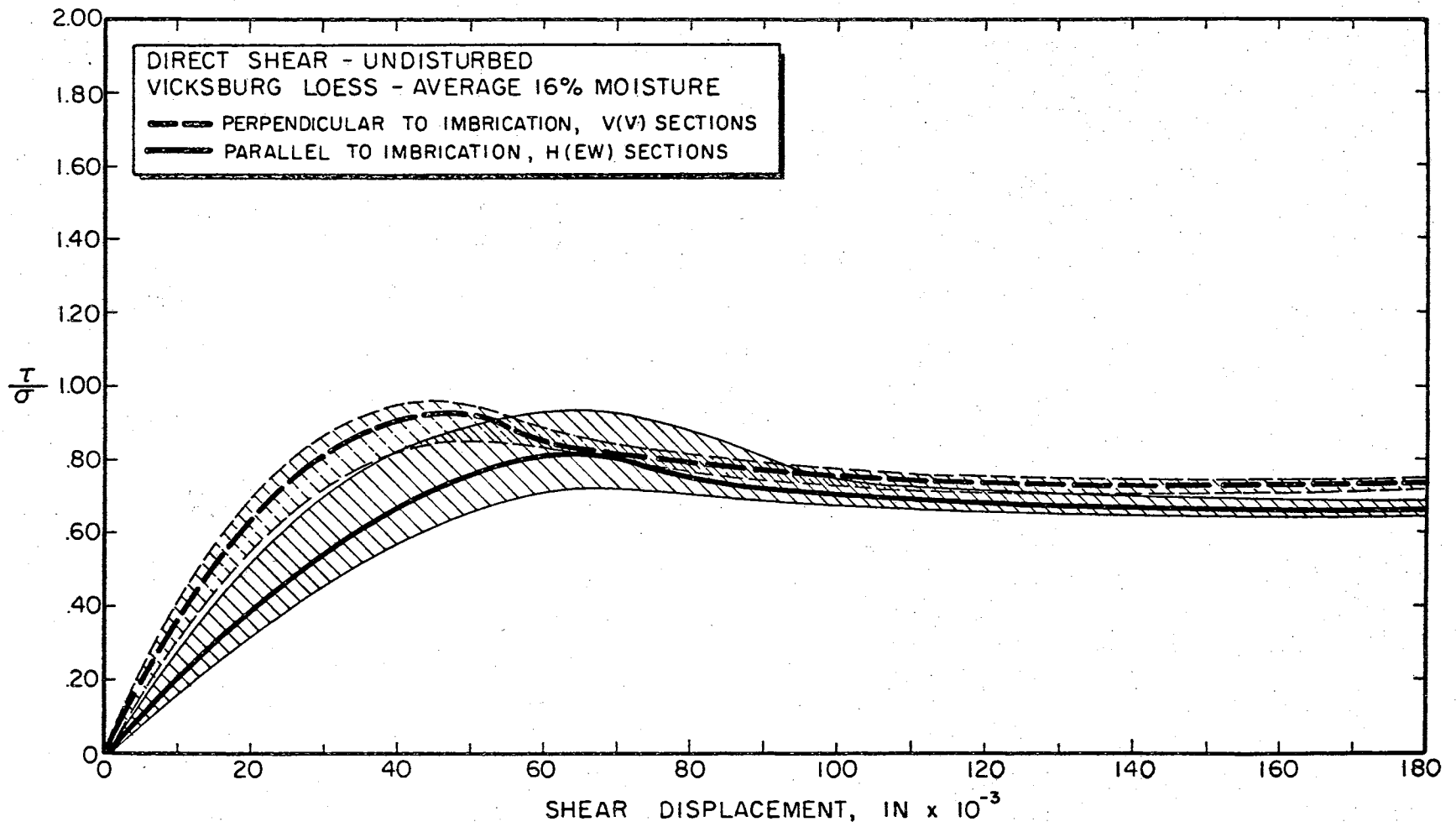


Figure 22. Effect of Imbrication on Direct Shear Tests of Moist Specimens

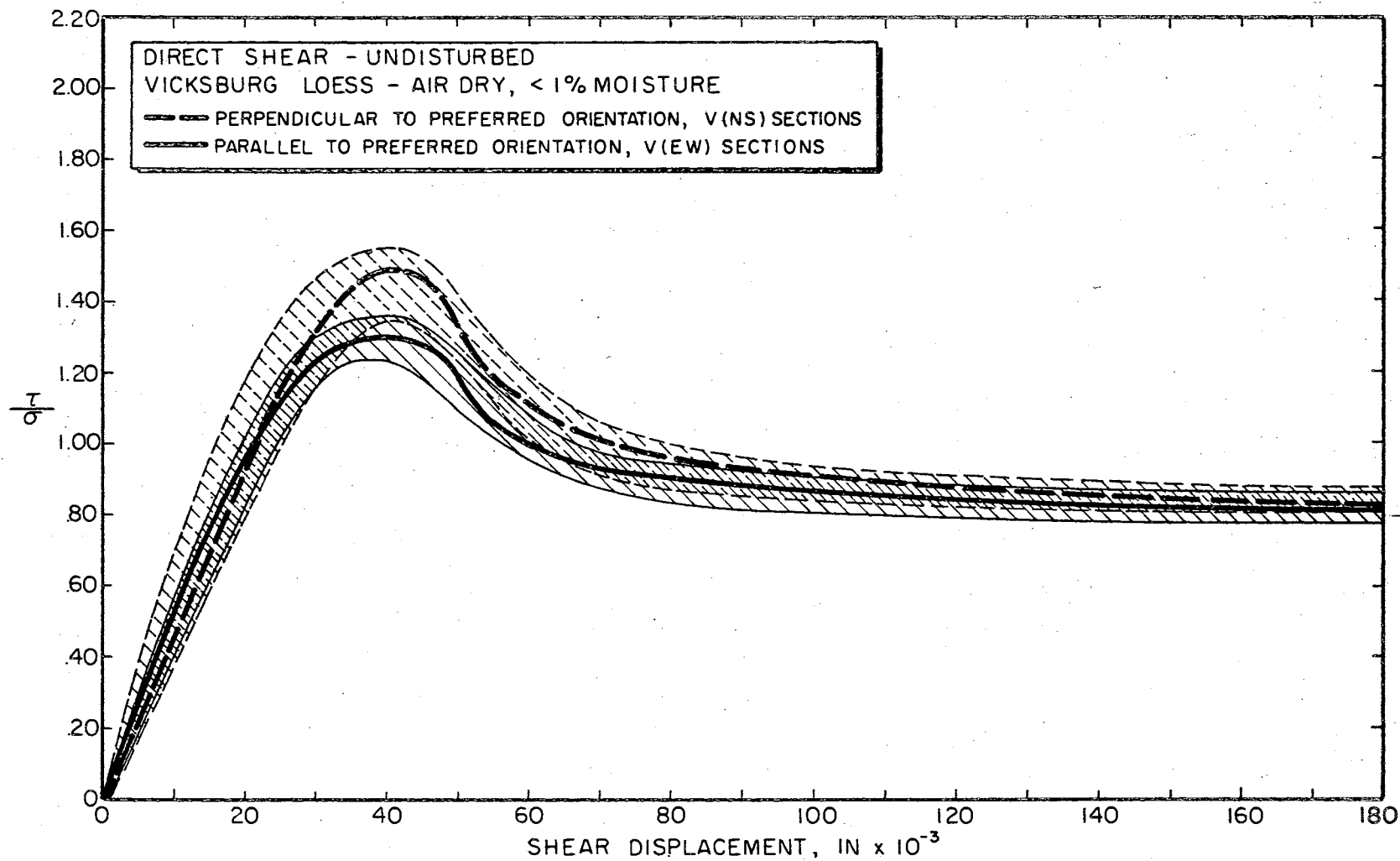


Figure 23. Effect of Preferred Grain Orientation on Direct Shear Tests of Dry Specimens

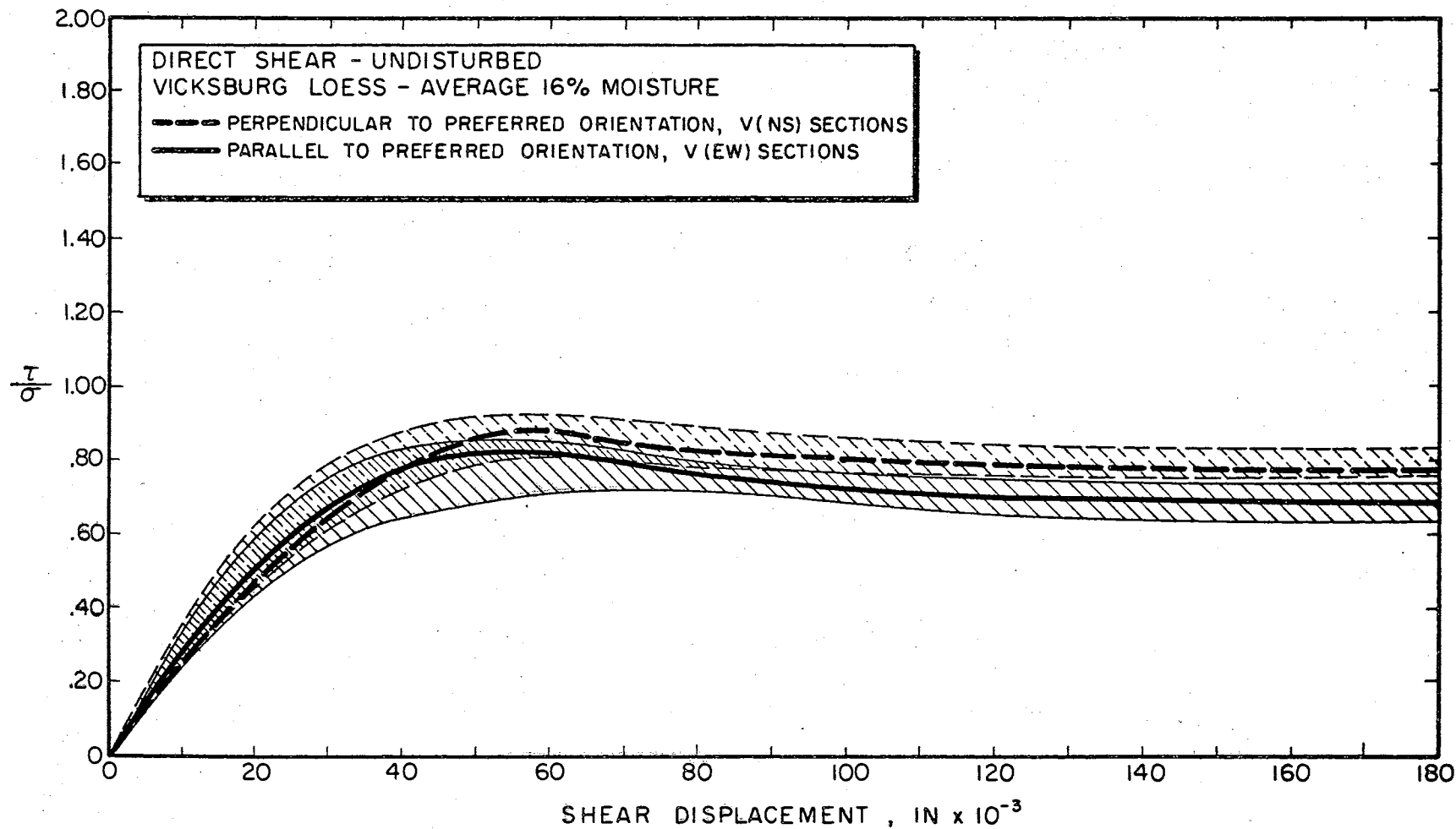


Figure 24. Effect of Preferred Grain Orientation on Direct Shear Tests of Moist Specimens

The heavy solid and broken lines represent the arithmetic average values of four specimens each stressed in the same orientation. The shaded region above and below each heavy line indicates the spread of values obtained from the four tests. The normal displacements resulting from the direct shear stresses were not included because no variation of any significance was observed. Normal displacements for dry specimens irrespective of stress orientation increased to an average of approximately 0.004 inches at peak strength and continued to increase at a reduced rate to an average ultimate value of 0.007 inches. Specimens at 16 per cent moisture followed a similar trend; however, normal displacements were slightly reduced to 0.002 inches and 0.005 inches, respectively.

The results of the direct shear test on Vicksburg loess are summarized in Table VI. Peak and residual shear strengths and shear displacements at peak and ultimate are indicated for both dry specimens and those with 16 per cent moisture.

D. Analysis of Data

Although graphically a difference in shear strength was noted between specimens loaded parallel and perpendicular to grain orientation, a statistical analysis of the data was considered necessary to evaluate the significance of this variation. As such, a taped IBM 7040 computer program prepared by Oklahoma State University Statistics

TABLE VI
SUMMARY OF DIRECT SHEAR TESTS

NORMAL STRESS, $\sigma = 6.6$ PSI AIR DRY, <1% MOISTURE	PARALLEL TO GRAIN ORIENTATION	PERPENDICULAR TO GRAIN ORIENTATION	PARALLEL TO IMBRICATION	PERPENDICULAR TO IMBRICATION
PEAK SHEAR STRENGTH (PSI)	8.65	9.85	10.95	12.05
SHEAR DISPLACEMENT AT PEAK (Inches)	.040	.042	.045	.037
RESIDUAL SHEAR STRENGTH (PSI)	5.35	5.55	6.05	6.80
SHEAR DISPLACEMENT AT RESIDUAL (Inches)	.180	.180	.180	.180
NORMAL STRESS, $\sigma = 4.4$ PSI AVERAGE 16% MOISTURE				
PEAK SHEAR STRENGTH (PSI)	3.65	3.90	3.65	4.10
SHEAR DISPLACEMENT AT PEAK (Inches)	.051	.058	.065	.046
RESIDUAL SHEAR STRENGTH (PSI)	3.05	3.45	2.90	3.25
SHEAR DISPLACEMENT AT RESIDUAL (Inches)	.180	.180	.180	.180

Laboratory was used to test the significance of the variation between the respective results. Table VII and the considerations that follow were used to establish a level of significance:

Testing for variation among directions:

$$H_0: B_1 = B_2 = B_3 = B_4$$

H_A : At least two B's are different

$$F_{\text{cal}} = 14.753 \text{ at } 99 \text{ per cent level,}$$

$$F_{\text{tab}} = 3.78 \text{ at } 99 \text{ per cent level.}$$

Since $F_{\text{cal}} > F_{\text{tab}}$, Reject H_0 .

To locate difference in direction, therefore, the least significant difference (LSD) test is performed as follows:

	<u>Means</u>
Direction B_1 = Section V(V) ,	0.89746
Direction B_2 = Section H(EW) ,	0.83350
Direction B_3 = Section V(NS) ,	0.84950
Direction B_4 = Section V(EW) ,	0.79683

$$\text{LSD}(.01) = t(.01) S_{\bar{x}} , \text{ (t at df of error)}$$

$$S_{\bar{x}} = \sqrt{\frac{\text{E.M.S.}}{r}} , \text{ r = number of observations per mean of given factor}$$

$$S_{\bar{x}} = \sqrt{\frac{0.0283}{240}} \quad \text{E.M.S. = error mean square}$$

$$S_{\bar{x}} = 0.0108$$

TABLE VII
ANALYSIS OF VARIANCE

Source	df	S.S.	M.S.	F_{cal}	F_{tab} (.01 level)
Total	959	84.93776			
Displacement (A)	29	35.13672	1.21161	42.813	1.70
Direction (B)	3	1.25254	0.41751	14.753	3.78
Material (C)	1	20.82842	20.82842	735.99	6.63
Displ x Direc (A x B)	87	.97906	0.01125	0.396	1.40
Displ x Mat'l (A x C)	29	3.20178	0.11041	3.901	1.70
Direc x Mat'l (B x C)	3	1.22222	0.40741	14.396	3.78
Displ x Direc x Mat'l (A x B x C)	87	1.93023	0.02219	.784	1.40
Experimental Error	720	20.38677	(0.0283) (E.M.S.)		

$$\begin{aligned} \text{LSD}_{(.01)} &= 2.576 (0.0108) \\ &= 0.02782 \end{aligned}$$

$$B_1 - B_2 = 0.89746 - 0.83350 = 0.06396.$$

Since $B_1 - B_2 > \text{LSD}$, difference between B_1 and B_2 is significant at 99 per cent level.

$$\text{Likewise, } B_3 - B_4 = 0.84950 - 0.79683 = 0.05267$$

which is greater than LSD; therefore, difference between B_3 and B_4 is significant at the 99 per cent level.

E. Failure Surfaces

According to several textbooks of structural geology, the smoother direction along fault planes, as felt with the fingers, indicates the sense of fault movement (Nevin, 1949). Recent publications, however, have cautioned against deducing sense of movement merely on the basis of rough or smooth appearance of slickensided surfaces, because in some cases the opposite direction was ascertained (Tjia, 1964; Riecker, 1965). Accordingly, the faces of the loess specimens loaded to residual strength under direct shear were exposed for examination of the features which developed on the surfaces.

Although more pronounced in dry specimens, shear surfaces in moist specimens also contain steps and ridges which face the direction of movement of the opposite block. Figures 25 and 26 illustrate the relative direction

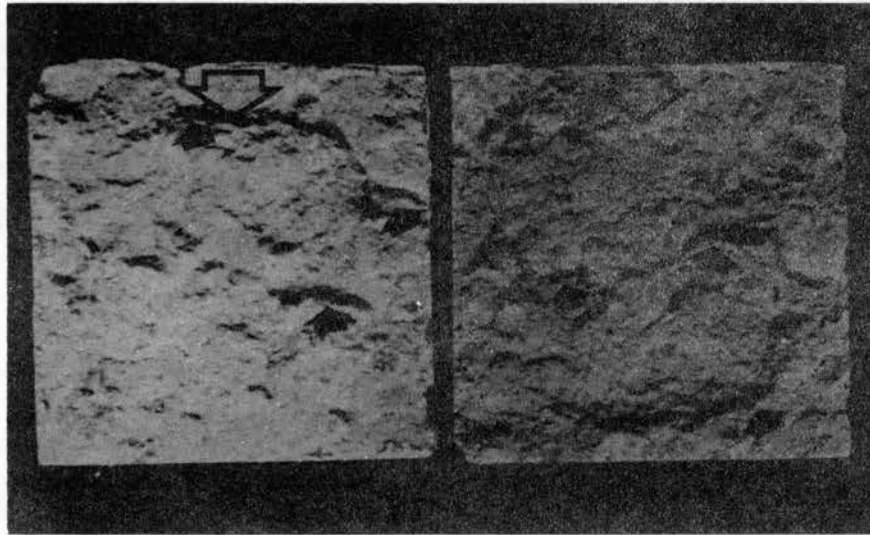


Figure 25. Exposed Direct Shear Surfaces (2" x 2") of Moist Vicksburg Loess. Large Arrows Indicate Direction of Movement; Small Arrows Indicate Steps Facing Oncoming Opposed Surface

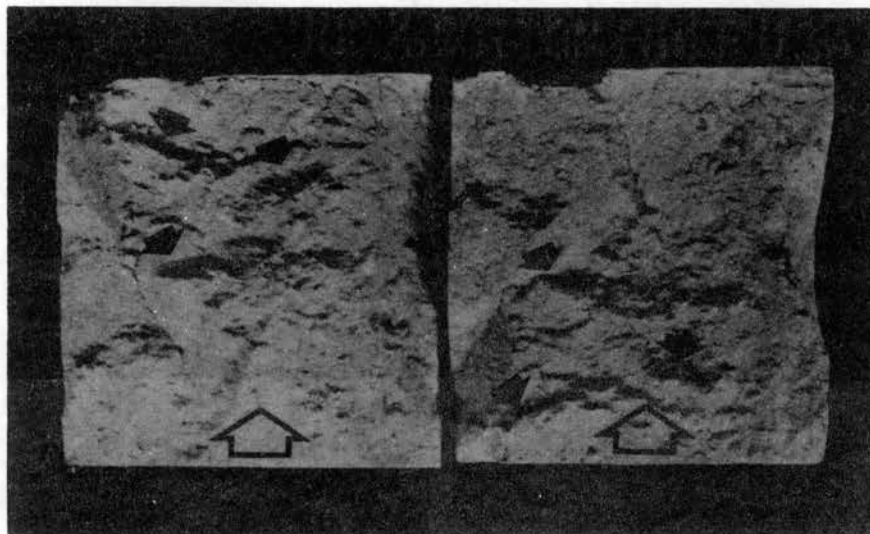


Figure 26. Exposed Direct Shear Surfaces (2" x 2") of Dry Vicksburg Loess. Large Arrows Indicate Direction of Movement; Small Arrows Indicate Steps Facing Oncoming Opposed Surface

of movement of the direct shear test and the resulting step-like features which would appear to have hindered or resisted slippage on the surface.

F. Shear Plane Development

The sequential development of the shear plane in moist specimens is illustrated in Figure 27. In Figure 27, thin section (a) reflects a condition at elastic equilibrium and (b) reflects the condition of a specimen terminated at peak strength. Thin sections (c) and (d) in the same figure reflect initial condition at stable yield, and final condition at residual strength, respectively. The four sections illustrated were prepared from specimens stressed perpendicular to imbrication.

Thin section examination indicates that specimens stressed parallel to imbrication generally reflect a slightly different failure pattern which is more pronounced at the residual strength condition. Figure 28 illustrates the failure planes of two moist specimens stressed in mutually perpendicular directions as indicated. A relatively uniform shear plane developed in most specimens which were stressed perpendicular to grain orientation (Figure 28a). By comparison, those stressed parallel to grain orientation developed a different pattern of failure (Figure 28b). The resulting overlapping pattern of failure suggests a separation of skeletal grains in the central region of the specimen. Shear

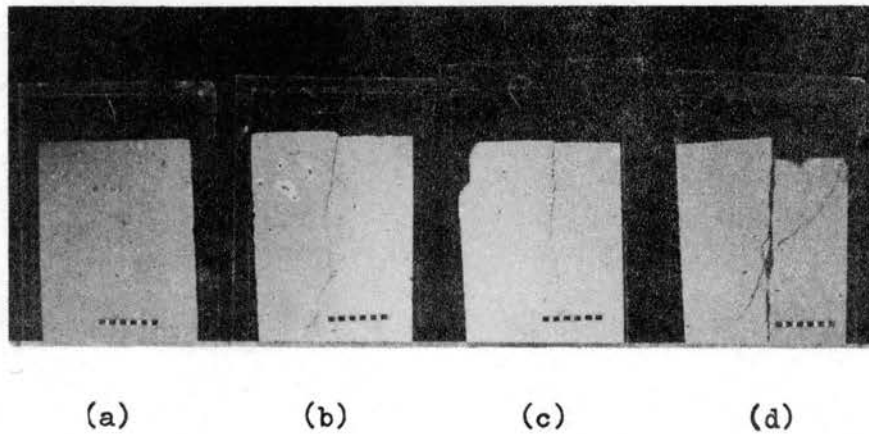


Figure 27. Thin Sections Illustrating Sequential Development of Failure Pattern (a, b, c, d) in Moist Specimens Sheared Normal to Grain Orientation; Crossed Polars

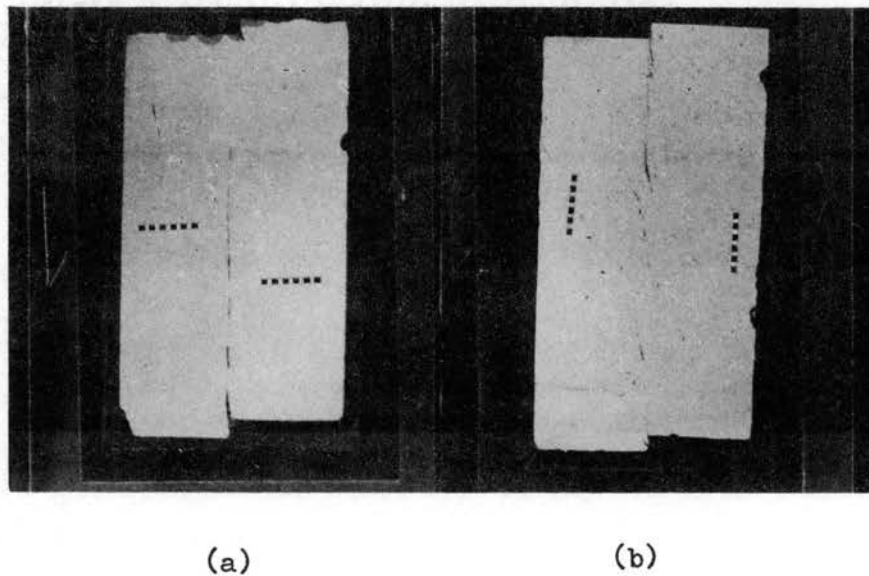


Figure 28. Thin Sections Illustrating Failure Pattern in Moist Specimens Sheared (a) Normal to Imbrication, and (b) Parallel to Imbrication; Crossed Polars; 1" x 2" Sections

perpendicular to grain orientation suggests a direct and more regular break between particles at the shear plane.

Microscopic observations of the shear plane further revealed the jagged steps noted on the failure surfaces aligned in a manner which would be expected to resist movement (Figure 29 and 30). Although larger displacements tended to reduce irregularities, it was also noted that the same general surface features were still present at 10 per cent strain.

G. Discussion

Complete explanation of all features noted at the failure surface and of the variation in strength is not possible. Although grain orientation affected the strength parameters and influenced the development of the failure pattern in some specimens, as explained above, it is also believed that the orientation and distribution of the clay matrix is also a controlling factor which requires further study. It is obvious, though, that shear failure occurred through the matrix and that skeletal grains remained intact. Nonetheless, some disaggregation of calcite particles was noted at the failure surface of dry specimens. However, this was suspected to have been a result of abrasion after failure.

The inconsistent variation in displacement required for peak strength was noted. Greater strain was required to achieve peak strength in both dry and moist samples

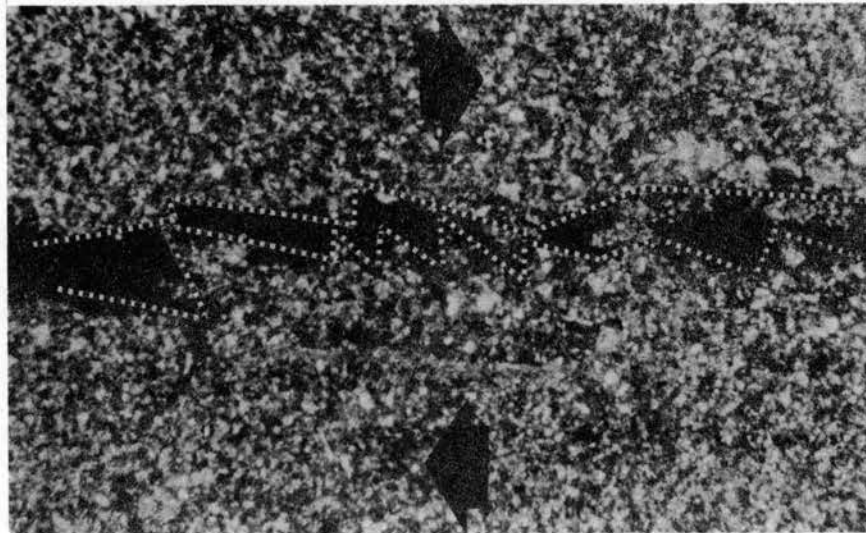


Figure 29. Photomicrograph of a Failure Plane in Specimen H(EW). Arrows Indicate Direction of Shear and Outline Indicates Steps Facing a Direction Which Apparently Opposes Movement; Crossed Nicols; 10x

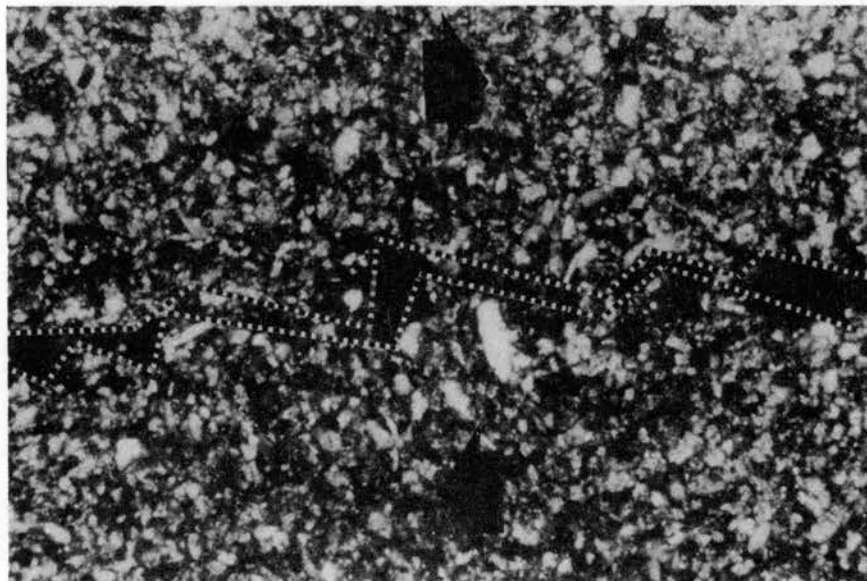


Figure 30. Photomicrograph of a Failure Plane in Specimen V(V). Arrows Indicate Direction of Shear and Outline Indicates Steps Facing a Direction Which Apparently Opposes Movement; Crossed Nicols; 20x

for shear stresses oriented parallel to imbrication. However, this trend was not maintained for shear stresses oriented parallel to preferred orientation (Table VI). The reason for this result is not apparent except that because the degree of grain orientation was greater in imbrication than in azimuthal orientation, a more pronounced difference in displacement might be expected in the former.

Moisture reduced the strength properties of loess and diminished the influence of grain orientation considerably (Figure 22 and 24). However, moisture accentuated the difference in failure pattern between specimens sheared parallel and perpendicular to grain orientation (Figure 28). It is believed that moisture permitted some rotation of skeletal grains and that shear-induced separation of particles in the failure zone was influenced by grain orientation. By comparison, grain orientation had no apparent influence on the failure pattern of dry specimens. The step-like surface features were still observed in dry specimens, although the shear plane was generally continuous irrespective of particle orientation.

In conclusion, the strength anisotropies of undisturbed Vicksburg loess were correlated with orientation of skeletal grains. Larger shear strengths were found where dry and moist specimens were stressed perpendicular to grain orientation, and lower strengths were found where specimens were stressed parallel to grain orientation.

The average peak shear strength of dry specimens stressed parallel to imbrication was 9 per cent lower than those stressed perpendicular to imbrication. The average peak strength of dry specimens stressed parallel to preferred grain orientation, was 12 per cent lower than those stressed perpendicular to grain orientation. For moist specimens, this same trend was maintained; however, the degree of strength variation was considerably reduced.

CHAPTER VI

INFLUENCE OF MICROSTRUCTURE ON SHEAR STRENGTH: TRIAXIAL TESTS

A. Introduction

The triaxial compression test is one of the more commonly used strength tests in soil mechanics laboratories for ascertaining the angle of internal friction (ϕ), and cohesion (c). Using these empirical constants, ϕ and c , Coulomb postulated the general equation which expresses the relationship between shear strength (s), and normal stress (σ) as:

$$s = c + \sigma \tan \phi.$$

Refinements and modifications of this equation depend on soil material and testing conditions. However, one consideration which pertained to this study involves the characteristic break of the Mohr-Coulomb failure envelope into two straight line segments.

Means and Parcher (1963), in a discussion of the failure properties of naturally cemented granular soils, postulated that the material undergoes two failures; one where the cohesive bond of cementation is broken, and one where the internal shearing resistance of the granular

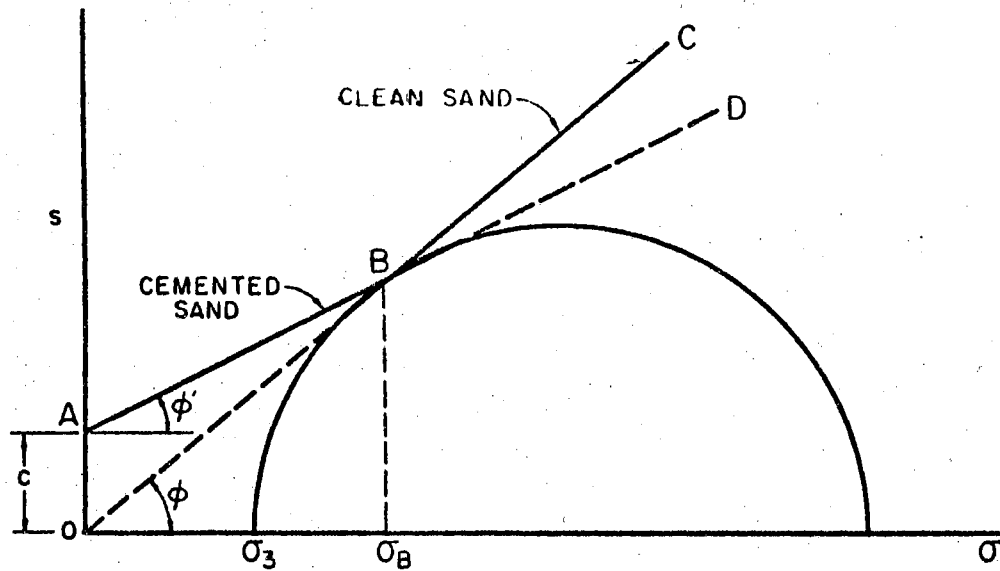
component is exceeded. This phenomenon is illustrated in Figure 31. Other investigators, however, found that this failure is not necessarily characteristic of artificially stabilized granular soils.

Another consideration of importance in this study was the relationship of the orientation of the inherent fabric anisotropy of soil specimens to the direction of applied axial stress. In most soils, this has been of little concern to investigators. However, if anisotropy is a known physical characteristic inherent in the material, its affect on strength and failure properties may be significant.

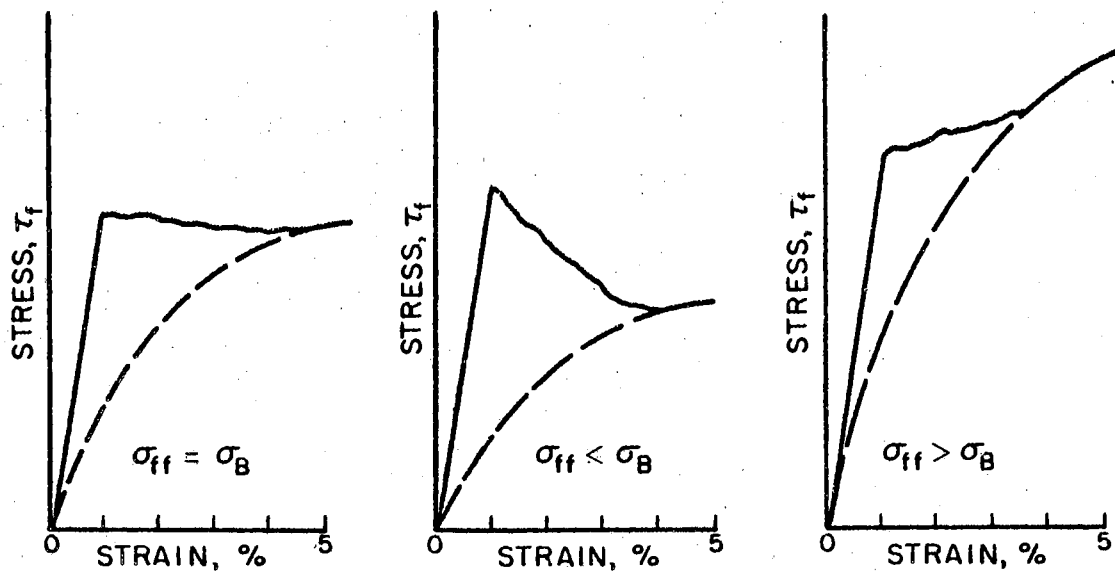
This chapter presents the results of triaxial tests for undisturbed and remolded Vicksburg loess. Because grain orientation analysis established an inherent structural anisotropy for the undisturbed material (Chapter IV), influence of fabric on strength parameters was examined by applying axial load at an arbitrary angle to the plane of anisotropy. These results were compared with triaxial tests of undisturbed specimens obtained from the same source but loaded perpendicular to the plane of the same structural anisotropy. Tests on remolded specimens were performed to evaluate the effect of the natural cementation on the behavior of undisturbed loess.

B. Procedure

Undisturbed specimens for triaxial testing were



a) STRENGTH LINE FOR CEMENTED GRANULAR SOIL.



b) STRESS-DEFORMATION CHARACTERISTICS OF CEMENTED SOIL.

Figure 31. Strength and Stress-Deformation Characteristics of Cemented Soils (after Means and Parcher, 1963)

obtained from one monolithic block of Vicksburg loess after the material was air dried to less than one per cent moisture. The block was appropriately marked and dry specimens approximately 2" x 2" and 5 inches in height were cut with a standard diamond saw. Both ends of the vertically oriented specimens were capped with wax and inserted in a standard motorized soil lathe for further trimming. Test specimens were trimmed to 1.4 inches in diameter, and cut to 2.8 inches in height after removal from the lathe.

A similar procedure was followed for preparing specimens to be axially loaded at an angle of 45 degrees to imbrication or bedding. However, for these specimens 2" x 2" x 5" blocks were initially cut at 45 degrees from the vertical and subsequently trimmed to size.

All moist specimens were prepared as previously outlined. Subsequently, the trimmed specimens were carefully sprayed with water until 16 per cent moisture was reached. The specimens were then wrapped, sealed and cured to permit uniform distribution of moisture prior to testing. After testing, the moisture content was again determined by oven drying, and only those specimens with 16 ± 0.5 per cent moisture were included in the strength analysis.

Remolded specimens, 1.4 inches in diameter and 2.8 inches in height, were prepared at optimum moisture of 16 per cent and compacted statically to an average density equal to that of the undisturbed loess. A sufficient

number of compacted specimens at 16 per cent moisture were wrapped in cellophane and wax sealed for subsequent testing. The remainder were air-dried to less than one per cent moisture before testing. In both dry and moist remolded specimens, the density of each sample used was within one per cent of the density of the respective undisturbed specimens.

In addition to unconfined compression tests, triaxial tests were conducted using 14.2, 28.4, 42.6, 56.8, and 85.2 psi confining pressures. Three tests for each material, each moisture condition, and each confining pressure were conducted, and the stress-strain behavior at each condition was plotted on a graph. The single stress-strain curve to represent the three tests was determined by averaging arithmetically the stresses at each increment of strain.

A strain rate of 0.004 inches per minute was maintained throughout all triaxial tests. Air was used as a confining medium and rubber membranes of 1.40 inch ID and 0.025 inch wall thickness were used. All tests were at drained conditions, and no attempt was made to measure pore water pressures for moist specimens. However, permeability of remolded and undisturbed specimens revealed good drainage qualities. Peak stresses were selected as failure criteria for establishing strength envelope.

C. Test Results

The dry and moist strength envelopes established by the triaxial tests are illustrated in Figures 32, 33, and 34 for undisturbed, undisturbed (45°), and remolded loess, respectively. The break in the strength envelope into two straight line segments for undisturbed specimens is evident (Figures 32 and 33). In contrast to these results, no break was noted in the strength envelope for remolded specimens (Figure 34). The break occurred at a normal stress (σ_B) of 59 psi and 53 psi for undisturbed and undisturbed (45°) dry specimens, respectively. Values of σ_B for moist specimens were each 45 psi.

Values of ϕ , and c for undisturbed dry and moist specimens were consistently greater than those for undisturbed (45°) specimens. However, values of ϕ' (as defined in Figure 31) were lower for undisturbed dry and moist specimens than those for undisturbed (45°) specimens. For remolded specimens, values of c were slightly lower than for all undisturbed specimens. Figure 35 illustrates the relative strength envelopes of all triaxial tests.

The average stress-strain behavior for undisturbed specimens at several confining pressures is illustrated in Figures 36 and 37. The consistently lower average strength behavior for specimens whose grain imbrication was oriented 45 degrees to axial stress was noted. However, the differences were not so pronounced in moist specimens. Although average axial strain at failure for dry specimens

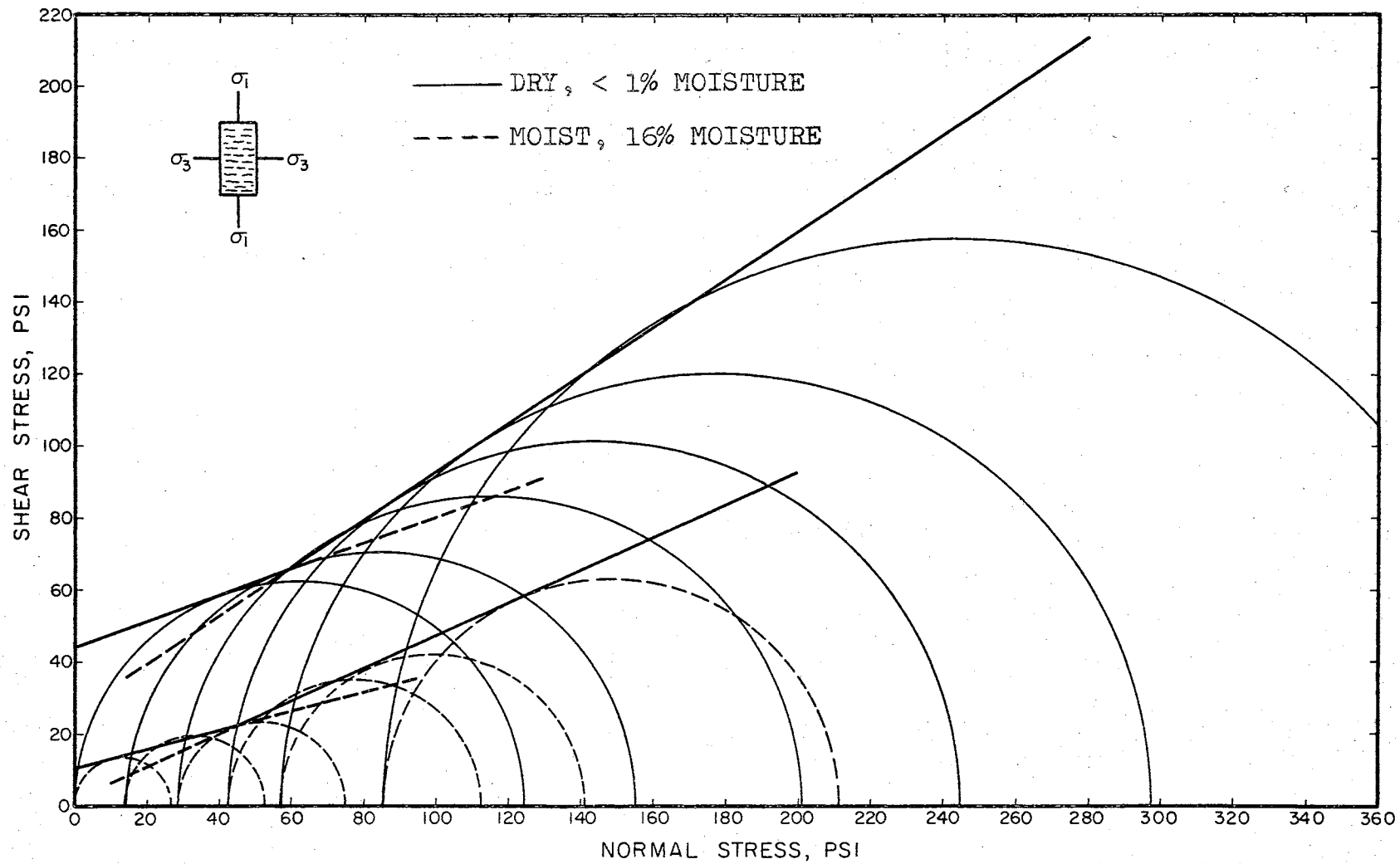


Figure 32. Triaxial Compression Tests on Undisturbed Vicksburg Loess

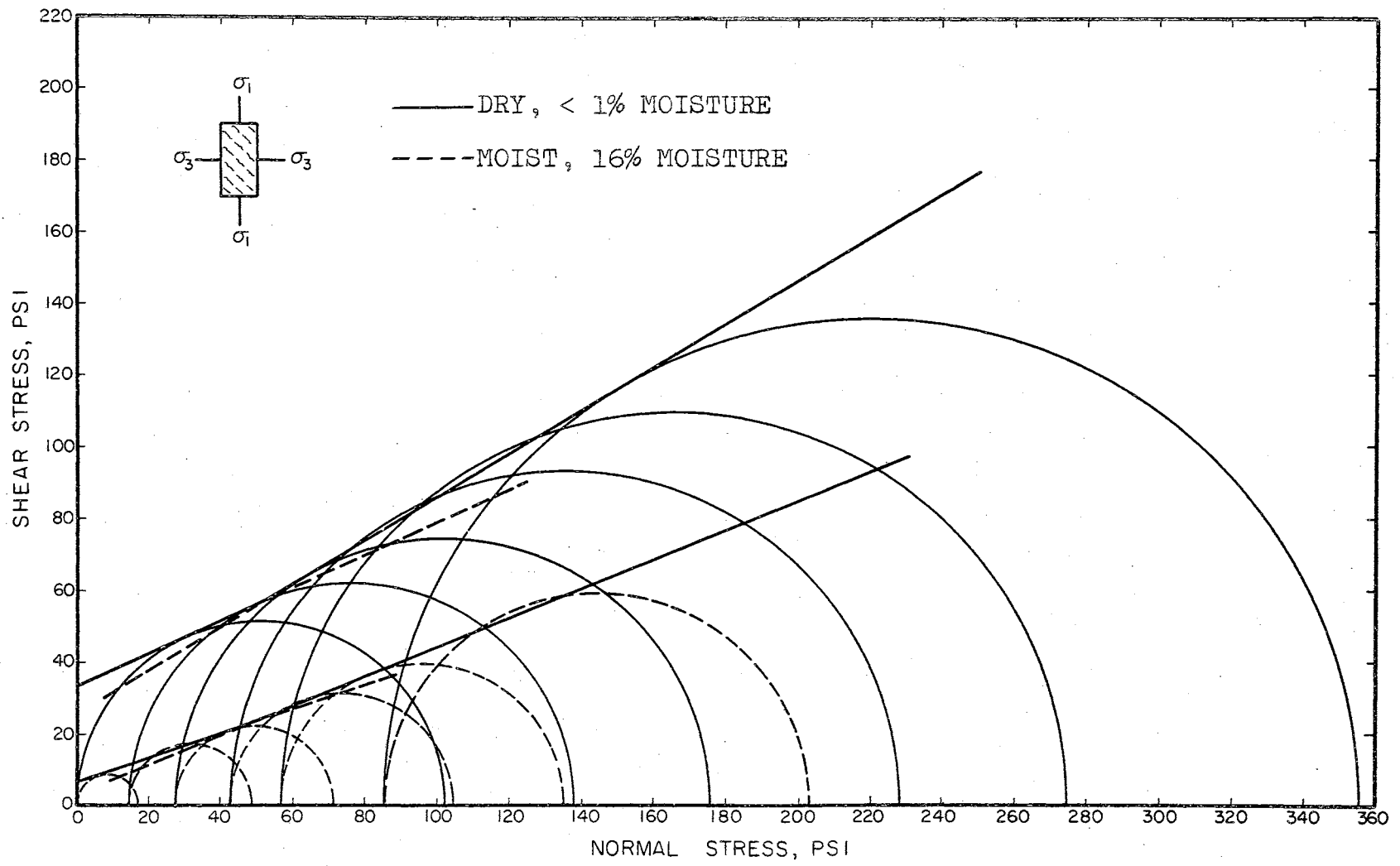


Figure 33. Triaxial Compression Tests on Undisturbed (45°) Vicksburg Loess

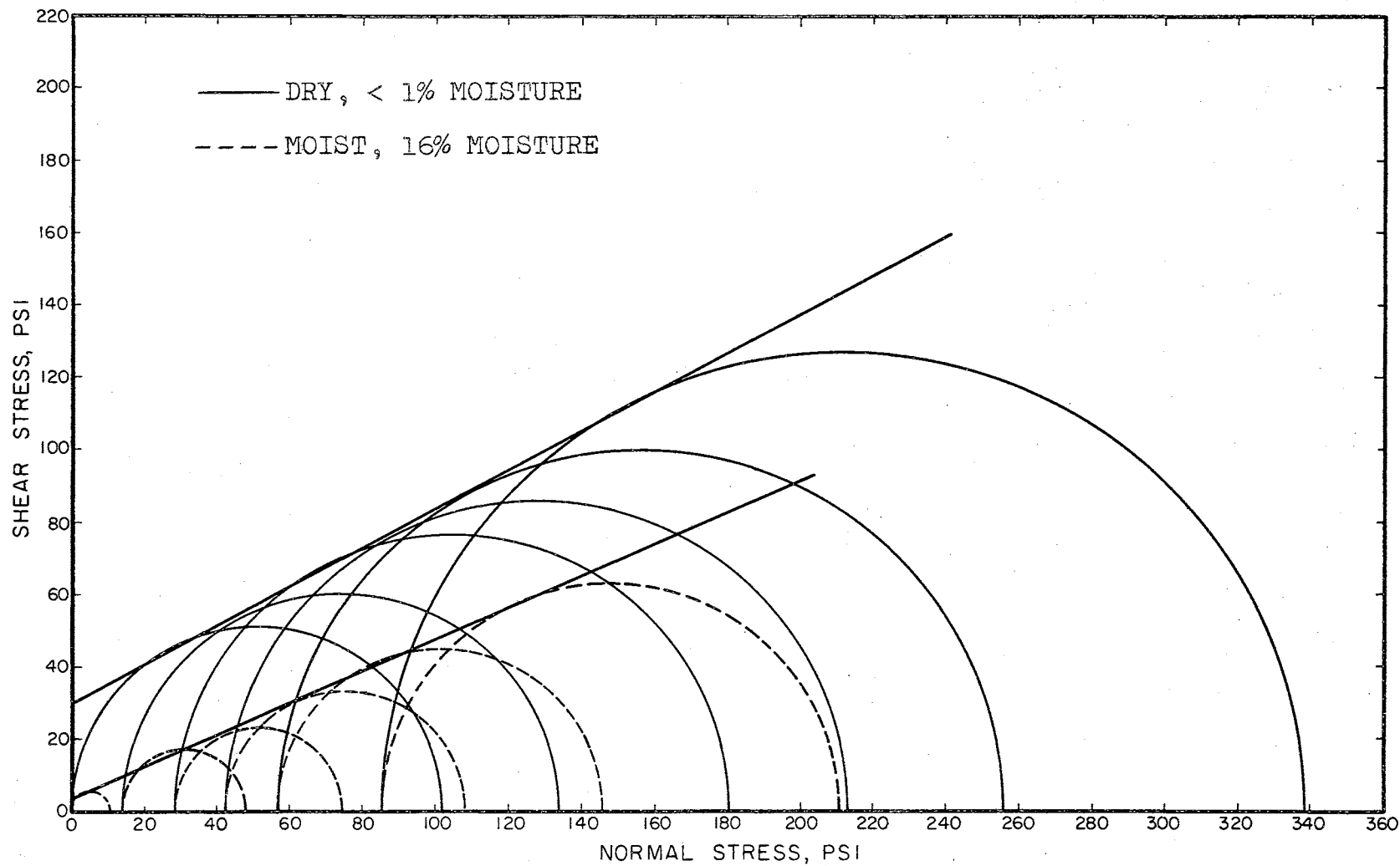


Figure 34. Triaxial Compression Tests on Remolded Vicksburg Loess

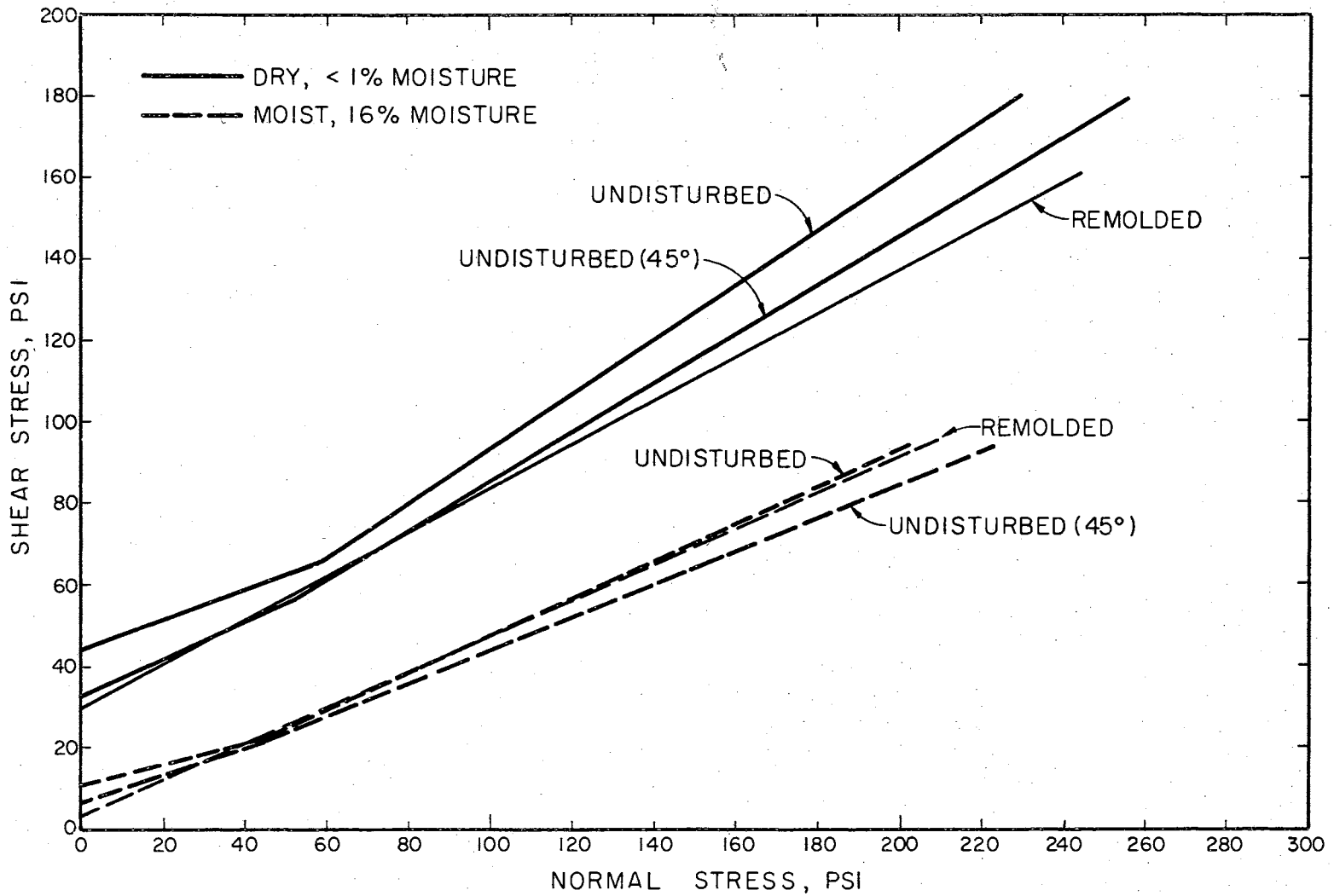


Figure 35. Triaxial Compression Strength Envelopes for Vicksburg Loess

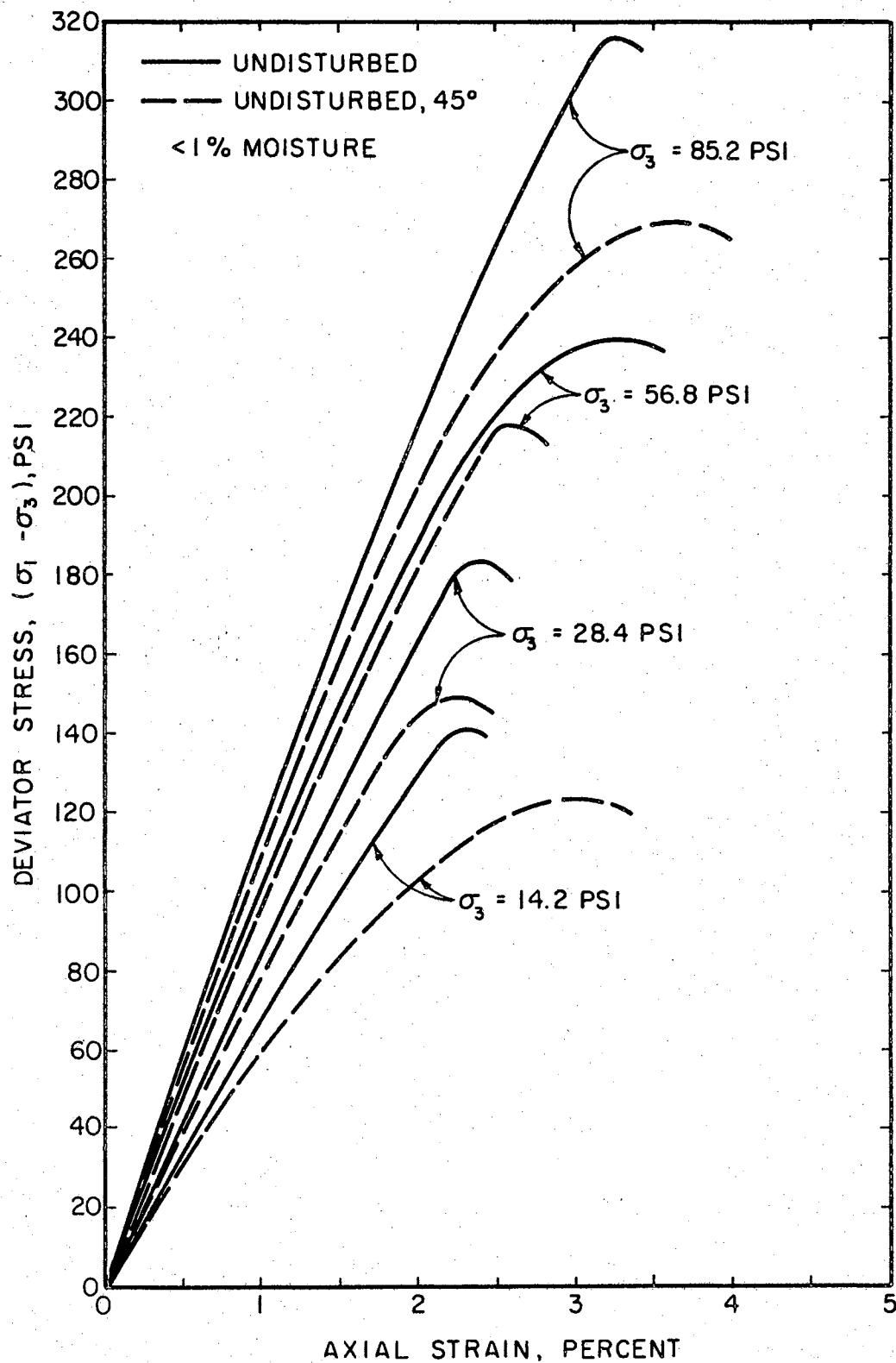


Figure 36. Average Stress-Strain Triaxial Test Results for Dry Vicksburg Loess

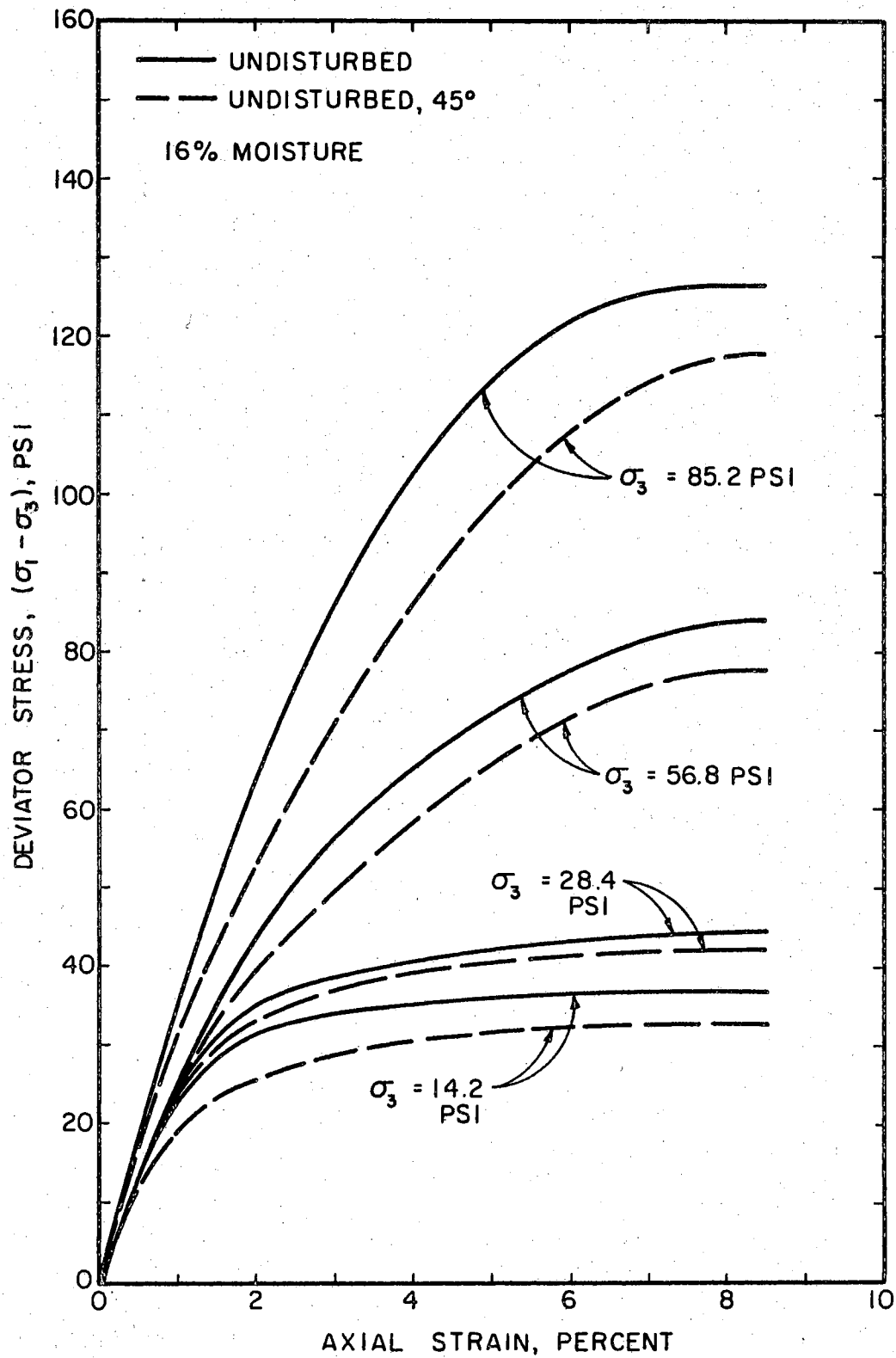


Figure 37. Average Stress-Strain Triaxial Test Results for Moist Vicksburg Loess

generally increased with increasing confining pressures, the pattern was not as uniform as expected (Figure 38). The reason for this cannot be explained. The average axial strain at failure for moist specimens did not vary.

A summary of all the results of the triaxial tests is presented in Table VIII.

D. Discussion

From the triaxial data obtained, the apparent two straight line segments of the failure envelope for undisturbed specimens is considered a significant engineering characteristic of Vicksburg loess. It is evident from the test results that this property was maintained when axial stresses were applied at 45 degrees to grain imbrication or bedding. It is suspected that this behavior might also result irrespective of orientation of axial stresses because of the unique natural cementation and fabric of loess.

The inherent structural anisotropy in loess as a result of skeletal grain orientation affects the strength properties considerably as was revealed by triaxial testing. Whether this is significant in field problems is not known, except that perhaps the vertical stability of loess might well be attributed in part to the relatively horizontal orientation of silt grains. The larger strength behavior which resulted when axial stresses were oriented normal to the imbrication indicates, to some extent,

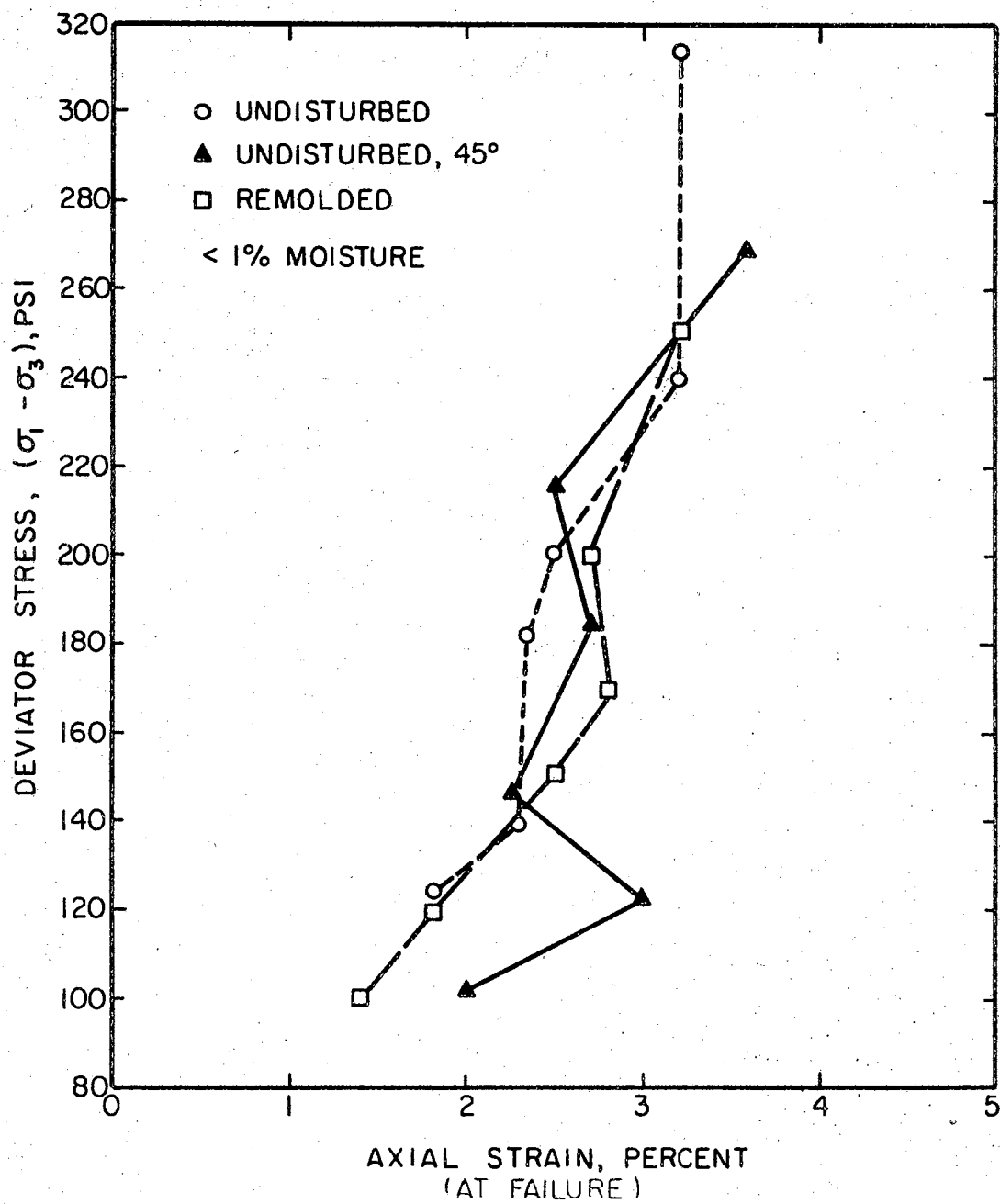


Figure 38. Axial Strains at Failure in Triaxial Compression Tests of Vicksburg Loess

TABLE VIII
SUMMARY OF TRIAXIAL COMPRESSION TESTS

	σ_3 (PSI)	MOISTURE	$\sigma_1 - \sigma_3$ (PSI)	σ_1 (PSI)	% STRAIN	σ_B (PSI)	STRENGTH PARAMETERS
UNDISTURBED	0	AIR DRY <1%	124.0	—	1.8	59	C = 44 PSI $\phi' = 20^\circ$ $\phi = 34^\circ$
	14.2		140.6	154.8	2.3		
	28.4		182.5	210.9	2.3		
	42.6		201.7	244.3	2.5		
	56.8		240.0	296.8	3.2		
85.2	314.6	399.8	3.2				
UNDISTURBED	0	16%	26.7	—	2.0	45	C = 11 PSI $\phi' = 15^\circ$ $\phi = 24^\circ$
	14.2		37.1	53.3	8.5		
	28.4		44.6	73.0	8.5		
	42.6		69.9	112.5	8.5		
	56.8		83.8	140.6	8.5		
85.2	126.3	211.5	8.5				
UNDISTURBED 45°	0	AIR DRY <1%	102.0	—	2.0	53	C = 33 PSI $\phi' = 24^\circ$ $\phi = 31^\circ$
	14.2		122.9	137.1	3.0		
	28.4		147.5	175.9	2.2		
	42.6		185.9	228.5	2.7		
	56.8		216.6	273.4	2.5		
85.2	269.8	355.0	3.6				
UNDISTURBED 45°	0	16%	16.8	—	2.0	45	C = 6 PSI $\phi' = 18^\circ$ $\phi = 21^\circ$
	14.2		33.9	48.1	8.5		
	28.4		43.0	71.4	8.5		
	42.6		62.3	104.9	8.5		
	56.8		77.9	134.7	8.5		
85.2	118.2	203.4	8.5				
REMOLDED	0	AIR DRY <1%	102.0	—	1.4	—	C = 30 PSI $\phi = 27^\circ$
	14.2		120.1	134.3	1.8		
	28.4		151.8	180.2	2.5		
	42.6		169.6	212.2	2.8		
	56.8		199.0	255.8	2.7		
85.2	253.1	338.3	3.2				
REMOLDED	0	16%	9.2	—	1.4	—	C = 3 PSI $\phi = 23^\circ$
	14.2		32.8	47.0	8.5		
	28.4		45.1	73.5	8.5		
	42.6		65.2	107.8	8.5		
	56.8		88.7	145.5	8.5		
85.2	125.2	210.4	8.5				

increased vertical stability.

The larger ϕ' values for undisturbed (45°) specimens, both dry and moist, suggests better frictional resistance properties when the cohesive bonds are on the verge of rupture and when a larger number of grains are oriented more parallel to the failure plane. An explanation of the increase in ϕ' values (within the "cohesive range") where failure occurs more parallel to grain orientation is not known. However, it is suspected that the sequence in which cohesive bonds rupture with strain might reflect greater frictional resistance. Although moisture reduced cementation considerably, the same relative difference between ϕ' values for undisturbed and undisturbed (45°) was maintained.

On the other hand, the lower ϕ values for undisturbed (45°) specimens, dry and moist, suggests a lower internal shearing resistance when a specimen is stressed so that a failure plane develops more nearly parallel to grain orientation. It is suspected that interlocking of skeletal grains is less effective in a direction which parallels grain orientation than in a direction which is normal to it.

Although grain orientation analyses of remolded specimens were not performed, it is suspected that static compaction at optimum moisture would only slightly, if any, orient grains normal to the direction of compression. In any event, the structure of natural loess was destroyed,

and the ϕ and c values reflect properties similar to other silts. Although composition and density of remolded specimens were equal to undisturbed specimens, the different strength behavior accentuates the influence that natural cementation and fabric arrangement have on engineering behavior of loess.

An examination of thin sections prepared after specimens were stressed triaxially did not reveal any distinguishing features which were not discussed in the previous chapter. The failure plane did not exhibit the step-like features as noted in the direct shear tests. However, failure occurred within the clay matrix and considerably more disaggregation of calcite particles along the failure plane was observed in dry specimens. At high confining pressures, dry specimens failed as a result of almost complete collapse and disintegration of the open structure. Thin sections in this situation were not prepared because it was found that the impregnating process destroyed and concealed any failure pattern. However, thin sections of moist specimens were prepared after drying and examined. Observations indicated some increased degree of grain packing; however, no quantitative evaluation was possible. Root holes and concretions were found intact, yet some reduction of intrapedal voids was apparent.

CHAPTER VII

SUMMARY AND CONCLUSIONS

A. Summary

After a number of hypotheses on the origin of loess have been offered, loess is now generally agreed to be an eolian deposit. Loess deposits cover large areas of central United States, the plains of Argentina, central and eastern Europe, Russia, and China and range from a few feet to several hundred feet in thickness. In the United States, loess deposits are generally found to thin logarithmically with distance from source. It is described as a well-sorted, porous, calcareous silt arranged in an open, cohesive fabric resulting in a natural dry density of 70-90 pounds per cubic foot. Loess maintains near vertical exposures and ordinarily contains concretions, root tubules, and snail shells.

Quartz was found to be the primary mineral in both Vicksburg and Pre-Vicksburg loess, averaging 65 per cent by volume. Other constituents of the two materials, by weight per cent, respectively, are: carbonates, 30.5 and 3.8; clays, 9.0 and 17.9; and organic matter, 0.5 and 1.9. Feldspars averaged 6.0 per cent and the heavy minerals were found to be chiefly hematite, limonite, hornblende,

epidote, zircon, and garnet.

Grain shape of both Vicksburg and Pre-Vicksburg loess was found to be subangular. A visual determination of average roundness and sphericity was 0.3-0.4 and 0.6-0.8, respectively. The average width to length axial ratio of the silt particles which was found to be 1:1.6 indicates definite grain elongation.

Based on direct measurements of grain sizes, the mean diameter of Vicksburg and Pre-Vicksburg loess was found to be 5.28ϕ and 5.84ϕ (0.026 and 0.018 mm), respectively. Mean diameters based on hydrometer and dry sieve analyses averaged 5.54ϕ and 6.10ϕ (0.021 and 0.015 mm), respectively. Standard deviation indicated moderate sorting for both materials irrespective of method of analysis used. Vicksburg loess reflected a slightly positive skewness toward coarser grain sizes; whereas, the Pre-Vicksburg loess values indicated a slightly negative skewness toward finer grain sizes. Conflicting kurtosis values determined from different equations supported the belief that kurtosis is an insensitive and insignificant parameter for grain size studies.

The regression equation for converting grain size distribution of loess based on long axis measurements of grains on thin sections to a sieve size distribution, in phi units, was derived as:

$$\phi_w = -1.247 + 1.350 \phi_{T.S.}$$

Similarly, the regression equation for converting grain size distribution based on short axis measurements of grains on grain mountings to sieve sizes, in phi units, was found to be:

$$\phi_w = -2.390 + 1.365 \phi_{G.M.}$$

The grain orientation data analyzed for Vicksburg and Pre-Vicksburg loess based on visual and dielectric anisotropy measurements are summarized as follows:

1. Visual grain orientation azimuth for Vicksburg loess is 288-289 degrees; imbrication, 3-5 degrees.
2. Visual grain orientation azimuth for Pre-Vicksburg loess is 285-288 degrees; imbrication, 4-8 degrees.
3. Dielectric azimuthal fabric mean for Vicksburg loess is 275 degrees; imbrication, 4 degrees.
4. Dielectric azimuthal fabric mean for Pre-Vicksburg loess is 284 degrees; imbrication, 10 degrees.
5. Statistical analysis of data reveals that preferred grain orientation and imbrication are highly significant.

The influence of grain orientation on directional shear strength of Vicksburg loess based on direct shear tests is summarized as follows:

1. A 12 per cent average peak shear strength reduction resulted where dry specimens under a normal stress of 6.6 psi were sheared first perpendicular to preferred grain orientation and then parallel to it. Similarly, a 9 per cent reduction resulted in peak shear strength where specimens were sheared first perpendicular to imbrication and then parallel to it.
2. Residual shear strength values under the same conditions as above were reduced 3 per cent and 12 per cent for grain orientation and imbrication considerations, respectively.
3. The average peak shear strength of moist specimens under a normal stress of 4.4 psi was reduced over 6 per cent where shear directions were changed from one perpendicular to grain orientation and imbrication to one parallel to them.
4. Similarly, residual shear strength values of moist specimens reflected a 12 per cent difference for the same considerations.
5. Slightly larger strains were generally required to achieve peak shear strength for stresses parallel to grain imbrication than perpendicular to it.

The influence of microstructure on shear strength of Vicksburg loess based on triaxial compression tests is summarized as follows:

1. The strength envelope for undisturbed dry and moist specimens consisted of two straight-line segments, the slope of which increased at larger normal stresses; whereas, no break in the straight line envelope was found for remolded specimens.
2. Values of ϕ for undisturbed specimens decreased from 34° to 31° when dry, and 24° to 21° when moist, as the axially applied stress was changed from a direction normal to imbrication to one inclined 45 degrees to it.
3. Values of ϕ' increased from 20° to 24° , and 15° to 18° under the same conditions explained in item 2.
4. Cohesion values decreased from 44 to 33 psi under dry conditions, and from 11 to 6 psi under moist as applied axial stresses were changed from a direction normal to one at 45° to imbrication.
5. Stress-strain considerations revealed a significant reduction in required axial stress to reach failure when the stress direction was inclined 45 degrees to

imbrication instead of normal. The reduction was not as pronounced in moist specimens as in dry ones.

6. As axial stresses increased to reach failure because of increased confining pressures, axial strains generally increased as well. However, the increase was not as uniform and consistent as might be normally expected.

B. Conclusions

Grain size distributions for Vicksburg and Pre-Vicksburg loess were determined with sufficient accuracy by direct measurement of long axes of grains in thin section and short axes in grain mounts. These distributions can further be correlated with sieve size distributions by applying regression equations derived in this study. If thin sections are to be prepared for other types of investigations, it is considered advantageous to determine grain sizes from these same sections by simply measuring 1000-1500 grains. Otherwise, preparation of grain mounts are rapid, and short axis measurements of grains can be performed without difficulty. In many fine-grained materials such as loess, accuracies based on sieving and hydrometer methods are sometimes questionable and procedures are usually time consuming. The frequency-by-number (direct measurement) data obtained for grain size

distributions in some cases may be more reliable for certain permeability, seepage, and moisture movement studies than other methods.

Definite grain orientation was found in both horizontal and vertical planes of Vicksburg and Pre-Vicksburg loess. Following the eolian theory of loess deposition, the preferred grain orientation and slight imbrication conform to postulated paleowind directions determined by the thinning pattern of the loess blanket and decreasing particle size. Accordingly, silt-sized particles were found to be oriented parallel with the depositing current and imbricated in conformity with established criteria of sedimentation. Furthermore, this study demonstrates that with care grain orientation of silt-sized particles can be measured both visually from thin sections and electronically using a dielectric anisotropy instrument.

The orientation of skeletal grains in the Vicksburg loess studied definitely influences the directional shear strength. Oriented silt grains caused a significant reduction of shear strength where stresses were applied parallel to the plane of preferred grain orientation and imbrication. Failure planes which developed parallel to grain orientation produced off lapping, short, discontinuous fractures; whereas, a uniform continuous fracture was produced for failure normal to grain orientation. Failure surfaces of direct shear tests also revealed steplike features which faced the oncoming opposed surface.

From triaxial tests, microstructural anisotropies in Vicksburg loess also reflected considerable variation in the shear strength. The two line segment of the failure envelope characterized undisturbed specimens apparently because of natural cement; whereas, a straight line envelope typified remolded specimens. Also, greater ϕ values and lower ϕ' values were found when principal stresses were applied normal to imbrication or bedding.

C. Recommendations for Further Research

Although failure of all stressed specimens occurred within the clay matrix, the role of clay particle orientation or arrangement was not determined in this study. It is suspected that zones of weakness might exist within the clay matrix caused by accumulations of fine quartz or carbonate on the planes of the clay particles which could conceivably influence strength properties.

Other suggestions for additional study of microstructure of loess are as follows:

1. Effect of grain orientation and grain size distribution on permeability.
2. Particle orientation in remolded specimens and its effect on directional shear strength.
3. Variation of shear strength at different angles to planes of structural anisotropy.
4. Effect of variations in quantity of clay

and carbonate on shear strength.

5. Development of additional engineering applications related to structural anisotropy.

SELECTED BIBLIOGRAPHY

- Arbogast, J. L., C. H. Fay, and S. Kaufman. Method and Apparatus for Determining Directional Dielectric Anisotropy in Solids. U. S. Patent Office, Patent 2,963,642, 1960.
- Berg, L. S. "Loess as a Product of Weathering and Soil Formation" (from Climate and Life, in Russian, Vol. 3). Israel Program for Scientific Translations, Jerusalem, 1964 (U. S. Department of Agriculture and the National Science Foundation, Washington, D. C.). 1947.
- Chamberlin, T. C. "Supplementary Hypothesis Respecting the Origin of the Loess of the Mississippi Valley," Journal of Geology, Vol. 5 (1897), p. 795-802.
- Chamberlin, T. C., and R. D. Salisbury. Geology, Vol. 3. New York: Henry Holt and Co., 1907, pp. 405-412.
- Chayes, F. "Statistical Analysis of Two-Dimensional Fabric Diagrams" published in Structural Petrology of Deformed Rocks. Cambridge, Mass.: Addison-Wesley Press, 1949, pp. 297-326.
- Chayes, F. "Discussion: Effect of Change of Origin on Mean and Variance of Two-Dimensional Fabrics." American Journal of Science, Vol. 252 (1954), pp. 567-570.
- Chayes, F. Petrographic Modal Analysis: An Elementary Statistical Appraisal. New York: John Wiley and Sons, Inc., 1956, 113 pp.
- Clevenger, W. A. "Experiences With Loess as Foundation Material." American Society of Civil Engineers Transactions, Vol. 123 (1958), pp. 151-169.
- Curray, J. R. "Dimensional Grain Orientation Studies of Recent Coastal Sands." American Association of Petroleum Geologists Bulletin, Vol. 40 (1956a), pp. 2440-2456.
- Curray, J. R. "The Analysis of Two-Dimensional Orientation Data." Journal of Geology, Vol. 64 (1956b), pp. 117-131.

- Dapples, E. C., and J. F. Rominger. "Orientation Analysis of Fine-Grained Clastic Sediments: A Report of Progress." Journal of Geology, Vol. 53 (1945), pp. 246-261.
- Davidson, D. T., et. al. "Geologic and Engineering Properties of Pleistocene Materials in Iowa." Iowa Engineering Experiment Station Bulletin No. 191 (1960), 250 pp.
- Doeglas, D. J. "Loess, an Eolian Product." Journal of Sedimentary Petrology, Vol. 19 (1949), pp. 112-117.
- Emerson, F. V. "Loess Depositing Winds in the Louisiana Region." Journal of Geology, Vol. 26 (1918), pp. 532-541.
- Fairbairn, H. W. "Gelatinized Slides for R. I. Immersion Mounting." American Mineralogist, Vol. 28 (1943), p. 396.
- Fisk, H. N. Geological Investigation of the Alluvial Valley of the Lower Mississippi River. Mississippi River Commission, Vicksburg, Miss. (1944), 78 p.
- Fisk, H. N. "Loess and Quaternary Geology of the Lower Mississippi Valley." Journal of Geology, Vol. 59, No. 4 (1951), pp. 333-356.
- Folk, R. L., and W. C. Ward. "Brazos River Bar, A Study in the Significance of Grain-Size Parameters." Journal of Sedimentary Petrology, Vol. 27 (1957), pp. 3-27.
- Friedman, G. M. "Determination of Sieve-Size Distribution From Thin-Section Data for Sedimentary Petrological Studies." Journal of Geology, Vol. 66 (1957), pp. 394-416.
- Friedman, G. M. "On Sorting Coefficients and the Lognormality of the Grain-Size Distribution of Sandstones." Journal of Geology, Vol. 70 (1962), pp. 737-753.
- Gibbs, H. J., and W. Y. Holland. Petrographic and Engineering Properties of Loess. Denver: Bureau Reclamation, Engineering Monograph No. 28 (1960), 37 p.
- Griffiths, J. C. Scientific Method in Analysis of Sediments. New York: McGraw-Hill Book Company (1967), 508 p.

- Griffiths, J. C., and M. A. Rosenfeld. "A Further Test of Dimensional Orientation of Quartz Grains in Bradford Sand." American Journal of Science, Vol. 251 (1953), pp. 192-214.
- Harrison, P. W. "New Technique for Three-Dimensional Fabric Analysis of Till and Englacial Debris Containing Particles From 3 to 40 mm. in size." Journal of Geology, Vol. 65 (1957), pp. 98-105.
- Ingles, O. G., and D. Lafeber. "The Influence of Volume Defects on the Strength and Strength Isotropy of Stabilized Clays." Engineering Geology, Vol. 1, No. 4 (1966), pp. 305-310.
- Inman, D. L. "Measure for Describing the Size Distribution of Sediments." Journal of Sedimentary Petrology, Vol. 22, No. 3 (1952), pp. 125-145.
- Jones, T. A. "Statistical Analysis of Orientational Data." Journal of Sedimentary Petrology, Vol. 38 (1968), pp. 61-67.
- Krinitzsky, E. L., and W. J. Turnbull. "Loess Deposits of Mississippi." Geological Society of America Special Paper (1967), 64 p.
- Krumbein, W. C. "Size Frequency Distribution of Sediments." Journal of Sedimentary Petrology, Vol. 4 (1934), pp. 65-77.
- Krumbein, W. C. "Sediments and Exponential Curves." Journal of Geology, Vol. 45 (1937), pp. 577-601.
- Krumbein, W. C. "Preferred Orientation of Pebbles in Sedimentary Deposits." Journal of Geology, Vol. 47 (1939), pp. 673-706.
- Krumbein, W. C., and L. L. Sloss. Stratigraphy and Sedimentation. California: W. H. Freeman and Co., 1955, 343 p.
- Lafeber, D. "Soil Structural Concepts." Engineering Geology, Vol. 1 (1966), pp. 261-290.
- Lafeber, D., and M. Kurbanovic. "Photographic Reproduction of Soil Fabric Patterns." Nature, Vol. 208, No. 5010 (1965), pp. 609-610.
- Larionov, A. K. "Structural Characteristics of Loess Soils for Evaluating Their Constructional Properties." Proceedings, 6th International Conference on Soil Mechanics and Foundation Engineering, Vol. 1, Canada (1965), pp. 64-68.

- Leighton, M. M., and H. B. Willman. "Loess Formation of the Mississippi Valley." Journal of Geology, Vol. 58, No. 6 (1950), pp. 599-623.
- Lohnes, R. A., and R. L. Handy. "Slope Angles in Friable Loess." Journal of Geology, Vol. 76 (1968), pp. 247-258.
- Martinez, J. D. "Photometer Method for Studying Quartz Grain Orientation." Bulletin of American Association of Petroleum Geologists, Vol. 42, No. 3 (1958), pp. 588-608.
- Means, R. E., and J. V. Parcher. Physical Properties of Soils. Columbus, Ohio: Charles E. Merrill Books, Inc., 1963, pp. 335-337.
- Mitchell, J. K. "The Fabric of Natural Clays and Its Relation to Engineering Properties." Proceedings Highway Research Board, Vol. 35 (1956), pp. 693-713.
- Morgenstern, N. R., and J. S. Tchalenko. "Microscopic Structures in Kaolin Subjected to Direct Shear." Géotechnique, Vol. 17 (1967), pp. 309-328.
- Nanz, R. H. Exploration of Earth Formations Associated With Petroleum Deposits. U. S. Patent Office, Patent 2,963,641 (1960).
- Nayudu, Y. R. "Rapid Methods for Studying Silt-Size Sediments and Heavy Minerals by Liquid Immersion." Journal of Sedimentary Petrology, Vol. 32, No. 2 (1962), pp. 326-331.
- Nevin, C. M. Principals of Structural Geology. 4th ed. New York: Wiley and Sons, 1949, 341 p.
- Orr, William R. Method for Determining Directional Inductive Anisotropy of Materials by Measuring Q Factor. U. S. Patent Office, Patent 3,151,292 (1964).
- Péwé, T. L. "An Observation on Wind-Blown Silt." Journal of Geology, Vol. 59, No. 4 (1951), pp. 399-401.
- Pincus, Howard J. "The Analysis of Aggregates of Orientation Data in the Earth Sciences." Journal of Geology, Vol. 61 (1953), pp. 482-509.
- Potter, P. E., and F. J. Pettijohn. Paleocurrents and Basin Analysis. New York: Academic Press Inc., 1963, 296 pp.

- Potter, P. E., and R. F. Mast. "Sedimentary Structures, Sand Shape Fabrics and Permeability." Journal of Geology, Vol. 71 (1963), pp. 441-471.
- Powers, M. "A New Roundness Scale for Sedimentary Particles." Journal of Sedimentary Petrology, Vol. 23 (1953), pp. 117-119.
- Reiche, P. "An Analysis of Cross-Lamination: The Coconino Sandstone." Journal of Geology, Vol. 46 (1938), pp. 905-932.
- Riecker, R. E. "Fault Plane Features: An Alternative Explanation." Journal of Sedimentary Petrology, Vol. 35, No. 3 (1965), pp. 746-770.
- Rodriguez, A. R., and S. J. Pirson. "The Continuous Diameter as a Tool for Studies in Directional Sedimentation and Tectonics." Society of Professional Well Log Analysts, Houston, Texas, 1968.
- Royster, D. L., and W. H. Rowan. "Highway Design and Construction Problems Associated With the Loessial Soils of West Tennessee." Highway Research Record Number 212, Highway Research Board (1968), pp. 28-32.
- Rusnak, G. A. "A Fabric and Petrological Study of the Pleasantview Sandstone." Journal of Sedimentary Petrology, Vol. 27, No. 1 (1957), pp. 41-55.
- Russell, R. J. "Lower Mississippi Valley Loess." Geological Society of America Bulletin, Vol. 55 (1944), pp. 1-40.
- Scheidig, Alfred. "Der Löss--und Seine Geotechnischen Eigenschaften." Dresden und Leipzig, Verlag von Theodor Steinkopf (1934), 233 p.
- Shapley, H. (editor). Climatic Change: Evidence, Causes, and Effects. Cambridge, Mass.: Harvard University Press (1953), 318 p.
- Sheeler, J. B. "Summarization and Comparison of Engineering Properties of Loess in the United States." Highway Research Record Number 212, Highway Research Board (1968), pp. 1-9.
- Simonson, R. W., and C. E. Hutton. "Distribution Curves for Loess." American Journal of Science, Vol. 252 (1954), pp. 99-105.

- Smith, G. D. "Illinois Loess, Variation in Its Properties and Distribution, a Pedologic Interpretation." University of Illinois Agriculture Experiment Station Bulletin 490 (1942), pp. 139-184.
- Snowden, J. O., Jr. "Petrology of Mississippi Loess." (Unpublished Ph.D. Dissertation, University of Missouri, Columbia, Missouri, 1966).
- Spencer, D. W. "The Interpretation of Grain Size Distribution of Clastic Sediments." Journal of Sedimentary Petrology, Vol. 33, No. 1 (1963), pp. 180-190.
- Steel, R. G. D., and J. H. Torrie. Principles and Procedures of Statistics. New York: McGraw-Hill Book Co., Inc., 1960, 481 pp.
- Steinmetz, R. "Analysis of Vectorial Data." Journal of Sedimentary Petrology, Vol. 32 (1962), pp. 801-812.
- Swineford, Ada, and J. C. Frye. "A Mechanical Analysis of Wind-Blown Dust Compared With Analyses of Loess." American Journal of Science, Vol. 243, No. 5 (1945), pp. 249-255.
- Swineford, A., and J. C. Frye. "Petrography of the Peoria Loess in Kansas." Journal of Geology, Vol. 59, No. 4 (1951), pp. 306-322.
- Teruggi, M. E. "The Nature and Origin of Argentine Loess." Journal of Sedimentary Petrology, Vol. 27, No. 3 (1957), pp. 322-332.
- Tjia, H. D. "Slickensides and Fault Movements." Geological Society of America Bulletin, Vol. 75 (1964), pp. 683-686.
- Trask, P. D. Origin and Environment of Source Sediments of Petroleum. Houston, Texas: Gulf Publishing Co., 1932.
- U. S. Department of Commerce, Weather Bureau. Local Climatological Data. Vicksburg, Mississippi, 1967.
- Visher, S. S. "The Time of Glacial Loess Accumulation." Journal of Geology, Vol. 30 (1922), pp. 472-479.
- Waggoner, P. E., and C. Bingham. "Depth of Loess and Distance From Source." Soil Science, Vol. 92, No. 6 (1961), pp. 396-401.

Wascher, H. L., R. P. Humbert, and J. G. Cady. "Loess in the Southern Mississippi Valley: Identification and Distribution of the Loess Sheets." Soil Science Society of America Proceedings, Vol. 12 (1948), pp. 389-399.

Zimmerle, W. and L. C. Bonham. "Rapid Methods for Dimensional Grain Orientation Measurements." Journal of Sedimentary Petrology, Vol. 32, No. 4 (1962), pp. 751-763.

APPENDIX A

RAPID PROCEDURE USED FOR MOUNTING GRAINS

1. Place a large drop of a one per cent gelatin solution on a clean dry slide and allow to dry to a thin film.
2. Place a drop of a mixture of two parts acetone and one part formalin directly on the film and spread the grains evenly over the drop with a needle.
3. Under the microscope, insure that grains are evenly spread and that only one layer of particles is on the glass slide.
4. If gelatin film solidifies, add more solution of acetone and formalin until layer of grains is evenly dispersed on the glass slide.
5. Allow to dry for subsequent examination.
6. For added effectiveness, certain refractive index liquids can be used and are discussed in other cited references.

APPENDIX B

RELATIONSHIP BETWEEN FREQUENCY-BY-NUMBER
AND WEIGHT-PER CENT GRAIN-SIZE
DISTRIBUTIONS

Problem: Establish the difference existing between data involving frequency-by-number and weight-per cent grain-size distributions.

Assumptions:

- a. Total of 10^7 grains form a hypothetical perfectly normal distribution (straight line) based on direct measurements of grain diameters (Figure 39).
- b. Specific Gravity = 2.71.
- c. All grains are perfect spheres.

Calculations:

At 10% cumulative, $\Phi = 4.2$; diameter = 0.0545 mm by conversion. (radius = 0.02725)

Weight:

$$\begin{aligned} \text{Number of grains} &= .10 \times 10^7 = 10^6 \\ \text{Volume of grains} &= \frac{4}{3} \pi r^3 (N) \\ &= \frac{4}{3} \pi (.02725)^3 \times 10^6 \\ &= 84.8 \text{ mm}^3 = 0.0848 \text{ c.c.} \\ \text{Weight of grains} &= \text{Vol.} \times \text{Density} \\ &= .0848 \times 2.71 \\ &= 0.23 \text{ gms.} \end{aligned}$$

Therefore, if 10% weighs .23 gms, the total weight of sample = $\frac{.23}{.10} = 2.3$ gms.

Then, from frequency-by-number (Figure 39), diameter at 90% cumulative = 5.35 Φ .

And, average diameter of particles coarser than 5.35 Φ (90%) equals 0.0425 mm, or radius = 0.02125 mm;

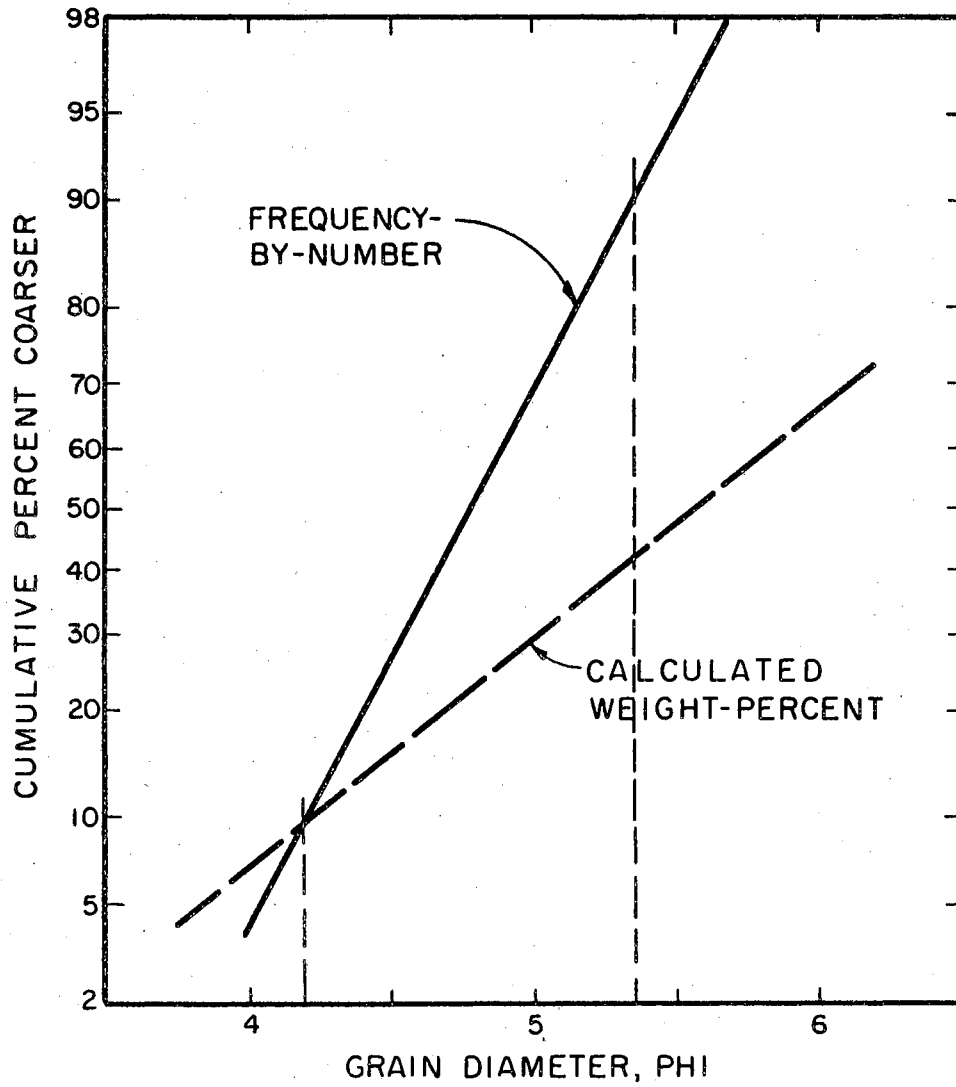


Figure 39. Perfectly Normal Grain Size Distribution Curves Plotted on Probability Paper

the volume of grains for the weight-per cent distribution is:

$$\text{number of grains} = .9 \times 10^7 = 9 \times 10^6$$

$$\begin{aligned} \text{volume of grains} &= \frac{4}{3} \pi r^3 N = \frac{4}{3} \pi (.02125)^3 \times 9 \times 10^6 \\ &= 0.362 \text{ cc} \end{aligned}$$

$$\text{Weight of grains} = .362 \times 2.71 = 0.98 \text{ gms.}$$

Therefore, the ratio of weight of grains coarser than 90% size to total weight is:

$$\frac{.98 \text{ gms.}}{2.3 \text{ gms.}} = .425$$

or 42.5% by weight (Figure 39).

This example shows that although a constant number of grains was used for calculation of distribution by weight-per cent, the phi diameter of 5.35 indicates a cumulative per cent of 90 for frequency-by-number; whereas, 42.5 per cent is calculated for a weight per cent distribution coarser than 5.35 ϕ .

APPENDIX C

GRAIN-SIZE DISTRIBUTION REGRESSION DATA

TABLE IX
 PHI VALUES DERIVED BY PLOTTING CUMULATIVE CURVES
 ON PROBABILITY PAPER

Cumulative Percentages	Vicksburg Loess			Pre-Vicksburg Loess		
	Average Sieve and Hydrometer	Thin Section	Grain Mount	Average Sieve and Hydrometer	Thin Section	Grain Mount
1	3.45	3.75	4.30	3.50	3.45	4.45
5	4.00	4.05	4.65	4.35	4.05	4.75
10	4.35	4.20	4.95	4.80	4.40	5.15
20	4.75	4.40	5.20	5.30	4.95	5.55
30	4.95	4.50	5.40	5.60	5.15	5.80
40	5.10	4.60	5.55	5.85	5.35	6.05
50	5.25	4.70	5.75	6.10	5.55	6.25
60	5.35	4.80	5.85	6.40	5.75	6.40
70	5.75	4.95	6.00	6.85	5.95	6.65

Thin section values as independent variable (X):

$$\begin{aligned}
 n &= 18 \\
 \Sigma X &= 84.550 & \Sigma Y &= 91.700 \\
 \bar{X} &= 4.697 & \bar{Y} &= 5.094 \\
 \Sigma X^2 &= 405.088 & \Sigma Y^2 &= 482.125 & \Sigma XY &= 441.457 \\
 (\Sigma X)^2/n &= \underline{397.150} & (\Sigma Y)^2/n &= \underline{467.160} & (\Sigma X)(\Sigma Y)/n &= 430.740 \\
 \Sigma x^2 &= 7.938 & \Sigma y^2 &= 14.965 & \Sigma xy &= 10.717
 \end{aligned}$$

$$\begin{aligned}
 b_1 &= \Sigma xy / \Sigma x^2 = 1.350 & r^2 &= (\Sigma xy)^2 / \Sigma x^2 \Sigma y^2 = 0.967 \\
 b_0 &= \bar{Y} - b_1 \bar{X} = -1.247 & r &= 0.984 \\
 \hat{Y} &= b_0 + b_1 X = -1.247 + 1.350(X)
 \end{aligned}$$

H_0 : No correlation between thin section values and weight-per cent values.

H_A : Thin section and weight-per cent values are correlated.

At 99 per cent confidence level, $r_{tab} = 0.647$.

Therefore, since $r_{cal} > r_{tab}$, Reject H_0 .

Grain mount values as independent variable (X):

$$n = 18$$

$$\Sigma X = 98.70 \quad \Sigma Y = 91.70$$

$$\bar{X} = 5.483 \quad \bar{Y} = 5.094$$

$$\Sigma X^2 = 549.080 \quad \Sigma Y^2 = 482.125 \quad \Sigma XY = 513.570$$

$$(\Sigma X)^2 / n = \underline{541.205} \quad (\Sigma Y)^2 / n = \underline{467.161} \quad (\Sigma X)(\Sigma Y) / n = \underline{502.822}$$

$$\Sigma x^2 = 7.875 \quad \Sigma y^2 = 14.964 \quad \Sigma xy = 10.748$$

$$b_1 = \Sigma xy / \Sigma x^2 = 1.365 \quad r^2 = (\Sigma xy)^2 / \Sigma x^2 \Sigma y^2 = 0.980$$

$$b_0 = \bar{Y} - b_1 \bar{X} = -2.390 \quad r = 0.990$$

$$\hat{Y} = b_0 + b_1 X = -2.390 + 1.365(X)$$

H_0 : No correlation between grain mount values and weight-per cent values.

H_A : Grain mount and weight-per cent values are correlated.

At 99 per cent confidence level, $r_{tab} = 0.647$.

Therefore, since $r_{cal} > r_{tab}$, Reject H_0 .

APPENDIX D

PROCEDURE FOR IMPREGNATING SAMPLES
FOR THIN SECTIONS

1. Soil specimens are appropriately marked oven-dried, placed in a container and then in a vacuum chamber with a desiccant for several hours (Figure 40)
2. While under vacuum, allow the epoxy plastic (4 parts R8-2038 Resin, to one part H2-3404 Hardener, Hysol Corporation, Olean, New York), thoroughly mixed, to completely submerge the specimen.
3. Keep under vacuum for 15-20 minutes, and then gradually release vacuum to allow atmospheric pressure to force impregnating plastic into pores.
4. Remove from vacuum chamber and allow to remain submerged as long as possible before plastic begins to polymerize.
5. Rapidly remove from container and place on paper towels to cure. To insure more rapid curing, place in oven at 90-100°F for a period of 24 hours.
6. Clean container, separatory funnel, and other apparatus rapidly with carbon tetrachloride or other solvent prior to hardening of plastic.
7. Note that plastic mixture used in this study polymerizes within 35-40 minutes of adding hardening agent. Allowance should be made to complete above procedure prior to such action. Polymerization of epoxy plastic is associated with high temperatures and toxic vapors, and all necessary precautions should be taken.

APPENDIX E

PROCEDURE FOR PREPARING SAMPLES FOR
DIELECTRIC ANISOTROPY
MEASUREMENTS

I. Consolidation of Loess Specimens

- a. Lucite tubing is cemented to lucite base plate as is illustrated in the upper portion of Figure 41.
- b. Layer of fine clean sand is placed beneath an oven-dried, marked, and undisturbed loess specimen.
- c. Fine silt is placed around the sample which acts as a seal.
- d. The sample in the lucite tube is placed in a vacuum chamber for several hours (configuration similar to Figure 40).
- e. While under vacuum, allow a solution of eposand 8A, 8B, and 8C (50:50:7 by volume, respectively), through a separatory funnel, to completely submerge the loess specimen.
- f. Release the vacuum slowly, with caution, to allow atmospheric pressure to force the eposand solution into the pores of the specimen.
- g. Remove excess solution until the level is approximately $\frac{1}{8}$ -inch below top of specimen.
- h. Cure for 24 hours at 140°F.
- i. Pour out excess solution after curing and drill several holes into base plate to the sand layer (Figure 41).
- j. Place on greased o-ring and clamp to vacuum

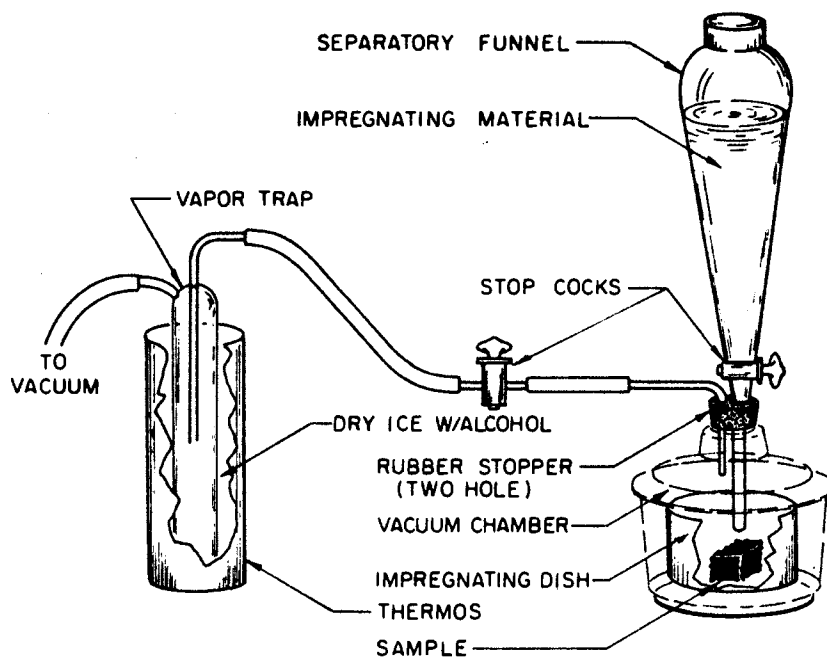


Figure 40. Apparatus for Standard Impregnation of Soils

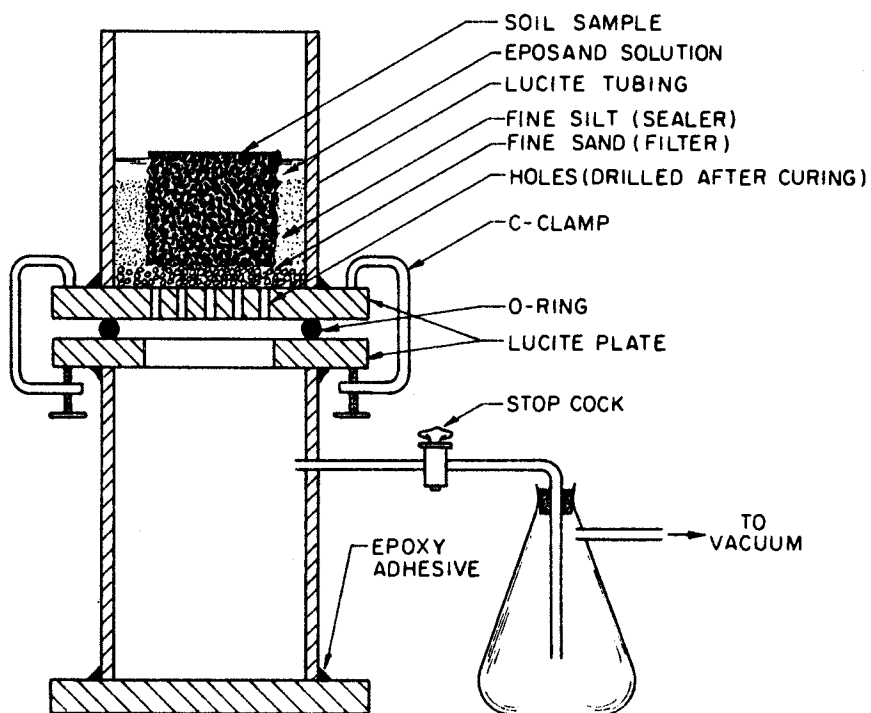


Figure 41. Apparatus for Consolidation of Soil Specimens

chamber as shown (Figure 41).

- k. Pour sufficient quantity of naphtha into upper lucite tube and flush through loess specimen with aid of a vacuum.
- l. Continue to add naphtha until specimen is considered free of eposand solvent.
- m. Add isopropyl alcohol until all of the naphtha is removed and specimen is considered completely flushed of all solvents. The fine silt seal insures that the naphtha and alcohol are flushed through the specimen and not around its boundary.
- n. The consolidated specimen is now ready for remarking and drilling.

II. Impregnating Drilled Plugs With Dielectric Fluid

- a. After specimen is drilled and appropriately marked, plugs are oven-dried and placed in a container and in a vacuum chamber with a desiccant for several hours (Figure 40).
- b. While under vacuum, add Dow Corning 550 dielectric fluid through separatory funnel until plugs are completely submerged.
- c. Release vacuum slowly to allow atmospheric pressure to force fluid into pores of specimen.
- d. Keep plugs submerged under fluid for at least 24 hours and until ready for dielectric anisotropy measurements.

APPENDIX F
COMPUTERIZED GRAIN ORIENTATION
STATISTICAL ANALYSIS

VECTOR MAGNITUDE METHOD USING TWO THETA ANGLES

```

DIMENSION THETA(100),RN(100),COS2(100),SIN2(100),RNCOS2(100)
DIMENSION RNSIN2(100),THETA2(100),IWHAT(80)
DATA RADIANS/57.29578/
5  FORMAT(1HL,2X,5HTHETA, 4X,1HN, 7X,2H2*, 6X,7HCOS(2*), 4X,
C   7HSIN(2*), 5X,9HNCOS(2*), 3X,9HNSIN(2*), /)
7  FORMAT(1HK,3F 7.1,4F12.3)
8  FORMAT(1HL, 14HSUM N(COS(2*)), 2X,14HSUM N(SIN(2*)), 2X,
C   10HSUM OF N'S, 3X,7HTAN(2*), 5X,1HR,12X,1HL)
9  FORMAT(1HL,2(F11.3,2X),3X,4F11.3)
  READ(5,1) N
1  FORMAT(I2)
  DO 20 KK=1,N
16  READ(5,11) IWHAT
11  FORMAT(80A1)
  READ (5,2) (RN(I),I=1,18)
2  FORMAT(18F4.0)
  DO 10 I=1,18
10  THETA(I)=10.0*FLOAT(I)
  DO 3 I=1,18
    THETA2(I)=2.0*THETA(I)
    COS2(I)=COS(2.0*(THETA(I)/RADIANS))
    SIN2(I)=SIN(2.0*(THETA(I)/RADIANS))
    RNCOS2(I)=RN(I)*COS2(I)
    RNSIN2(I)=RN(I)*SIN2(I)
3  CONTINUE
  SX=0.0
  CY=0.0
  ZN=0.0
  DO 4 I=1,18
    SX=SX+RNSIN2(I)
    CY=CY+RNCOS2(I)
    ZN=ZN+RN(I)
4  CONTINUE
  WRITE(6,12) IWHAT
12  FORMAT(1H1,1X,80A1)
  WRITE(6,5)
  DO 6 I=1,18
6  WRITE(6,7) THETA(I),RN(I),THETA2(I),COS2(I),SIN2(I),RNCOS2(I),
  *RNSIN2(I)
  TAN2=SX/CY
  R=SQRT(SX**2+CY**2)
  RL=(R/ZN)*100.0
  WRITE(6,8)
  WRITE(6,9) CY,SX,ZN,TAN2,R,RL
20  CONTINUE
  STOP
  END
$ENTRY
20
C   SPECIMEN NUMBER 100 TOTALS SECTION H-1 1,2,3 VICKS LOESS
139.122.108.099.116.111.111.095.094.079.077.068.073.076.087.104.116.135.

```

TABLE X
GRAIN ORIENTATION BY VECTOR MAGNITUDE METHOD

C SPECIMEN NUMBER 100 TOTALS SECTION H-1 1,2,3 VICKS LBESS						
THETA	N	2*	COS(2*)	SIN(2*)	NCOS(2*)	NSIN(2*)
10.0	139.0	20.0	0.940	0.342	130.617	47.541
20.0	122.0	40.0	0.766	0.643	93.457	78.420
30.0	108.0	60.0	0.500	0.866	54.000	93.531
40.0	99.0	80.0	0.174	0.985	17.191	97.496
50.0	116.0	100.0	-0.174	0.985	-20.143	114.238
60.0	111.0	120.0	-0.500	0.866	-55.500	96.129
70.0	111.0	140.0	-0.766	0.643	-85.031	71.349
80.0	95.0	160.0	-0.940	0.342	-89.271	32.492
90.0	94.0	180.0	-1.000	0.000	-94.000	0.000
100.0	79.0	200.0	-0.940	-0.342	-74.236	-27.020
110.0	77.0	220.0	-0.766	-0.643	-58.985	-49.495
120.0	68.0	240.0	-0.500	-0.866	-34.000	-58.890
130.0	73.0	260.0	-0.174	-0.985	-12.676	-71.891
140.0	76.0	280.0	0.174	-0.985	13.197	-74.845
150.0	87.0	300.0	0.500	-0.866	43.500	-75.344
160.0	104.0	320.0	0.766	-0.643	79.669	-66.850
170.0	116.0	340.0	0.940	-0.342	109.004	-39.674
180.0	135.0	360.0	1.000	-0.000	135.000	-0.000
SUM NCOS(2*)	SUM N(SIN(2*))	SUM OF N'S	TAN(2*)	R	L	
151.794	167.187	1810.000	1.101	225.816	12.476	

$$\tan 2\theta = 1.101$$

$$2\theta = 47^{\circ} 45'$$

$$\theta = 24^{\circ}$$

$$\text{Minus } 5^{\circ} \text{ (to mid-point)} = 19^{\circ}$$

$$\text{North Azimuth} = 270^{\circ} + 19^{\circ} = 289^{\circ}$$

$$\text{Bearing} = \text{N } 71^{\circ} \text{ W}$$

PREFERRED ORIENTATION BY CHAYES MIN VARIANCE METHOD

```

DIMENSION Y(20),X(20),SY(20),AX(20),Z(20),DIFF(20),AK(20),VI(20)
READ11,IPAR
11 FORMAT(I4)
DO 12 J = 1,IPAR,1
  READ 14, X(1),X(2),X(3),X(4),X(5),X(6),X(7),X(8),X(9),SPEC
  READ 14,X(10),X(11),X(12),X(13),X(14),X(15),X(16),X(17),X(18)
14 FORMAT (F4.0,F4.0,F4.0,F4.0,F4.0,F4.0,F4.0,F4.0,F4.0,F4.0,28X,F8.1)
  READ 14,Y(1),Y(2),Y(3),Y(4),Y(5),Y(6),Y(7),Y(8),Y(9)
  READ 14,Y(10),Y(11),Y(12),Y(13),Y(14),Y(15),Y(16),Y(17),Y(18)
  PRINT 101
101 FORMAT (//1H1,16H SPECIMEN NUMBER)
  PRINT 103, SPEC
103 FORMAT (36X,28X,F8.1)
  SF = 0.0
  SY 18 = 0.0
  DO 15 I = 1,18,1
15 SY 18 = SY 18 + Y(I)
  SYY = 0.0
  DO 5 I = 1,18,1
  CUM = X(I)*Y(I)
  SF = SF + CUM
  SYY = SYY + Y(I)
  SY(I) = SYY/SY 18
  5 AX(I) = SF/SYY
  GO TO 31
31 AVEX = SF/ SY 18
  SZ = 0.0
  I = 1
  DO 7 I = 1,18,1
  Z(I) = X(I)*X(I)*Y(I)
  SZ = SZ + Z(I)
  7 CONTINUE
  S2MOM = SZ/SY 18
  VAR = (S2MOM - (AVEX**2))
  STDV = VAR**0.5
  SNED = 2700.0/ VAR
  PRINT 13
13 FORMAT (//5X,7H AVEX,4X,10H VARIANCE,4X,8H STDV)
  PRINT 27, AVEX,VAR,STDV
27 FORMAT (5X,F7.2,4X,F10.3,4X,F8.3)
  PRINT 28
28 FORMAT (//5X,8H SNED,4X,7H SY 18)
  PRINT 29,SNED,SY 18
29 FORMAT (5X,F8.4,4X,F7.1)
  PRINT 8
  8 FORMAT (///10X,3HLCL,4X,4HFREQ,6X,2HVI)
  DO90 I=1,18,1
  DIFF(I) = AX(I) - AX(18)
  AK(I) = 90.0*(1.0-SY(I))
  VI(I) = (DIFF(I) + AK(I))*(SY(I))
90 PRINT 9,X(I),Y(I),VI(I)
  9 FORMAT (10X,F4.0,3X,F4.0,3X,F7.4)
  VIMX = VI(1)
  KK = 1
  DO 20 K = 2,18,1
  IF (VIMX - VI(K)) 21,20,20
21 VIMX = VI(K)
  KK = K
20 CONTINUE
  PRINT 16
16 FORMAT (//5X,8H VIMX,5X,4H KK,5X,5HX(KK))

```



```

PRINT 10,VIMX,KK,X(KK)
10 FORMAT (5X,F8.4,5X,14,5X,F5.0)
XX = X(KK)
DO 40 I = 1,18,1
X(I) = X(I) - XX
IF (XX) 30,105,32
30 IF (X(I) - 90.0) 40,40,41
41 X(I) = X(I) - 180.0
GO TO 40
105 PRINT 107
107 FORMAT (11H VAR IS MIN)
GO TO 12
32 IF (X(I) + 85.0) 50,50,40
50 X(I) = X(I) + 180.0
40 CONTINUE
SF = 0.0
SY 18 = 0.0
DO 18 I = 1,18,1
18 SY 18 = SY 18 + Y(I)
SYY = 0.0
DO 1 I = 1,18,1
CUM = X(I)*Y(I)
SF = SF + CUM
SYY = SYY + Y(I)
SY(I) = SYY/SY 18
1 AX(I) = SF/SYY
GO TO 33
33 AVEX = SF/ SY 18
SZ = 0.0
I = 1
DO 3 I = 1,18,1
Z(I) = X(I)*X(I)*Y(I)
SZ = SZ + Z(I)
3 CONTINUE
S2MOM = SZ/SY 18
VAR = (S2MOM - (AVEX**2))
STDV = VAR**0.5
SNED = 2700.0/ VAR
PRINT 80
80 FORMAT (/5X,7H AVEX,4X, 9H VARIANCE,4X,8H STDV)
PRINT 81, AVEX,VAR,STDV
81 FORMAT (5X,F7.2,4X,F10.3,4X,F8.3)
PRINT 82
82 FORMAT (/5X,8H SNED,4X,7H SY 18)
PRINT 83,SNED,SY 18
83 FORMAT (5X,F8.4,4X,F7.1)
12 CONTINUE
GO TO 140
140 STOP
END
$ENTRY
0030
-80.-70.-60.-50.-40.-30.-20.-10.000.
010.020.030.040.050.060.070.080.090.
139.122.108.099.116.111.111.095.094.
079.077.068.073.076.087.104.116.135.
100.0

```

TABLE XI
GRAIN ORIENTATION BY CHAYES' MINIMUM
VARIANCE TECHNIQUE

SPECIMEN NUMBER		
100.0		
AVEX	VARIANCE	STDV
1.54	3052.044	55.245
SNED	SY 18	
0.8847	1810.0	
LCL	FREQ	VI
-80.	139.	0.1188
-70.	122.	0.0223
-60.	108.	-0.1487
-50.	99.	-0.3216
-40.	116.	-0.5684
-30.	111.	-0.8835
-20.	111.	-1.2623
-10.	95.	-1.5992
0.	94.	-1.9014
10.	79.	-2.0943
20.	77.	-2.1869
30.	68.	-2.1639
40.	73.	-2.0186
50.	76.	-1.7585
60.	87.	-1.3697
70.	104.	-0.8761
80.	116.	-0.3857
90.	135.	0.0000
VIMX	KK	X(KK)
0.1188	1	-80.
AVEX	VARIANCE	STDV
8.35	2298.100	47.938
SNED	SY 18	
1.1749	1810.0	
<p>X(KK) = Lower Class Limit = -80 = N 80° W</p> <p>AVEX = Mean (overall) = 8.35° (additive)</p> <p>Bearing = N 72° W</p> <p>North Azimuth = 288°</p> <p>Standard Deviation = 48°</p> <p>Variance Ratio, F = 1.17</p>		

VITA

2

Rudolph Vincent Matalucci
Candidate for the Degree of
Doctor of Philosophy

Thesis: THE MICROSTRUCTURE OF LOESS AND ITS RELATIONSHIP
TO ENGINEERING PROPERTIES

Major Field: Engineering

Biographical:

Personal Data: Born in Goshen, New York, February 6,
1938, the son of Luigi and Concetta Matalucci.

Education: Graduated from Goshen Central School in
1956; received the Bachelor of Science degree
from the University of New Hampshire, with a
major in Civil Engineering, in June, 1960;
received the Master of Science degree from
Oklahoma State University, with a major in
Civil Engineering, in May, 1962; completed
requirements for the Doctor of Philosophy degree
in May, 1969.

Professional Experience: Sales Engineer Trainee,
Ingersoll-Rand Company, Summer, 1960; Planning
and Programming Officer, Engineering Officer,
Engineering Management Officer, and Base Civil
Engineer with the U. S. Air Force Strategic Air
Command and U. S. Air Force Europe Bases from
1962-1966.

Professional Societies: Associate Member, American
Society of Civil Engineers; Registered
Professional Engineer, State of New Hampshire.